

# Characterization of quantum correlations with strong non-classical properties

Ph.D. Thesis

By  
**MAHASWETA PANDIT**

**Supervisor:** Wiesław Laskowski  
**Co-supervisor:** Waldemar Kłobus



**Institute of Theoretical Physics and Astrophysics**

University of Gdańsk, Poland

To my beloved parents.

# Acknowledgement

I would foremost like to thank my supervisors Prof. dr hab. Wiesław Laskowski and dr. Waldemar Kłobus for their continuous guidance throughout my Ph.D. and providing me with the necessary motivation and knowledge to conduct my research.

I would like to thank Prof. Ujjwal Sen, dr hab. Tomasz Paterek and dr hab. Marcin Wieśniak for numerous useful discussions and learning opportunities.

My heartiest gratitude to all my collaborators, who have been part of fruitful research endeavours that have contributed greatly to the shaping of my academic outlook as an independent researcher.

I want to thank my friends Souradeep Purkayastha, Ray Ganardi, Palash Pandya and Chirag Srivastava in particular for proofreading the thesis and providing helpful inputs throughout its preparation. I also feel grateful to my fellow graduate students, post-graduates and friends, *Bianka Wołoncewicz*, Anubhav Chaturvedi, Omer Sakarya, Jacek Aleksander Gruca, Tanmoy Biswas, Tamoghna Das, Adrian Kołodziejski and Ekta Panwar for countless useful discussions, coffee breaks, and keeping my motivation up during these difficult pandemic times. Also, a very special mention to my dear friend Małgorzata Szczekocka who has been the kindest and helped me through every administrative tasks and many more.

Finally, I would like to convey my heartiest gratitude and love to my parents Mahitosh and Nandita Pandit for their eternal love and support.

# Streszczenie

Nieklasyczne korelacje w układach wielocząstkowych stanowią złożony problem, który nie został jeszcze w pełni zbadany. W szczególności interesują nas korelacje pomiędzy wieloma układami, które nie są biseparowalne i mogą być określane mianem "silnie nieklasycznych".

Pierwszym przykładem układów przejawiających "silną nieklasyczność", który rozpatrujemy są  $N$ -cząstkowe stany  $k$ -jednorodne. Takie stany posiadają cechę bycia maksymalnie mieszanymi na podukładach zredukowanych do  $k$  cząstek dla wszystkich podziałów układu i stanowią naturalne uogólnienie stanów maksymalnie splątanych. Prezentujemy metodę konstrukcji takich stanów. Znajdujemy również  $N$ -cząstkowe stany  $k$ -jednorodne o największej możliwej czystości dla przypadków, w których czyste stany  $k$ -jednorodne nie istnieją. Takie stany mają najwyższe wielocząstkowe korelacje spośród wszystkich stanów o zadanej czystości.

W następnej części prezentujemy teorio-informacyjną wielkość charakteryzującą "silne" wielocząstkowe korelacje. Wielkość ta,  $N$ -współzależność, określa zysk w sensie teorio-informacyjnym, uzyskiwany na drodze wzajemnej współpracy między różnymi podukładami wielocząstkowego układu. Ta wielkość różni się od miar wielocząstkowych korelacji, jako że nie spełnia ich wszystkich postulatów. Pokazujemy, że  $N$ -współzależność może mieć różne zastosowania, jak choćby w kwantowym protokole współdzielenia sekretu.

W kolejnym rozdziale rozpatrujemy "silną nieklasyczność" pod kątem metrologii kwantowej. W tym względzie, prezentujemy metodę estymacji wielofazowej w układach złożonych wykorzystującą 3- i 4-modowe interferometrię Macha-Zehndera. Pokazujemy, że możliwe jest uzyskanie fundamentalnego limitu narzuconego na precyzję pomiaru (tj. limit Heisenberga), uzyskiwanego przez bezszumowe złożone układy kwantowe. Prezentujemy metodę jednoczesnej estymacji  $d - 1$  faz w  $d$ -modowym układzie, gdzie pozostały mod służy w charakterze odniesienia.

W ostatniej części rozpatrujemy inny aspekt "silnej nieklasyczności", który ma duże znaczenie w kwestii zrozumienia znaczenia efektów świata kwantowego, mianowicie tzw. prawdziwej wielocząstkowej nielokalności (GMNL). Rozpatrujemy dwa różne ujęcia GMNL i prezentujemy dowody numeryczne celem zbadania łamania ograniczeń na GMNL dla różnych kwantowych układów wielocząstkowych. Jako wskaźnik nieklasyczności używamy dwóch miar: siły nielokalności i prawdopodobieństwa łamania.

# Abstract

Non-classical correlations present a wide range of complexity and variation in the multipartite setup that is yet to be explored to its full extent. In particular, correlations between many parties that are not separable in any bipartition can be referred to as "strongly" non-classical. In this dissertation aimed to investigate such strong non-classical correlations especially in the multipartite scenario.

The first candidate exhibiting such "strong" non-classicality that we consider are the  $k$ -uniform  $N$ -partite states. These states are such that they become maximally mixed if reduced to a  $k$ -partite state considering any permutation of the subsystems and referred to as a natural generalization of the maximally entangled Bell states. We propose a generator scheme to construct such states. We also find  $k$ -uniform  $N$ -partite states with the highest possible purity when one such pure state does not exist. These states possess the most multipartite correlations among all quantum states of the same purity.

Following the construction of the states displaying strong multipartite correlations, we next propose an information-theoretic quantifier that can address such correlations. This quantifier, namely  $N$ -dependence, quantifies the information gained from the cooperation among different subsystems about a particular subsystem within a multipartite system. This quantifier is distinct from measures of multipartite correlations as it does not satisfy all their postulates. We show that  $N$ -dependence can have several applications such as in symmetric quantum secret sharing.

We next take a step further and provide a metrological aspect of strong non-classicality. We, in a composite system scenario, propose a multiphase estimation scheme using a setup consisting of a 3-4-mode Mach-Zehnder interferometer. We show that it is possible to attain the fundamentally imposed limit on measurement precision, i.e., the Heisenberg limit, achievable by noiseless composite quantum systems. We present a scheme for simultaneous estimation of  $d - 1$  phases for a  $d$ -mode system.

Lastly, we investigate another notion of strong non-classicality which has major significance in understanding the advantages that the quantum world has to offer, namely genuine multipartite nonlocality (GMNL). We consider two different notions of GMNL and present numerical evidence to investigate the violations of the constraints corresponding to these different notions of GMNL by a number of multipartite quantum states. As an indicator of non-classicality, we employ two measures: strength of nonlocality and probability of violation.

# Contents

<b>Dedicate</b>	<b>i</b>
<b>Acknowledgement</b>	<b>ii</b>
<b>Abstract</b>	<b>iii</b>
<b>Contents</b>	<b>v</b>
<b>List of Figures</b>	<b>vii</b>
<b>List of papers</b>	<b>viii</b>
<b>Introduction</b>	<b>1</b>
<b>1 <math>k</math>-uniform mixed states</b>	<b>4</b>
1.1 Correlations of $k$ -uniform states . . . . .	5
1.1.1 Bloch representation of states . . . . .	5
1.1.2 Length of correlations . . . . .	6
1.2 Numerical methods . . . . .	7
1.2.1 PRAXIS optimization routine . . . . .	7
1.2.2 Numerical method based on semidefinite programming . . . . .	8
1.3 State construction scheme . . . . .	9
1.4 Orthogonal arrays . . . . .	11
1.5 Examples . . . . .	13
1.5.1 General schemes . . . . .	14
1.5.2 $N$ arbitrary, $k = 1$ . . . . .	15
1.5.3 $N$ arbitrary, $k = N - 1$ . . . . .	16
1.5.4 $N = 4, k = 2$ . . . . .	16
1.5.5 $N = 5, k = 2$ . . . . .	18
1.5.6 $N = 5, k = 3$ . . . . .	19
1.5.7 $N = 6, k = 2$ . . . . .	19
1.5.8 $N = 6, k = 3$ . . . . .	20
1.5.9 $N = 6, k = 4$ . . . . .	20

1.5.10	$N = 7, k = 2$ . . . . .	21
1.5.11	$N = 7, k = 3$ . . . . .	21
1.5.12	$N = 7, k = 5$ . . . . .	22
1.5.13	$N > 7, k = N - 2$ . . . . .	22
1.5.14	$N = 9, k = 5$ . . . . .	23
1.5.15	$N = 12, k = 5$ . . . . .	23
1.6	Characteristics of $k$ -uniform states . . . . .	25
1.6.1	Genuine multipartite entanglement . . . . .	25
1.6.2	Fisher information . . . . .	26
1.6.3	Violation of Bell inequality . . . . .	27
1.7	Quantum circuits for $k$ -uniform states . . . . .	29
1.8	Higher dimensional $k$ -uniform states . . . . .	31
1.9	Threshold values for the number of generators . . . . .	33
1.10	Conclusions . . . . .	36
<b>2</b>	<b>Cooperation and dependencies in multipartite systems</b> . . . . .	<b>37</b>
2.1	Definition of multipartite Dependence . . . . .	39
2.1.1	Tripartite dependence . . . . .	40
2.1.2	Multipartite dependence ( $N > 3$ ) . . . . .	42
2.1.3	Pure states . . . . .	44
2.1.4	Relevant Examples . . . . .	44
2.1.5	$k$ -partite $N$ -Dependence . . . . .	46
2.2	General Properties . . . . .	47
2.2.1	Extremal values of dependence . . . . .	47
2.2.2	Key properties of $\mathcal{D}_N$ . . . . .	53
2.2.3	Partial extension of classical interpretations . . . . .	56
2.3	Comparison with other quantifiers of correlations . . . . .	58
2.3.1	$N$ -dependence versus $N$ -partite correlations . . . . .	58
2.3.2	Dependence without correlations . . . . .	61
2.3.3	Entanglement without dependence . . . . .	61
2.3.4	Connections to the costs of merging and Markov Chains . . . . .	62
2.4	Applications . . . . .	63
2.4.1	Quantum secret sharing . . . . .	63
2.4.2	Witnessing entanglement . . . . .	66
2.4.3	Data science . . . . .	67
2.5	Conclusions . . . . .	69
<b>3</b>	<b>Simultaneous multiphase estimation with Heisenberg scaling</b> . . . . .	<b>70</b>
	Introduction . . . . .	70
3.1	Prerequisites and the Setup . . . . .	72

3.1.1	General introduction to multiphase estimation . . . . .	72
3.1.2	Setup for the estimation procedure . . . . .	76
3.2	Main Results . . . . .	79
3.2.1	Generalised Mach-Zehnder interferometer . . . . .	79
3.2.2	Precision of the multiphase estimation scheme . . . . .	83
3.2.3	Optical implementation of Single-interferometer . . . . .	90
3.2.4	Symmetric 5-mode multiport . . . . .	91
3.3	Conclusion . . . . .	93
<b>4</b>	<b>Optimal tests of genuine multipartite nonlocality</b>	<b>94</b>
4.1	Definitions and Methodology . . . . .	96
4.1.1	Bell nonlocality . . . . .	96
4.1.2	Tripartite nonlocality . . . . .	96
4.1.3	Indicators of genuine multipartite nonlocality . . . . .	99
4.1.4	Linear Programming for tripartite nonlocality . . . . .	100
4.2	Results . . . . .	104
4.2.1	Qubits . . . . .	104
4.2.2	Qutrits . . . . .	105
4.3	Conclusion . . . . .	107
	<b>Bibliography</b>	<b>109</b>

## List of Figures

1.1	Maximum purity of different $k$ -uniform states. . . . .	24
1.2	Quantum circuit to generate 2-uniform 4-qubit state. . . . .	30
3.1	Schematic of the multiphase estimation setup. . . . .	78
3.2	$\text{Tr} \left( (\mathcal{F}(\alpha_1, \alpha_2)_{\mathcal{I}, \mathcal{I}})^{-1} \right)$ vs $\alpha_1$ vs $\alpha_2$ . . . . .	88

# List of papers

This dissertation is based on the following published works and ongoing project:

1. Waldemar Kłobus, Adam Burchardt, Adrian Kołodziejski, Mahasweta Pandit, Tamás Vértesi, Karol Życzkowski, and Wiesław Laskowski,  $k$ -uniform mixed states, *Physical Review A* **100**, 032112 (2019).
2. Waldemar Kłobus, Marek Miller, Mahasweta Pandit, Ray Ganardi, Lukas Knips, Jan Dżiewior, Jasmin Meinecke, Harald Weinfurter, Wiesław Laskowski, and Tomasz Paterek, Cooperation and dependencies in multipartite systems, *New Journal of Physics* **23**, 063057 (2021).
3. Marcin Markiewicz, Mahasweta Pandit, and Wiesław Laskowski, Simultaneous estimation of multiple phases in generalised Mach–Zehnder interferometer, *Sci Rep* **11**, 15669 (2021).
4. Mahasweta Pandit, Artur Barasiński, István Márton, Tamás Vértesi, and Wiesław Laskowski, Optimal tests of genuine multipartite nonlocality, in preparation.

Other published articles and preprints under review:

1. Mahasweta Pandit, Sreetama Das, Sudipto Singha Roy, Himadri Shekhar Dhar, and Ujjwal Sen, Effects of cavity–cavity interaction on the entanglement dynamics of a generalized double jaynes–cummings model, *J. Phys. B: At. Mol. Opt. Phys.*, **51**, 045501 (2018).
2. Mahasweta Pandit, Anindita Bera, Aditi Sen(De), and Ujjwal Sen. Quantum reciprocity relations for fluctuations of position and momentum, *Physical Review A*, **100**, 012131 (2019).
3. Chirag Srivastava, Mahasweta Pandit, and Ujjwal Sen, Entanglement witnessing by arbitrarily many independent observers recycling a local quantum shared state, arXiv: 2109.10310 (2021).
4. Mahasweta Pandit, Chirag Srivastava, and Ujjwal Sen, Recycled entanglement detection by arbitrarily many sequential and independent pairs of observers, arXiv: 2201.02594 (2022).

# Introduction

Quantum theory is the basis of modern physics that departs from the long running "classical lines of thought" [1] which has enabled several advantages in quantum information processing and quantum computation. Quantum theory casts aside assumptions such as determinism of a physical theory and joint measurability of observables. This allowed quantum theory to uncover different phenomena such as entanglement, uncertainty relations, Bell nonlocality, contextuality, etc. These are referred as the *non-classicality* of quantum theory that appears due to the presence of *non-classical* correlations which do not have any classical counterpart. In [2], the authors first introduced the distinction between classical and quantum correlations in bipartite systems. Results also show that quantum correlations can exist in the absence of any classical correlation [3]. Therefore, it is of utmost importance to investigate and characterize quantum correlations. Numerous works have been done in this direction so far [4, 5, 6, 7, 8, 9, 10, 11, 12, 13, 14], especially in the bipartite scenario. However, the knowledge concerning the correlations shared by multi-qubit or multi-qudit states, i.e., systems involving more than two parties, remains inadequate given their ubiquity throughout quantum technologies. Therefore, quantification and characterization of correlations in multipartite systems [15] is one of the most fundamental tasks in quantum information theory.

The aim of this thesis is to develop methods that can help characterizing the nature of the multipartite quantum mechanical systems. In particular, in the following chapters, we do extensive study of genuine multipartite entanglement and genuine nonlocality which displays the "strong non-classical" nature of multipartite systems.

This thesis is divided into four chapters, each addressing ways to characterize and quantify strong non-classical correlations from a different perspective. Our investigations and results especially focus on systems that have three or more number of parties.

In the first chapter, we investigate a special family of states, namely, the  $k$ -uniform states,

in order to characterize multipartite entanglement. The  $k$ -uniform states are  $N$ -partite entangled states such that given  $N - k$  number of subsystems are traced out at random, the reduced state becomes maximally mixed [16]. Such situation can be understood as complete absence of stored information of an  $N$  partite quantum state in any subset of  $k$  collaborating parties. Pure  $k$ -uniform states with  $k = \lfloor N/2 \rfloor$  are called *absolutely maximally entangled* (AME) [17]. These AME states are natural generalization of the maximally entangled Bell States ( $k = 1$ ) [18] in a sense that it is maximally mixed in any  $k \leq \lfloor N/2 \rfloor$  reduction.. Such states are found to be useful for several quantum information protocols [19, 20, 21]. However, there are instances, that in certain scenarios AME states which are pure  $k$ -uniform states do not exist. In this chapter, we relax this constrain of purity and rather try to find the  $k$ -uniform states that are of highest possible purity. We reformulate the notion of  $k$ -uniformity in terms of the correlation tensor and propose a new scheme to construct these states using  $N$ -qubit Pauli operators. We present a relation between this construction scheme and the notion of orthogonal arrays [22, 23]. We also give specific examples of  $k$ -uniform  $N$ -qubit states and provide numerical evidence of having highest purity given specific values of  $k$  and  $N$ . We present an example of a specific quantum circuit which enables generating of the respective  $k$ -uniform state. We also provide some results concerning  $k$ -uniform  $N$ -qudit states that have a higher dimensionality of subsystems.

In the second chapter, we proceed to investigate mutual dependencies between subsystem within a composite multipartite system. We propose a quantifier of their dependencies which relies on the information advantage that can be gained from cooperation among different parties. This new quantifier highlights the complex nature of multipartite systems from a different point of view. This quantifier, in turns, captures the degree of dependency between subsystems of a global system. We refer to this as *multipartite dependence*,  $\mathcal{D}_N$ . We discuss the key properties of this quantifier and calculate its value for several relevant examples. Importantly, we show that this quantifier conforms to some desired postulates that establish it as a figure of merit of genuine multipartite correlations while being distinct from the conventional measures of multipartite correlations constructed in terms of the three fundamental postulates in Ref. [15, 24]. It does, however, share many of their characteristics. We show how to use this measure in numerous scenarios, including quantum secret sharing [25, 26, 27, 28] and witnessing entanglement [29, 30, 31]. In addition, we establish and explain an inequality that characterises the lack of monotonicity of conditional mutual information under local operations.

In the third chapter, we take a metrological approach in order to investigate multipartite correlation and its effect on multiphase estimation. Our aim is to make high precision measurements of some unknown parameters using quantum systems and quantum resources. Our setup consists of generalized 3,4-mode Mach-Zehnder interferometer that are used to

---

perform simultaneous estimation of phases that are encoded into a probe state which is highly correlated. We assume that the unknown phases are placed in each of the modes in the interferometer. In this chapter, we provide an estimation scheme and show that it is still possible to obtain the Heisenberg-like scaling of precision concerning the joint estimation of any subset of  $d - 1$  phases where  $d$  is the total number of modes. In order to do so, we opt for a completely fixed experimental setup where we use the fixed initial state and set of measurements. We also show that our estimation scheme can be applied to the task of quantum-enhanced sensing in three-dimensional interferometric configurations.

In the fourth chapter, we investigate strong nonlocal correlations, i.e., *genuine multipartite nonlocality* (GMNL). Such correlations are retained by multipartite entangled states and are also distinguishable from the correlations that are local to some bipartition. We construct linear optimization problem to attain optimal values of two different quantifiers of GMNL, the strength of nonlocality and probability of violation. Using this linear programming routine, we investigate three particular families of nonlocal correlations who violate either of the inequalities upon satisfying which a given correlation point  $\mathbf{p}$  belongs to one of the following sets: Bell local correlations, Svetlichny-local ( $S_2$ ) correlations and no-signaling bilocal ( $NS_2$ ) correlations. From the collected numerical evidences we then give observation of how the amount of nonlocality be effected by parameters line number of settings of the measurements and dimension of the subsystems.

## $k$ -uniform mixed states

Over the years, multipartite entanglement has gained a lot of attention. It has many applications in the field of quantum information such as quantum teleportation [32, 33], superdense coding [34], quantum key distribution [35, 36, 37], quantum error correcting code [16] etc. But, despite of much effort, it has been difficult to quantify entanglement among higher number of parties. However, a very special kind of states has been proven to be very useful in this matter in recent years. Referred as the  $k$ -uniform states, these are  $N$ -partite states such that after tracing out  $N - k$  number of subsystems arbitrarily, the remaining  $k$  subsystems become maximally mixed [16].

If the initial state is pure, then the integer number  $k$  cannot be more than  $\lfloor N/2 \rfloor$  [38]. This is because for  $k > \lfloor N/2 \rfloor$  the dimension of the reduced state is larger than that of the auxiliary space and as a result, a maximally mixed state cannot be attained. The states with  $k = \lfloor N/2 \rfloor$  are called the absolutely maximally entangled states (AME) which are considered to be the "natural generalisation" of the Bell States ( $k = 1$ ) [18]. We extend the notion of being "maximally entangled" in a sense that we now demand any  $k$ -partite reduced state of an  $N$ -partite state to be maximally mixed which marks them to be "even more entangled" and hence "maximally entangled" when  $k = \lfloor N/2 \rfloor$ , given that for a pure state, such property can hold only for  $k \leq \lfloor N/2 \rfloor$ . AME states has been proven to be useful to design holographic quantum codes and perfect tensors [19]. AME states are also have been utilized for determining threshold quantum secret sharing schemes and teleportation protocols [20, 21].

Several construction methods has been proposed to find such states, among them, state construction from orthogonal arrays, Latin squares, symmetric matrices, graph states, quantum error correcting codes [16, 39, 40, 41, 42, 43, 44]. More recently, Acín *et al.* [45] has presented a symmetric method to construct the  $k$ -uniform and AME states. It has been shown that for any  $d \geq 2$  and  $N \geq 2$ , 1-uniform states exist which are the so called *GHZ* states and the 2, 3-uniform states exist for almost every  $N$ -qudits [44].

However, not every AME can be found by any of these construction methods. While AME states for five and six qubits have been constructed explicitly [16, 46, 47], such states do not exist for systems consisting of four [48] and seven qubits [49]. These results motivated us to investigate states that possess similar property, namely the property of  $k$ -uniformity, while attaining highest possible purity. Moreover, it has been shown that there exist no AME states for systems with a larger number of qubits [50, 51]. Interestingly, if the local dimension is chosen to be large enough, AME states always exist [52]. For example, it has been proven that there exist AME states for three and four qudits, for every prime  $d > 2$  [17]. A necessary condition was also provided in [16, 53] for the existence of  $N$ -partite AME state of arbitrary dimension  $d$ ,

$$N \leq \begin{cases} 2(d^2 - 1) & N \text{ even,} \\ 2d(d + 1) - 1 & N \text{ odd.} \end{cases} \quad (1.1)$$

As described earlier, for many cases, one cannot construct such pure  $k$ -uniform states. For such cases, the next best thing is to find a mixed state of highest possible purity which will show the same attributes as a pure  $k$ -uniform state. In this chapter, we construct  $k$ -uniform states with the highest possible purity for which the corresponding pure  $k$ -uniform states or AME states do not exist.

## 1.1 Correlations of $k$ -uniform states

### 1.1.1 Bloch representation of states

Throughout this chapter, we have opted for the Bloch representation to describe any arbitrary states. In this formalism, an arbitrary state in the Hilbert space of  $N$  qubits, i.e.,  $\mathcal{H}_2^{\otimes N}$ , can be represented as:

$$\rho = \frac{1}{2^N} \sum_{\mu_1, \dots, \mu_N=0}^3 T_{\mu_1 \dots \mu_N} \sigma_{\mu_1} \otimes \dots \otimes \sigma_{\mu_N}, \quad (1.2)$$

where  $\sigma_0$  is the identity operator,  $\sigma_\mu$  are the Pauli matrices and  $\{T_{\mu_1 \dots \mu_N}\}$  represent the *correlation tensor*. The elements of the correlation tensor are real and given by the correlation function values for measurements of products of Pauli operators,

$$T_{\mu_1 \dots \mu_N} = \langle \sigma_{\mu_1} \otimes \dots \otimes \sigma_{\mu_N} \rangle_\rho = \text{Tr}(\rho \sigma_{\mu_1} \otimes \dots \otimes \sigma_{\mu_N}), \quad (1.3)$$

which we will refer to as *correlations*.

### 1.1.2 Length of correlations

The correlation that an arbitrary state possesses plays a vital role in characterising  $k$ -uniform states. Let us define *the length of correlations*, among any  $r$  subsystems

$$M_r(\rho) = \sum_{\pi} \sum_{i_1, i_2, \dots, i_r=1}^3 T_{\pi(i_1 i_2 \dots i_r)}^2, \quad (1.4)$$

where  $\pi(i_1 \dots i_r)$  stands for all permutations of  $r$  non-zero indices on  $N$  positions. A  $k$ -uniform state of  $N$  particles  $\rho_N^k$  does not have any  $k$ -partite correlations, as well as correlations between a smaller number of parties. Therefore by definition,

$$M_r(\rho_N^k) = 0, \quad \text{for } 1 \leq r \leq k. \quad (1.5)$$

In other words,

$$T_{\pi(i_1 i_2 \dots i_r)} = 0, \quad \text{for } r \leq k. \quad (1.6)$$

Whereas, the total length of the non-vanishing part of the correlations are defined as,

$$\widetilde{M}_r^N = \sum_{r=k+1}^N M_r(\rho_N^k). \quad (1.7)$$

The definition of  $M_r(\rho)$  allows us to express the purity of a  $N$ -qubit state in the following form,

$$\text{Tr} \rho^2 = \frac{1}{2^N} \sum_{i_1, i_2, \dots, i_N=0}^3 T_{i_1 i_2 \dots i_N}^2 = \frac{1}{2^N} \left( 1 + \sum_{r=1}^N M_r(\rho) \right). \quad (1.8)$$

Furthermore, because of Eq. (1.5), the sum can be reduced only to the last  $N - k - 1$  elements

$$\text{Tr}(\rho_N^k)^2 = \frac{1}{2^N} \left( 1 + \sum_{r=k+1}^N M_r(\rho) \right). \quad (1.9)$$

For a given purity, now one can calculate the total length of correlations,

$$\sum_{r=1}^N M_r(\rho) = 2^N \text{Tr} \rho^2 - 1 \quad (1.10)$$

The amount of the total correlation is constant and state independent. The absence of correlation for  $r \leq k$  results in the fact that all available correlations occur between a large number of qubits ( $r > k$ ). This, combined with a relatively high purity, can manifest strong non-classical properties, for instance the genuine multipartite entanglement.

## 1.2 Numerical methods

Numerical methods played a vital role in acquiring preliminary qualitative evidence in support of the proposed state generation scheme. We ran a non-linear optimization over the state space and confirmed that the states constructed using the generator method are of the highest purity. We extend our search based on semidefinite programming to further strengthen our claim. In this section we discuss these two methods.

### 1.2.1 PRAXIS optimization routine

To find the  $k$ -uniform  $N$ -partite mixed states of a high purity, we numerically searched over the complete set of multipartite quantum states using non-linear optimization. The calculation was carried out utilizing the Nlopt Package [54] available under the GNU LGPL.

In particular, we implemented PRAXIS (PRincipal AXIS) optimization routine which is an algorithm for gradient-free local optimization based on Richard Brent's 'principal axis method' [55], specifically designed for unconstrained optimization. This algorithm minimizes a multivariate function without using derivatives. It is a refinement of Powell's conjugate search method [56] of optimizing quadratic functions which is devised to determine a set of search directions which are repeatedly updated until they reach a set of conjugate directions up to a desired number of iterations. Brent modified the the algorithm further to ensure that the directions remain conjugate by replacing the matrix of the search direction by its principal axes. And in the last iteration the minimum will be found if the function was indeed quadratic.

To identify the  $k$ -uniform states, we introduce a cost function defined in the following way,

$$p_{\max}(N, k) = \max_{\rho} \left[ \widetilde{M}_r^N - \beta \sum_{i=1}^k M_i(\rho) \right], \quad (1.11)$$

where  $p_{\max}$  is the sum over the lengths of all non-zero correlations, maximized over the entire state space of  $N$  parties. According to the definition of a  $k$ -uniform state, the correlations between the subsystems up to total of  $k$  subsystems should vanish, whereas the rest is incorporated in the term  $\widetilde{M}_r^N$ , the total length of the non-vanishing part of the correlations. To ensure that the constraint of vanishing correlations has been satisfied, we associate a regression coefficient  $\beta$  to the lengths of correlations among the  $k$  subsystems. To efficiently determine the global maximum for the cost function one takes the constant  $\beta$  large enough, for which cost part vanishes, hence  $\beta > 2^{N-1}$ .

### 1.2.2 Numerical method based on semidefinite programming

Another way to find  $N$ -partite  $k$ -uniform states,  $\rho_N^k$  of the highest possible purity by searching over the entire state space is to use an iterative procedure based on semidefinite programming (SDP) [57]. In this method, we first need to fix the number of parties  $N$ , the number of subsystems  $k$  and the dimension  $d$  of each local Hilbert spaces. Two important constraints that are to impose in our case are the vanishing correlations for  $k$  or less number of parties and an arbitrary but same dimension for each subsystems. In addition to that, we fix the parameter  $\epsilon \in [0, 1]$ , which sets the speed of convergence, typically 0.3.

A standard SDP is a convex optimization algorithm that optimizes a linear function which is subjected to the constraint that an affine combination of symmetric matrices is positive semidefinite. A standard algorithm can be defined as follows:

$$\begin{aligned} & \text{maximize} && P = \text{Tr}(GZ) \\ & \text{subject to} && \text{Tr}(F_i Z) = c_i \quad i = 1, \dots, p \\ & && Z \geq 0, \end{aligned} \tag{1.12}$$

where the problem variable is the  $n \times n$  matrix  $Z$  and the problem parameters are the  $n \times n$  matrices  $G, F_i$  and the scalars  $c_i$ .

The algorithm for this particular work as follows:

1. Generate randomly a  $k$ -uniform state  $\rho \in \mathbb{C}^{(d^N)}$ .
2. Solve the following semidefinite program:

$$\begin{aligned} P = \max_{\sigma} & \quad \text{Tr}(\rho \cdot \sigma), \\ \text{s.t.} & \quad \rho_{\epsilon} \geq 0, \text{Tr}(\rho_{\epsilon}) = 1, \\ & \quad \sigma = (1 - \epsilon)\rho + \epsilon\rho_{\epsilon}, \\ & \quad \sigma \text{ is } k\text{-uniform}, \end{aligned} \tag{1.13}$$

where the optimization is carried out over the set of  $k$ -uniform density matrices  $\sigma$ , and the constraints within the optimization are either linear or semidefinite.

3. Set  $\rho = \sigma$ . Compute purity  $\text{Tr}(\rho^2)$  of the state  $\rho$ .
4. Repeat steps 2-4 until convergence of the purity  $\text{Tr}(\rho^2)$  is reached.

Generating  $N$ -partite  $k$ -uniform states is, however, may not always be an easy task. In such a case, we can sidestep this issue by generating a random  $N$ -party state instead and setting  $\epsilon = 1$  within the very first iteration. Then, from the second step, we ensure that  $\sigma$

is  $k$ -uniform. Therefore the state that is found in step 3 is also ensured to be  $k$ -uniform. It is worth mentioning that the  $P$  that is defined above is a non-decreasing function with the sequence of iterations. However, the above optimization may still get stuck in local maxima of the purity. Therefore, we may have to run the above procedure several times before obtaining global optimal solution.

### 1.3 State construction scheme

In this section we present a scheme for constructing  $k$ -uniform states from particular sets of  $N$ -qubit Pauli matrices. This scheme is comprised of the building blocks that resemble with the generators as used within the framework of stabilizer codes [58, 59]. Here, however, we do not employ stabilizer codes as such. For further convenience, if not stated otherwise, we will use the simplified notation for multi-qubit Pauli operators as

$$\sigma_0 \otimes \sigma_1 \otimes \sigma_2 \otimes \sigma_3 \otimes \cdots \equiv \mathbb{1}XYZ \dots \quad (1.14)$$

We then assume that there exists a set of  $N$ -qubit Pauli operators

$$\mathcal{G} = \{G_1, \dots, G_m\}, \quad (1.15)$$

where  $G_i$ 's are, having the form  $G_i = \sigma_{i_1} \otimes \cdots \otimes \sigma_{i_N}$ , the operators referred as the *generators* and  $m$  is the total number of such operators required to construct a target  $k$ -uniform state. The requirements to define such operators  $G_i$ 's are as follows:

- **mutual commutation:**

$$[G_i, G_j] = 0 \quad \text{for all } i \text{ and } j;$$

- **independence:**

$$G_1^{i_1} \dots G_m^{i_m} \sim \mathbb{1}_{2^N} \quad \text{only for } i_j = \cdots = i_m = 0 \quad \text{with } i_j = \{0, 1\};$$

and  $\mathbb{1}_{2^N}$  is the identity operator in  $\mathcal{H}_2^{\otimes N}$ ;

- **$k$ -uniformity:**  $G_1^{i_1} \dots G_m^{i_m}$  ( $i_j = \{0, 1\}$ ) results in  $N$ -qubit Pauli operator in Eq. (1.14) containing the identity operators on at most  $N - k - 1$  positions of the form of  $G_i$ 's that is given in Eq. (1.15).

For example, the generators constructing an 2-uniform 5-qubit state as described in

Subsec.1.5.5 have the following form,

$$\begin{aligned} G_1 &= \mathbb{1}XYXY; \\ G_2 &= \mathbb{1}ZXX\mathbb{1}; \\ G_3 &= XYY\mathbb{1}Z; \\ G_4 &= XZYZY; \\ G_5 &= ZXZ\mathbb{1}X. \end{aligned}$$

As we can see that these generators have the identity operators on at most  $(N - k - 1) = 2$  positions. Hence we can call them 2-uniform generators, and thus they are suitable for construction of a 2-uniform state.

These generators will be the key element for constructing a  $k$ -uniform state. To do so, we need to add all possible products of the elements from  $\mathcal{G}$  in the following way,

$$\rho = \frac{1}{2^N} \sum_{j_1, \dots, j_m=0}^1 G_1^{j_1} \dots G_m^{j_m}. \quad (1.16)$$

The above construction leads to a valid physical state by virtue of the following argument. Consider a set of  $m$  mutually commuting  $N$ -qubit Pauli operators  $\mathcal{G} = \{G_1, \dots, G_m\}$ . Let us rewrite the state in Eq. (1.16) into the form

$$\rho = \frac{1}{2^N} (\mathbb{1} + G_1)(\mathbb{1} + G_2) \dots (\mathbb{1} + G_m). \quad (1.17)$$

Therefore, we see that the eigenvalues of  $\rho$  can be written in the form

$$\lambda^i = \frac{1}{2^N} (1 + \lambda_1^i)(1 + \lambda_2^i) \dots (1 + \lambda_m^i), \quad (1.18)$$

where  $\lambda_j^i = \pm 1$  is the  $i$ -th eigenvalue of the  $j$ -th generator in common eigenbasis of mutually commuting operators from the set  $\mathcal{G}$ . Now from equation (1.16), we have  $\text{Tr}\rho = 1$ , while  $\lambda^i$  are either 0 or  $2^{m-N}$ , hence  $\rho$  constitutes a physical state with exactly  $m$  nonzero eigenvalues. Naturally, the case  $m = N$  corresponds to a pure state with exactly one eigenvalue equal to 1.

Now, the state in Eq. (1.16) has  $2^m$  number of non-vanishing correlations equal to  $\pm 1$  and its purity can be calculated simply as

$$\text{Tr}\rho^2 = \frac{1}{2^N} 2^m = 2^{m-N}. \quad (1.19)$$

Here, for any given  $N$ , the larger the set  $\mathcal{G}$ , i.e., larger the value of  $m$ , the higher the pu-

rity of the resulting state is. We observe that the problem of constructing  $k$ -uniform states is therefore directly related to the problem of finding the largest possible set of generators  $\mathcal{G}$ . Consequently, in the case of  $k = \lfloor \frac{N}{2} \rfloor$  and  $m = N$  the construction leads to an AME state with purity equal to 1.

Due to the construction method we expect to obtain  $k$ -uniform states of high purity. In all considered cases (up to  $N = 6$ ) we also have numerical evidence that there are no  $k$ -uniform states of higher purity. For that we have opted nonlinear optimization method which we have briefly introduced in the previous Sec. (1.2.1).

## 1.4 Orthogonal arrays

It has been established that orthogonal arrays are often useful for find  $k$ - uniform  $N$  qudit states as well as AME states [17]. But it turns out that these orthogonal arrays are also useful in order to determine the set of generators  $\mathcal{G}$ . In general, to find such a set, we have to search the full set of  $4^N$   $N$ -qubit operators. However, we observed that it is possible to construct a set of generators with the help of orthogonal arrays  $OA(r, N, l, s)$ , which significantly reduces the initial set of  $4^N$  operators.

The orthogonal arrays [22, 23] are combinatorial arrangements, tables with entries satisfying given orthogonal properties. It has several applications in the ground of error-correcting codes, difference schemes, Latin squares etc. And most importantly, orthogonal arrays are heavily used in statistics and experiment designing. An orthogonal array  $OA(r, \mathbf{N}, \mathbf{l}, s)$  is a  $r \times N$  array with entries taken from  $0, \dots, l - 1$  in such a way that each subset of  $s$  columns contains all possible combination of symbols with the same number of repetitions. The number of such repetitions is called the index of the OA; if  $l^s = r$  the orthogonal array is of index unity. An example of of OA,  $OA(16, 5, 4, 2)$  is given in (1.1).

To find  $\mathcal{G}$  for a  $k$ -uniform state of  $N$  qubits one can use an orthogonal array  $OA(r, N, 4, s)$  with 4 levels (corresponding to four different Pauli matrices). We treat each row of OA as a string of indices  $a_1 \dots a_N$  ( $a_i \in \{0, 1, 2, 3\}$ ) where each element in a string specifies a particular Pauli operator in the Hilbert space of each qubit,  $N$  in total for  $N$  subsystems. Then, we construct specific  $N$ -qubit Pauli operators of the form  $A_1 \dots A_N$  ( $A_i \in \{\mathbb{1}, X, Y, Z\}$ ) using

0	0	0	0	0
0	1	1	1	1
0	2	2	2	2
0	3	3	3	3
1	0	1	2	3
1	1	0	3	2
1	2	3	0	1
1	3	2	1	0
2	0	2	3	1
2	1	3	2	0
2	2	0	1	3
2	3	1	0	2
3	0	3	1	2
3	1	2	0	3
3	2	1	3	0
3	3	0	2	1

Table 1.1: Orthogonal arrays of strength three, symbolically OA(16,5,4,2).

the standard convention:

$$\begin{aligned}
 a_i = 0 &\rightarrow A_i = \mathbb{1}, \\
 a_i = 1 &\rightarrow A_i = X, \\
 a_i = 2 &\rightarrow A_i = Y, \\
 \text{and } a_i = 3 &\rightarrow A_i = Z.
 \end{aligned}$$

Following this we get a set of  $r$  operators, from which we have to choose the largest set  $\mathcal{G}$  such that its elements meet the conditions (1-2) from Eq. (1.15). By satisfying those conditions, we guarantee that the desired state is physical and determine its purity. The parameter  $k$  for which the property (3) from Eq. (1.15) holds does not depend explicitly on the presented construction but rather on a particular example of OA. The maximal number of  $\mathbb{1}$ 's in each row of OA equals to  $s - 1$ , which may suggest  $(N - s)$ -uniformity of obtained state. In condition (3), however, we require that the number of  $\mathbb{1}$ 's is limited not only for generators but also for all elements of the form  $G_1^{i_1} \dots G_m^{i_m}$ . In some of the presented examples (see Secs. 1.5.4, 1.5.6, 1.5.8) the number of  $\mathbb{1}$ 's is also limited by  $s - 1$  for all such elements. Hence the desired states are indeed  $(N - s)$ -uniform. In other examples, however, uniformity of the desired state is slightly smaller than the prediction from the generators. Although the states obtained from OA of index unity coincide with  $(N - s)$ -uniform states, the precise connection has to be established. In general, the relation between uniformity  $k$  and quantities  $s$  and  $N$  seems to be irregular.

It has been established in [48] that in the case of four qubits there is no 2-uniform pure

state. In other words, the AME state for 4-qubit does not exist. However, if we lift the assumption that desired state is pure, the orthogonal array  $OA(16, 4, 4, 2)$  can be utilized to construct the mixed 4-qubit 2-uniform state. It leads to the following set of operators

$$\begin{aligned}
0000 &\rightarrow \mathbb{1}\mathbb{1}\mathbb{1}\mathbb{1}, & 0111 &\rightarrow \mathbb{1}XXX, \\
0222 &\rightarrow \mathbb{1}YYY, & 0333 &\rightarrow \mathbb{1}ZZZ, \\
1012 &\rightarrow X\mathbb{1}XY, & 1103 &\rightarrow XX\mathbb{1}Z, \\
1230 &\rightarrow XYZ\mathbb{1}, & 1321 &\rightarrow XZYX, \\
2023 &\rightarrow Y\mathbb{1}YZ, & 2132 &\rightarrow YXZY, \\
2201 &\rightarrow YY\mathbb{1}X, & 2310 &\rightarrow YZX\mathbb{1}, \\
3031 &\rightarrow Z\mathbb{1}ZX, & 3120 &\rightarrow ZXY\mathbb{1}, \\
3213 &\rightarrow ZYXZ, & 3302 &\rightarrow ZZ\mathbb{1}Y.
\end{aligned} \tag{1.20}$$

Within this set we can find  $m = 3$  operators conforming to the properties from Sec. 1.3, which constitute the set  $\mathcal{G}$ , e.g.:

$$\begin{aligned}
G_1 &= \mathbb{1}YYY, \\
G_2 &= XZYX, \\
G_3 &= YXZY
\end{aligned} \tag{1.21}$$

and by virtue of Eq. (1.16), leads to the state  $\rho_4^2$  of purity  $1/2$ . This is one example of how orthogonal arrays can be utilised to efficiently construct  $k$ -uniform states.

## 1.5 Examples

In this section, we present  $k$ -uniform states with the highest possible purity for several cases of  $k$  and  $N$  that have been constructed using a unique set of generators as shown in Sec.1.3. We begin with giving a formal declaration of the "purity" constraint that we consider to construct a  $k$ -uniform state.

- An  $N$ -qubit state,  $\rho_N^k$ , is our desired  $k$ -uniform state if the following holds,

$$\begin{aligned}
\text{Tr}_{i_1 \dots i_{N-k}} \rho_N^k &= \frac{1}{d^k} \mathbb{1}_2^{\otimes k} \quad \text{for any } \{i_j\} \subset \{1, \dots, N\}, \\
\text{s.t. } \text{Tr}(\rho_N^k)^2 &= \max_{S'(\mathcal{H})} \text{Tr}(\rho^2),
\end{aligned} \tag{1.22}$$

where  $\mathcal{S}'(\mathcal{H}) \subset \mathcal{H}_2^{\otimes N}$  contains only the  $k$ -uniform states and  $\rho \in \mathcal{S}'(\mathcal{H})$ .

In the next step, we show how the generator scheme works. Let us consider that  $m$  number of generators are required to construct a particular  $N$ -qubit  $k$ -uniform state  $\rho_N^k$ . The set of generators are given by,

$$\begin{aligned} G_1 &= A_1^1 \otimes \cdots \otimes A_1^N \equiv A_1^1 \dots A_1^N; \\ &\vdots \\ G_m &= A_m^1 \otimes \cdots \otimes A_m^N \equiv A_m^1 \dots A_m^N; \end{aligned}$$

where,  $A_m^i \in \{\mathbb{1}, X, Y, Z\}$  for  $i = 0, 1, 2, 3$ . The resultant state will then be,

$$\rho_N^k = \frac{1}{2^N} \sum_{j_1, \dots, j_m=0}^1 G_1^{j_1} \dots G_m^{j_m}. \quad (1.23)$$

We now present some general schemes followed by some examples which are also present a summarized version in Fig. 1.

### 1.5.1 General schemes

As described in Sec. 1.3, the generator scheme needs to satisfy the properties (1–3). And with increasing number of parties, the verification of these properties becomes computationally demanding. However, for some particular cases, such difficulties can be overcome by employing simple schemes for the construction procedure.

1. As presented in [60, 61], protocols can be used to generate a certain  $k$ -uniform state if the other particular  $(k - 1)$ -uniform state is known. Importantly, this protocol works only when  $(k - 1)$  is even. This method allows us to eliminate all correlations between odd number of subsystems without changing the remaining even ones.

In this method, we first need to know the notion of ‘antistate’ of any given  $N$ -qubit state  $\rho_N$ ,

$$\bar{\rho}_N = \sigma_y^{\otimes N} \text{conj}(\rho_N) \sigma_y^{\otimes N}, \quad (1.24)$$

where the  $\text{conj}(\cdot)$  denotes the complex conjugation. The state  $\bar{\rho}_N$  has its  $N$ -partite correlations inverted with respect to the  $\rho_N$ .

Given the definition of the ‘antistate’, for any odd number  $N$ , if we have a state  $|\psi\rangle_N$ , then we can construct the corresponding ‘antistate’  $|\bar{\psi}\rangle_N$ . Thereafter, by evenly

mixing these two states we get,

$$\rho_\psi^{nc} = \frac{1}{2}|\psi\rangle\langle\psi|_N + \frac{1}{2}|\bar{\psi}\rangle\langle\bar{\psi}|_N. \quad (1.25)$$

Hence the state  $\rho_\psi^{nc}$  has no  $N$ -partite correlations.

To this end if we evenly mix the original state  $\rho_N^{k-1}$  with its ‘antistate’:

$$\rho_N^k = \frac{1}{2}(\rho_N^{k-1} + \bar{\rho}_N^{k-1}), \quad (1.26)$$

where  $\bar{\rho}_N^{k-1}$  is the corresponding ‘antistate’. Since  $k$  is odd for even  $k-1$ , the  $k$ -partite correlations vanish and the state becomes  $k$ -uniform.

2. We can also obtain  $k$ -uniform  $N$ -qubit states by tracing out some of the subsystems from a  $k$ -uniform state which has a higher number of parties  $N'$ , i.e.,  $N' > N$ . Given a  $N'$ -qubit  $k$ -uniform state, a  $N$ -qubit  $k$ -uniform state is given by,

$$\rho_N^k = \text{Tr}_{j_1 \dots j_{N'-N}} \rho_{N'}^k, \quad (1.27)$$

where  $j_i \in [1, N']$  with  $j_i \neq j_k$ .

By the construction of these  $k$ -uniform states, there is no correlation among  $k$  or smaller number of parties. Therefore, tracing out one or some of the subparts from a  $k$ -uniform state with a higher number of parties maintains the monotonicity of correlation. Therefore, the resultant state will be a  $k$ -uniform  $(N-1)$ -qubit state.

However, in the first method, because of taking equal mixtures, the purity of the resulting state is reduced by a half. And the same happens for the second method as the removed subsystem will be in maximally mixed state with a purity  $\frac{1}{2}$ . These methods, therefore, do not guarantee that the obtained states are of the highest possible purity.

Bellow we present several examples which are found using generator scheme.

### 1.5.2 $N$ arbitrary, $k = 1$

This is one state which can be easily found regardless of the total number of parties. The 1-uniform state is pure and is turns out to be the  $N$ -qubit GHZ state given by,

$$|\text{GHZ}\rangle_N = \frac{1}{\sqrt{2}}(|0\dots 0\rangle + |1\dots 1\rangle). \quad (1.28)$$

The largest number of generators to construct this state is

$$m = N.$$

The generators are given by,

$$\begin{aligned} G_1 &= ZX \cdots XX, & G_2 &= XZ \cdots XX, \\ & & \dots & \\ G_{N-1} &= XX \cdots ZX, & G_N &= XX \cdots XZ. \end{aligned} \quad (1.29)$$

The purity of the state is,

$$\text{Tr}\rho^2 = 2^{m-N} = 1. \quad (1.30)$$

### 1.5.3 $N$ arbitrary, $k = N - 1$

When  $k = N - 1$ , the only correlations that the state can possess are the  $N$ -partite ones. Now, having an identity operator at one of the sites equivalently means that the corresponding party is not correlated with other parties. Therefore, the generators cannot have identity operator  $\mathbb{1}$  on any position.

For  $N$  odd, it is enough to have only one generator ( $m = 1$ ) in the set  $\mathcal{G}$ :

$$G_1 = Z \cdots Z. \quad (1.31)$$

Therefore the purity of the state is,

$$\text{Tr}\rho^2 = 2^{N-m} = 2^{N-1}. \quad (1.32)$$

However, for  $N$  even, the set  $\mathcal{G}$  consists of two generators  $m = 2$ :

$$G_1 = X \cdots X, \quad G_2 = Z \cdots Z. \quad (1.33)$$

And then the purity of the state is,

$$\text{Tr}\rho^2 = 2^{N-m} = 2^{N-2}. \quad (1.34)$$

Therefore it can also be noted that the  $k$ -uniform mixed state for an even  $N$  is of higher purity than that of for an odd  $N$ .

### 1.5.4 $N = 4, k = 2$

$N = 4, k = 2$  stands for a AME state by definition. As mentioned in the introduction, such a pure state does not exist [48]. Therefore, one cannot have four generators. Hence we

look for the highest possible purity that can be attained for a 4-qubit state with 2-uniformity. The largest number of generators to construct this state is

$$m = 3.$$

the set  $\mathcal{G}$  consists of elements:

$$\begin{aligned} G_1 &= XXXX, & G_2 &= YYYY, \\ G_3 &= \mathbb{1}XYZ; \end{aligned} \quad (1.35)$$

then the purity of the state is,

$$\text{Tr}\rho^2 = 2^{N-m} = \frac{1}{2}. \quad (1.36)$$

Interestingly, this particular state can be represented as a symmetric mixture of following two pure states:

$$\begin{aligned} |\varphi_1\rangle &= \frac{1}{\sqrt{2}}\left(|\phi_1\rangle + |\phi_2\rangle\right), \\ |\varphi_2\rangle &= \frac{\sigma_x^{\otimes 4}}{\sqrt{2}}\left(|\phi_1\rangle - |\phi_2\rangle\right), \end{aligned} \quad (1.37)$$

where

$$\begin{aligned} |\phi_1\rangle &= \frac{1}{2}\left(|0010\rangle + |1110\rangle + i|1000\rangle - i|1001\rangle\right), \\ |\phi_2\rangle &= \frac{1}{2}\left(|1111\rangle - |0011\rangle + i|0100\rangle + i|0101\rangle\right), \end{aligned}$$

and the  $\sigma_x$  corresponds to a bit-flip ( $0 \iff 1$ ) operation on all particles. We investigate these states in Eq. (1.37) and determine the  $\binom{4}{2}$  number of possible 2-qubit reduced states. For  $|\varphi_1\rangle$  they are given by,

$$\begin{aligned} \text{Tr}_{12}|\varphi_1\rangle\langle\varphi_1| &= \text{Tr}_{14}|\varphi_1\rangle\langle\varphi_1| = \text{Tr}_{23}|\varphi_1\rangle\langle\varphi_1| = \text{Tr}_{34}|\varphi_1\rangle\langle\varphi_1| = \frac{1}{4}\mathbb{1}_2; \\ \text{Tr}_{13}|\varphi_1\rangle\langle\varphi_1| &= \frac{1}{4} \begin{pmatrix} 1 & -1 & 0 & 0 \\ -1 & 1 & 0 & 0 \\ 0 & 0 & 1 & 1 \\ 0 & 0 & 1 & 1 \end{pmatrix}; \\ \text{Tr}_{24}|\varphi_1\rangle\langle\varphi_1| &= \frac{1}{4} \begin{pmatrix} 1 & 1 & 0 & 0 \\ 1 & 1 & 0 & 0 \\ 0 & 0 & 1 & -1 \\ 0 & 0 & -1 & 1 \end{pmatrix}. \end{aligned}$$

For  $|\varphi_2\rangle$  they are given by,

$$\mathrm{Tr}_{12}|\varphi_2\rangle\langle\varphi_2| = \mathrm{Tr}_{13}|\varphi_2\rangle\langle\varphi_2| = \mathrm{Tr}_{24}|\varphi_2\rangle\langle\varphi_2| = \mathrm{Tr}_{34}|\varphi_2\rangle\langle\varphi_2| = \frac{1}{4}\mathbb{1}_2;$$

$$\mathrm{Tr}_{14}|\varphi_2\rangle\langle\varphi_2| = \frac{1}{4} \begin{pmatrix} 1 & -1 & 0 & 0 \\ -1 & 1 & 0 & 0 \\ 0 & 0 & 1 & 1 \\ 0 & 0 & 1 & 1 \end{pmatrix};$$

$$\mathrm{Tr}_{23}|\varphi_2\rangle\langle\varphi_2| = \frac{1}{4} \begin{pmatrix} 1 & 1 & 0 & 0 \\ 1 & 1 & 0 & 0 \\ 0 & 0 & 1 & -1 \\ 0 & 0 & -1 & 1 \end{pmatrix}.$$

As evident above, 4 out of these  $\binom{4}{2}$  times its reductions to 2 qubits turned out to be maximally mixed. This means that they almost have a similar symmetry as a 2-uniform state. It can be noted that the sum of those two matrices is proportional to  $\mathbb{1}$ , which is relevant to the fact that the mixture of  $|\varphi_1\rangle$  and  $|\varphi_2\rangle$  is 2-uniform.

### 1.5.5 $N = 5, k = 2$

The 5-qubit AME state happens to be pure [16, 47, 46] and hence the largest number of generators to construct this state is

$$m = 5.$$

The set of generators are given by,

$$\begin{aligned} G_1 &= \mathbb{1}XYXY, & G_2 &= \mathbb{1}ZXX\mathbb{1}, \\ G_3 &= XYY\mathbb{1}Z, & G_4 &= XZYZY, \\ G_5 &= ZXZ\mathbb{1}X. \end{aligned} \tag{1.38}$$

The purity of the state is,

$$\mathrm{Tr}\rho^2 = 2^{N-m} = 1. \tag{1.39}$$

The generators give  $\rho_{\frac{5}{2}}^2 = |\psi\rangle\langle\psi|_{\frac{5}{2}}^2$  where,

$$|\psi\rangle_{\frac{5}{2}} = \frac{1}{\sqrt{8}} \left( |01111\rangle + |10011\rangle + |10101\rangle + |11100\rangle + |00000\rangle + |00110\rangle + |01001\rangle + |11010\rangle \right).$$

This state is equivalent to the AME(5,2) state constructed via the link with quantum error correction codes [62].

### 1.5.6 $N = 5, k = 3$

The 5-qubit 3-uniform mixed state can be obtained from OA(16, 5, 4, 2) which is given in Tab.1.1. We took four of the rays that reproduces the state  $\rho_5^3$ . The largest number of generators to construct this state is

$$m = 4.$$

The generators are given by,

$$\begin{aligned} G_1 &= \mathbb{1}XXXX, & G_2 &= \mathbb{1}YYYY, \\ G_3 &= X\mathbb{1}XYZ, & G_4 &= Y\mathbb{1}YZX. \end{aligned} \quad (1.40)$$

The purity of the state is,

$$\text{Tr}\rho^2 = 2^{N-m} = \frac{1}{2}. \quad (1.41)$$

The corresponding state can again be represented in the form given in Eq.(1.37), i.e., symmetric mixture of the two pure states,

$$\begin{aligned} |\varphi_1\rangle &= \frac{1}{\sqrt{2}}\left(|\phi_1\rangle + |\phi_2\rangle\right), \\ |\varphi_2\rangle &= \frac{\sigma_x^{\otimes 4}}{\sqrt{2}}\left(|\phi_1\rangle - |\phi_2\rangle\right), \end{aligned} \quad (1.42)$$

with

$$\begin{aligned} |\phi_1\rangle &= \frac{1}{2}\left(|00101\rangle + |01010\rangle + i|00110\rangle + i|01001\rangle\right), \\ |\phi_2\rangle &= \frac{1}{2}\left(|10000\rangle + |11111\rangle - i|10011\rangle - i|11100\rangle\right). \end{aligned}$$

An interesting property of the state is the fact that it contains only four-qubit correlations as all the correlation matrix elements corresponding to  $r < 4$ , i.e., involving identity operation at any of the sites, are zero.

### 1.5.7 $N = 6, k = 2$

The 6-qubit 2-uniform state is a pure state and hence the largest number of generators to construct this state is

$$m = 6.$$

The generators are given by,

$$\begin{aligned} G_1 &= XXYYZZ, & G_2 &= XXZZYY, \\ G_3 &= XZZXXZ, & G_4 &= XYYX1Z, \\ G_5 &= YX1ZXY, & G_6 &= YYY11. \end{aligned} \quad (1.43)$$

The purity of the state is,

$$\text{Tr}\rho^2 = 2^{N-m} = 1. \quad (1.44)$$

This state is equivalent to the state presented in [39].

### 1.5.8 $N = 6, k = 3$

The 6-qubit AME state, again a pure state, can be obtained from OA(64, 6, 4, 3) similarly from the rays as shown for the case of  $\rho_5^3$ . The largest number of generators to construct this state is,

$$m = 6.$$

The generators are given by,

$$\begin{aligned} G_1 &= 11ZZZZ, & G_2 &= 1XYZ1X, \\ G_3 &= 1ZXY1Z, & G_4 &= XYZ1Z1, \\ G_5 &= Z1Z1XY, & G_6 &= ZYYZZY. \end{aligned} \quad (1.45)$$

The purity of the state is,

$$\text{Tr}\rho^2 = 2^{N-m} = 1. \quad (1.46)$$

The state  $\rho_6^3 = |\psi\rangle\langle\psi|_6^3$  was explicitly found where,

$$\begin{aligned} |\psi\rangle_6^3 &= \frac{1}{4} \left( |000110\rangle + |011100\rangle + |100000\rangle + |111010\rangle \right. \\ &\quad - |001001\rangle - |010011\rangle - |101111\rangle - |110101\rangle \\ &\quad + i|000101\rangle + i|010000\rangle + i|101100\rangle + i|111001\rangle \\ &\quad \left. - i|001010\rangle - i|011111\rangle - i|100011\rangle - i|110110\rangle \right). \end{aligned}$$

This state is equivalent to the one found in [17].

### 1.5.9 $N = 6, k = 4$

The 4-uniform 6-qubit is a mixed state and the largest number of generators to construct this state is,

$$m = 3.$$

The generators are given by,

$$\begin{aligned} G_1 &= \mathbb{1}XXXXX, & G_2 &= Y\mathbb{1}YYYY, \\ G_3 &= ZZ\mathbb{1}XYZ. \end{aligned}$$

The purity of the state is,

$$\mathrm{Tr}\rho^2 = 2^{N-m} = \frac{1}{8}. \quad (1.47)$$

### 1.5.10 $N = 7, k = 2$

The 2-uniform 7-qubit is a pure state and hence the largest number of generators to construct this state is,

$$m = 7.$$

The generators are given by,

$$\begin{aligned} G_1 &= \mathbb{1}XXYYZZ, & G_2 &= \mathbb{1}Z\mathbb{1}\mathbb{1}Z\mathbb{1}Z, \\ G_3 &= XXZXZZX, & G_4 &= YYZYZZY, \\ G_5 &= \mathbb{1}\mathbb{1}ZXYYX, & G_6 &= \mathbb{1}YY\mathbb{1}\mathbb{1}YY, \\ G_7 &= Z\mathbb{1}Z\mathbb{1}Z\mathbb{1}Z, \end{aligned} \quad (1.48)$$

The purity of the state is,

$$\mathrm{Tr}\rho^2 = 2^{N-m} = 1. \quad (1.49)$$

The state of the following form [39]:

$$\begin{aligned} |\psi\rangle_7^2 &= \frac{1}{\sqrt{8}} \left( |0000000\rangle + |0110011\rangle + |1011010\rangle + |1101001\rangle \right. \\ &\quad \left. - |1111111\rangle - |0111100\rangle - |1010101\rangle - |1100110\rangle \right). \end{aligned}$$

### 1.5.11 $N = 7, k = 3$

The 3 uniform 7 qubit state is another AME state which does not exist [49]. Therefore we cannot specify 7 generators to construct the state. Here, however, we can employ the scheme for eliminating all the correlations of the rank given by even number. Therefore, using the 7-qubit 2-uniform state  $\rho_7^2$  mentioned in the previous section, we can construct 7-qubit 3-uniform mixed state  $\rho_7^3$  which indeed is the highest possible purity that can be attained in this case. The largest number of generators to construct this state is,

$$m = 6.$$

The generators are given by,

$$\begin{aligned} G_1 &= Y\mathbb{1}YXZZXZ, & G_2 &= \mathbb{1}XXYYZZ, \\ G_3 &= ZXYYXZ\mathbb{1}, & G_4 &= ZZ\mathbb{1}YXXY, \\ G_5 &= YY\mathbb{1}Y\mathbb{1}Y, & G_6 &= ZXYZ\mathbb{1}YX. \end{aligned} \quad (1.50)$$

And the purity of the state is,

$$\mathrm{Tr}\rho^2 = 2^{N-m} = \frac{1}{2}. \quad (1.51)$$

### 1.5.12 $N = 7, k = 5$

The 7-qubit 5-uniform mixed state and the largest number of generators to construct this state is,

$$m = 3.$$

The generators are given by,

$$\begin{aligned} G_1 &= \mathbb{1}XXXXXX, & G_2 &= X\mathbb{1}XYYYY, \\ G_3 &= YYY\mathbb{1}XYZ. \end{aligned}$$

The purity of the state is,

$$\mathrm{Tr}\rho^2 = 2^{N-m} = \frac{1}{16}. \quad (1.52)$$

### 1.5.13 $N > 7, k = N - 2$

For 7-qubit and  $k = N - 2$  case, only  $(N - 1)$ -partite correlations are possible. Therefore, the generators will have the identity operator  $\mathbb{1}$  on at most one position. For either the case of  $N$  being even or odd, at least two generators can be found. Therefore the largest number of generators to construct these states is,

$$m = 2.$$

For  $N$  odd, the generators are given by,

$$G_1 = \mathbb{1}X \cdots X, \quad G_2 = \mathbb{1}Y \cdots Y, \quad (1.53)$$

For  $N$  even, the generators are given by,

$$G_1 = \mathbb{1}X \cdots X, \quad G_2 = X\mathbb{1}Y \cdots Y. \quad (1.54)$$

The purity of the state is,

$$\text{Tr}\rho^2 = 2^{N-m} = \frac{1}{2^{N-2}}. \quad (1.55)$$

#### 1.5.14 $N = 9, k = 5$

The 9-qubit 5-uniform mixed state can also be obtained from OA(32, 9, 4, 2). The largest number of generators to construct this state that are derived from the rays of the corresponding OA is,

$$m = 4.$$

The generators are given by,

$$\begin{aligned} G_1 &= XXXXXXXX1, & G_2 &= YYYYYYYY1, \\ G_3 &= 1XYZ1XYZ, & G_4 &= 11ZZYYXX1. \end{aligned} \quad (1.56)$$

The purity of the state is,

$$\text{Tr}\rho^2 = 2^{N-m} = \frac{1}{32}. \quad (1.57)$$

#### 1.5.15 $N = 12, k = 5$

Another example that was found by investigating an orthogonal array (OA(4096,12,4,5)) is the 12-qubit 5-uniform state  $\rho_{12}^5$  and the largest number of generators to construct this state is,

$$m = 6.$$

The generators are given by,

$$\begin{aligned} G_1 &= XYY1ZZX11111, \\ G_2 &= YZZ1XXY11111, \\ G_3 &= 1XYY1ZZX1111, \\ G_4 &= 1YZZ1XXY1111, \\ G_5 &= XXXXXXXXXXXXX, \\ G_6 &= YYYYYYYYYYYY. \end{aligned} \quad (1.58)$$

The purity of the state is,

$$\text{Tr}\rho^2 = 2^{N-m} = \frac{1}{64}. \quad (1.59)$$

$k \backslash N$	4	5	6	7	8	9
1	1	1	1	1	1	1
2	$\frac{1}{2}$	1	1	1		
3	$\frac{1}{2^2}$	$\frac{1}{2}$	1	$\frac{1}{2}$		
4		$\frac{1}{2^4}$	$\frac{1}{2^3}$			
5			$\frac{1}{2^4}$	$\frac{1}{2^4}$		$\frac{1}{2^5}$
6				$\frac{1}{2^6}$	$\frac{1}{2^6}$	
7					$\frac{1}{2^6}$	$\frac{1}{2^7}$
8						$\frac{1}{2^8}$

Figure 1.1: The purity of the states presented in Sec. 1.5. States that can be obtained by one of two general procedures described in Sec. 1.5.1 are indicated by horizontal (i) and vertical (ii) arrows. The red boxes corresponds to the pure states and shade of blue darkens with increasing purity.

## 1.6 Characteristics of $k$ -uniform states

### 1.6.1 Genuine multipartite entanglement

The characterization and detection of genuine multipartite entanglement in many-body systems has been one of the most important questions in the field of quantum information. It has relevance in several grounds such as superconducting qubits, optical lattices etc besides being considered as a resource in order to implement information theoretical tasks such as measurement based quantum computation [63] or high-precision metrology [64]. Therefore it is only relevant to investigate what is the characteristic nature of our  $k$ -uniform  $N$ -qubit states with respect to genuine  $N$ -partite entanglement.

We calculate an entanglement monotone  $W$  for the states given in Ref. [65] to witness genuine  $N$ -partite entanglement.  $W$  is an *entanglement witness* which yields a non-negative value if the state is biseparable and is negative for at least one entangled state. In multipartite scenario ( $N > 2$ ), such a witness is called *fully decomposable*,

$$\forall M : W = P_M + Q_M^{T_M}, \quad (1.60)$$

where  $M$  is the subset of all systems for which it is decomposable with respect to a bipartition between  $M$  and its complement  $\bar{M}$ .  $P$  and  $Q_M$  are positive semidefinite, ( $P, Q \geq 0$ ) and  $T_M$  is the partial transpose with respect to  $M$ .

$W$  is positive on all PPT mixtures. Nonzero value of  $W$  indicates genuine multipartite entanglement for the considered state. The convex optimization method SDP was used to optimize over all fully decomposable witnesses where for a multipartite state  $\rho$ ,

$$\begin{aligned} & \min \text{Tr}(W\rho) \\ & \text{s.t. } \text{Tr}(W) = 1 \end{aligned} \quad (1.61)$$

$$\forall M : W = P_M + Q_M^{T_M}, P_M \geq 0, Q_M \geq 0. \quad (1.62)$$

By employing this technique for the  $k$ -uniform  $N$ -qubit states, we find that most of the studied states exhibit genuine multipartite entanglement. The values of  $W$  for considered states are presented in Tab. 1.2.

For 7-qubit  $k$ -uniform states with  $k = 1, 2$ , and 3, we derive the witnesses using the method designed for the stabilizer states shown in [59, 58]. The witnesses have the following form,

$$W_7^k = \alpha_7^k - \rho_7^k, \quad (1.63)$$

$N$	$k$	$W$
2	1	0.5
3	1	0.5
	2	0
4	1	0.5
	2	0.5
	3	0
5	1	0.5
	2	0.5
	3	0.5
	4	0

Table 1.2:  $W$  - witness genuine multipartite entanglement (GME) for  $k$ -uniform  $N$ -qubit states

where  $\alpha_7^1 = \alpha_7^2 = 1/2$  and  $\alpha_7^3 = 1/4$ . And for all considered  $k$ , the states turn out to possess genuine multipartite entanglement.

### 1.6.2 Fisher information

Quantum fisher information is one of the most important concept in theoretical quantum metrology as it plays significant role in parameter estimation and therefore is useful in understanding the non-classical nature of a physical state. Below we investigate quantum fisher information for the  $k$ -uniform  $N$ -qubit states.

Let us first consider a  $N$ -qubit Hamiltonian that allows observers to perform a different evolution on each particle. The local evolutions are generated by the operators

$$\sigma_{\vec{n}}^{(j)} = \vec{n}^{(j)} \cdot \vec{\sigma}^{(j)} \quad (j = 1, \dots, N), \quad (1.64)$$

where  $\vec{n} \in \mathbb{R}^3$  and  $\vec{\sigma} = (\sigma_1, \sigma_2, \sigma_3)$ . The Hamiltonian takes the form

$$\mathbb{H} = \frac{1}{2} \sum_j \sigma_{\vec{n}_j}^{(j)}, \quad (1.65)$$

which is a generalization of a standard collective Hamiltonian for which  $\sigma_{\vec{n}_j}^{(j)} = \sigma_{\vec{n}}^{(j)}$  for all  $j$ .

For a pure state  $\rho = |\psi\rangle\langle\psi|$ , the quantum Fisher information [66] can be easily calculated as the variance of the Hamiltonian,

$$F(\rho, \mathbb{H}) = 4\text{Tr}((\Delta\mathbb{H})^2\rho). \quad (1.66)$$

The square of the Hamiltonian is given by

$$\mathbb{H}^2 = \frac{N}{4} + \frac{1}{2} \sum_{i < j} \sigma_{\vec{n}}^{(i)} \sigma_{\vec{m}}^{(j)}. \quad (1.67)$$

Therefore the quantum Fisher information can be expressed in terms of correlation tensor elements in the following way (see [67] for comparison with a collective case):

$$\begin{aligned} F(\rho, \mathbb{H}) &= 4\{\text{Tr}(\mathbb{H}^2 \rho) - (\text{Tr}(\mathbb{H} \rho))^2\} \\ &= N + 2(T_{n_1 n_2 0 \dots 0} + T_{n_1 0 n_3 0 \dots 0} + \dots + T_{0 \dots 0 n_{N-1} n_N}) \\ &\quad - (T_{n_1 0 \dots 0} + T_{0 n_2 0 \dots 0} + \dots + T_{0 \dots 0 n_N})^2 \end{aligned} \quad (1.68)$$

Since for  $k$ -uniform states (with  $k \geq 2$ ) all two- and single-qubit correlation tensor elements vanish, the quantum Fisher information,

$$F(\rho_N^{k \geq 2}, \mathbb{H}) = N. \quad (1.69)$$

Therefore it depends only on the number of qubits. Hence the quantum Fisher information in Eq.(1.69) does not depend on a particular choice of the vectors  $\vec{n}_j$ . This implies that the quantum Fisher information  $F_{avg}$  averaged over all directions  $\vec{n}$  is also equal to  $N$ . As for all product states  $F_{avg} < 2N/3$  [68, 69], this fact verifies that the states  $\rho_N^{k \geq 2}$  always have some entanglement present.

However, the situation for mixed states is more complicated. For a mixed state of the form,

$$\rho = \sum_k p_k |\psi_k\rangle \langle \psi_k| = \sum_k p_k \rho_k, \quad (1.70)$$

the quantum fisher information has the form given by

$$F(\rho, \mathbb{H}) = 4 \inf_{\{p_k, |\psi_k\rangle\}} \sum_k p_k \text{Tr}((\Delta \mathbb{H})^2 \rho_k), \quad (1.71)$$

where the infimum is over all decompositions of the density matrix. Therefore, in the case of mixed states, Eq. (1.69) provides only an upper bound on the quantum Fisher information. In general it can now be a function of higher order correlations. In spite of this, in several cases of mixed states we observe similar behavior as for pure states that have been presented in Tab. 1.3.

### 1.6.3 Violation of Bell inequality

We investigated considered families of  $k$ -uniform states (up to 7 qubits) with a numerical method based on linear programming [70]. The method allows us to reveal non-

$N$	$k$	$F$
2	1	$F_x = 4, F_y = 0, F_z = 4$
3	1	$F_x = 3, F_y = 3, F_z = 9$
	2	$F_x = 0, F_y = 3, F_z = 3$
4	1	$F_x = 4, F_y = 4, F_z = 16$
	2	$F_x = F_y = F_z = 4$
	3	$F_x = F_y = F_z = 4$
5	1	$F_x = F_y = F_z = 25$
	2	$F_x = F_y = F_z = 5$
	3	$F_x = 5, F_y = 4, F_z = 5$
	4	$F_x = 0, F_y = 5, F_z = 5$
6	1	$F_x = 6, F_y = 6, F_z = 36$
	2	$F_x = F_y = F_z = 6$
	3	$F_x = F_y = F_z = 6$
	4	$F_x = 1, F_y = 6, F_z = 5$
	5	$F_x = F_y = F_z = 6$
7	1	$F_x = 7, F_y = 7, F_z = 49$
	2	$F_x = F_y = F_z = 7$
	3	$F_x = F_y = F_z = 7$

Table 1.3:  $F$  - quantum Fisher information,  $F_i = F(\rho, J_i)$ , where  $J_i$  is the collective angular momentum operator of  $k$ -uniform  $N$ -qubit states given in Sec. 1.5.

classicality even without direct knowledge of Bell's inequalities which can be satisfied by local realistic models, but violated by some quantum predictions for the given problem. But in the discussed method we calculate the minimal admixture of white noise that is necessary for the quantum correlations to vanish  $f_{crit}$  and the probability of violation of local realism  $p_v$  for randomly sampled settings [71] for a given state.  $f_{crit}$  is the critical visibility of a quantum state. It can be realised in the following way.

With the given  $N$ -qubit quantum state  $\rho$ , we mix some amount of white noise. The density matrix obtained by such a process is given by

$$\rho(f) = f\rho + (1-f)\frac{1}{2^N}\mathbb{1}^{\otimes N}, \quad (1.72)$$

where  $f$  is the visibility of the state.  $f = 0$  implies that a local realistic model exists whereas  $f = 1$  implies that no local realistic model can reproduce the predictions of quantum mechanics for the given state. For the states with no corresponding local realistic model, there exists a critical value  $f_{crit}$  such that for  $f \leq f_{crit}$  there exists a local realistic probability distribution for which a local realistic model can be found.

We calculate  $f_{crit}$  for each state and observe that in all non-trivial case  $f_{crit} > 0$ . This

means that a conflict with local realism is present and that can be resolved by mixing the state with white noise. The results are presented in Tab. 1.4.

$N$	$k$	$f_{crit}$
2	1	0.293
3	1	0.5
	2	0
4	1	0.647
	2	0.422
	3	0.292
5	1	0.75
	2	0.568
	3	0.460
	4	0
6	1	0.823
	2	0.666
	3	0.591
	4	0.293
	5	0.293
7	1	0.875
	2	0.785
	3	0.644

Table 1.4:  $f_{crit}$  - white noise robustness of  $k$ -uniform  $N$ -qubit states given in Sec. 1.5.

## 1.7 Quantum circuits for $k$ -uniform states

Quantum circuits have recently been designed to generate absolutely maximally entangled state [72]. Using their designs, maximally entangled states can be availed to investigate the strength of multipartite correlations in quantum computers. Therefore, we can employ a similar scheme in order to generate mixed  $k$ -uniform states.

Now we give such an example where a quantum circuit can be used to generate a 4-qubit 2-uniform state. The circuit comprises of Hadamard gate ( $H$ ), phase gate ( $S$ ), nonlocal CNOT and SWAP operations as described in Fig. 1.2. The definition of the gates and operations are as defined in Ref. [18]:

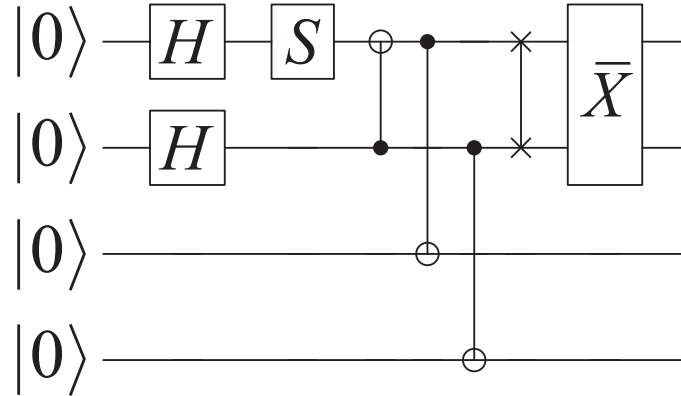


Figure 1.2: A scheme for constructing a 2-uniform 4-qubit state. The last transformation applied at random (i.e. with probability  $\frac{1}{2}$ ) outputs an equal mixture of two pure states.

$$\begin{aligned}
 H &= \frac{1}{\sqrt{2}} \begin{pmatrix} 1 & 1 \\ 1 & -1 \end{pmatrix}, \\
 S &= \begin{pmatrix} 1 & 0 \\ 0 & i \end{pmatrix},
 \end{aligned} \tag{1.73}$$

$$\begin{aligned}
 \text{CNOT} &= \begin{pmatrix} 1 & 0 & 0 & 0 \\ 0 & 1 & 0 & 0 \\ 0 & 0 & 0 & 1 \\ 0 & 0 & 1 & 0 \end{pmatrix}, \\
 \text{SWAP} &= \begin{pmatrix} 1 & 0 & 0 & 0 \\ 0 & 0 & 1 & 0 \\ 0 & 1 & 0 & 0 \\ 0 & 0 & 0 & 1 \end{pmatrix}.
 \end{aligned}$$

The output of this quantum circuit upto the SWAP operation is a pure state. However,  $\rho_4^2$  is actually a mixed state. But we know that it can be represented as a symmetric mixture of two pure states (Sec. 1.5.4). To construct the desired mixed state, we then apply one last gate on the first two bits at random. It then perform either  $\bar{X} = X \otimes X$  transformation or absolutely nothing at random. Hence, the resulting state is an equal mixture of two pure states given in Eq. (1.37) which, in turns, gives us  $\rho_4^2$ .

## 1.8 Higher dimensional $k$ -uniform states

The generalization of  $k$ -uniform states for higher dimensional subsystems is rather straightforward. We have observed that a scheme for higher dimensions can be achieved with the use of a specific set of generators. Here, instead of  $N$ -qubit Pauli operators  $G_i$ , we use  $N$ -qudit operators referred as  $G_i^{(d)}$  that are composed of  $d$ -dimensional Weyl-Heisenberg matrices given by

$$S_{kl}^{(d)} = (X^{(d)})^k (Z^{(d)})^l, \quad (1.74)$$

where,

$$X^{(d)} = \sum_{i=0}^{d-1} |i\rangle\langle i+1|; \quad (1.75)$$

$$Z^{(d)} = \sum_{i=0}^{d-1} \omega^i |i\rangle\langle i|, \quad (1.76)$$

with  $\omega = e^{2i\pi/d}$  and  $k, l = 0, \dots, d-1$ . The set of generators  $\mathcal{G}^{(d)}$  must also satisfy the same set of properties defined in Sec. 1.3. And the obtained  $k$ -uniform  $N$ -qudit state is given by

$$\rho = \frac{1}{d^N} \sum_{j_1, \dots, j_m=0}^{d-1} (G_1^{(d)})^{j_1} \dots (G_m^{(d)})^{j_m}. \quad (1.77)$$

By construction, this state has a purity  $d^{m-N}$ . It is worth noting that if a pure  $k$ -uniform state does not exist, the highest attainable purity for such state is  $1/d$ . And, the purity of such states are already small for  $d = 3$ .

The described scheme can be utilized to construct the so called graph states that include the 1-uniform  $N$ -qudit GHZ-type state which can be obtained from the generator scheme. In this case, the largest number of generators is given by,

$$m = N,$$

and the generators [73] are given by,

$$\begin{aligned}
G_1^{(d)} &= Z^{(d)} X^{(d)} \dots X^{(d)} X^{(d)}, \\
G_2^{(d)} &= X^{(d)} Z^{(d)} \dots X^{(d)} X^{(d)}, \\
&\vdots \\
G_{N-1}^{(d)} &= X^{(d)} X^{(d)} \dots Z^{(d)} X^{(d)}, \\
G_N^{(d)} &= X^{(d)} X^{(d)} \dots X^{(d)} Z^{(d)}.
\end{aligned} \tag{1.78}$$

Evidently, the purity of these states is 1.

For four qutrit case, on the contrary to its qubit counterpart, there exists a pure AME(4,3) state. Therefore it can be determined by  $m = 4$  number of generators and they are given by,

$$\begin{aligned}
G_1^{(3)} &= \mathbb{1}^{(3)} Z^{(3)} Z^{(3)} (Z^{(3)})^2, \\
G_2^{(3)} &= \mathbb{1}^{(3)} X^{(3)} X^{(3)} (X^{(3)})^2, \\
G_3^{(3)} &= Z^{(3)} \mathbb{1}^{(3)} Z^{(3)} Z^{(3)}, \\
G_4^{(3)} &= X^{(3)} \mathbb{1}^{(3)} X^{(3)} X^{(3)}.
\end{aligned} \tag{1.79}$$

The last example that we provide for the  $q$ -dit case is the 3-qutrit 2-uniform state. The largest number of generators to construct is state is,

$$m = 2.$$

And the generators are given by,

$$\begin{aligned}
G_1^{(3)} &= X^{(3)} X^{(3)} X^{(3)}, \\
G_2^{(3)} &= Z^{(3)} Z^{(3)} Z^{(3)}.
\end{aligned} \tag{1.80}$$

And the purity is given by,

$$\text{Tr} \rho^2 = 3^{N-m} = \frac{1}{3}. \tag{1.81}$$

Interestingly, this state can also be expressed as a symmetric mixture of the following three pure states:

$$\begin{aligned}
|\alpha_1\rangle &= \frac{1}{\sqrt{3}}(|000\rangle + |111\rangle + |222\rangle), \\
|\alpha_2\rangle &= \frac{1}{\sqrt{3}}(|021\rangle + |102\rangle + |210\rangle), \\
|\alpha_3\rangle &= \frac{1}{\sqrt{3}}(|012\rangle + |201\rangle + |120\rangle).
\end{aligned} \tag{1.82}$$

And despite of acquiring a relatively low purity  $1/3$ , this state exhibits genuine multipartite entanglement ( $W = 1$ ). Interestingly, the purity of the 3-qutrit 2-uniform state is higher than that for the corresponding qubit state (Sec.1.5.3), which is equal to  $1/4$ .

To determine the maximal purity of  $k$ -uniform qudit states, we used an iterative method based on semidefinite programming [57] that has been described briefly in Sec.1.2.2. Using this algorithm, we were able to reproduce all purity values up to  $N = 6$  parties as provided in Tab. 1.5.

We proceed further and also ran the algorithm for other states with a higher  $d(d > 2)$  values. And for the qutrit scenario, the maximal purity of a ( $N = 3, k = 2$ ) state was found to be  $1/3$  which agrees with Eq. (1.82). Whereas, for  $d = 4$ , the purity is  $1/4$ . Also, for the case ( $N = 4, k = 3, d = 3$ ), we get the purity to be  $1/9$ . In this particular case the purity seems to decay with the increase of dimension.

## 1.9 Threshold values for the number of generators

For a given number of qubits  $N$ , the number of generators  $m$  decreases while the purity of the state increases as evident in Tab. 1.5. This observation raises the natural question of threshold functions for the number of generators; in other words, what are the constraints on  $N$  and  $k$  for being able to find  $m$  generators? It turns out that the answer to this question is not straightforward and seems to be the difficult one in its full generality. However, for a small number of generators we provide an answer.

By combining Examples in Sec. 1.5.3 and Sec. 1.5.13 we get the threshold for two generators. Indeed, the number of generators  $m$  satisfies the following:

$$\begin{cases} m = 1 & \text{for } k = N - 1 \text{ and } N \text{ odd,} \\ m \geq 2 & \text{for } k > N - 1 \text{ or } N \text{ even.} \end{cases} \quad (1.83)$$

For three generators the number of generators  $m$  satisfies the following:

$$\begin{cases} m \leq 2 & \text{for } k > \frac{6}{7}N - 1, \\ m \geq 3 & \text{for } k \leq \frac{6}{7}N - 1. \end{cases} \quad (1.84)$$

For  $k = \frac{6}{7}N - 1$  there exist three generators of the following form:

$$\begin{aligned}
 G_1 &= \mathbb{1} \cdots \mathbb{1} & X \cdots X \\
 G_2 &= X \cdots X & \mathbb{1} \cdots \mathbb{1} & X \cdots X & Y \cdots Y & Y \cdots Y & Y \cdots Y & Y \cdots Y \\
 G_3 &= \underbrace{Y \cdots Y}_s & \underbrace{Y \cdots Y}_s & \underbrace{Y \cdots Y}_s & \underbrace{\mathbb{1} \cdots \mathbb{1}}_s & \underbrace{X \cdots X}_s & \underbrace{Y \cdots Y}_s & \underbrace{Z \cdots Z}_s
 \end{aligned} \tag{1.85}$$

where  $s = N - k - 1$  is equal to the maximal number of  $\mathbb{1}$ 's in each non-trivial element of  $\mathcal{G}$ . For  $k < \frac{6}{7}N - 1$  and  $N$  being odd, it is sufficient to remove the relevant number of last elements in Eq. (1.85). For even  $N$ , it is sufficient to remove the relevant number of last elements from the following generators:

$$\begin{aligned}
 G_1 &= \mathbb{1}XX & \mathbb{1} \cdots \mathbb{1} & X \cdots X \\
 G_2 &= Y\mathbb{1}Y & X \cdots X & \mathbb{1} \cdots \mathbb{1} & X \cdots X & Y \cdots Y & Y \cdots Y & Y \cdots Y \\
 G_3 &= ZZ\mathbb{1} & \underbrace{Y \cdots Y}_{s-1} & \underbrace{Y \cdots Y}_{s-1} & \underbrace{Y \cdots Y}_{s-1} & \underbrace{\mathbb{1} \cdots \mathbb{1}}_{s-1} & \underbrace{X \cdots X}_s & \underbrace{Y \cdots Y}_s & \underbrace{Z \cdots Z}_s.
 \end{aligned} \tag{1.86}$$

$N$	$k$	purity	$W$	$M$	$F$	$f_{crit}$	$p_v(\%)$
2	1	1	0.5	$M_2 = 3$	$F_x = 4, F_y = 0, F_z = 4$	0.293	28.32
3	1	1	0.5	$M_3 = 4, M_2 = 3$	$F_x = 3, F_y = 3, F_z = 9$	0.5	74.69
	2	1/4	0	$M_3 = 1$	$F_x = 0, F_y = 3, F_z = 3$	0	0
4	1	1	0.5	$M_4 = 9, M_2 = 6$	$F_x = 4, F_y = 4, F_z = 16$	0.647	94.24
	2	1/2	0.5	$M_4 = 3, M_3 = 4$	$F_x = F_y = F_z = 4$	0.422	35.11
	3	1/4	0	$M_4 = 3$	$F_x = F_y = F_z = 4$	0.292	0.024
5	1	1	0.5	$M_5 = 16, M_4 = 5, M_3 = 10$	$F_x = F_y = F_z = 25$	0.75	99.60
	2	1	0.5	$M_5 = 6, M_4 = 15, M_3 = 10$	$F_x = F_y = F_z = 5$	0.568	99.96
	3	1/2	0.5	$M_4 = 15$	$F_x = 5, F_y = 4, F_z = 5$	0.460	63.65
	4	1/16	0	$M_5 = 1$	$F_x = 0, F_y = 5, F_z = 5$	0	0
6	1	1		$M_6 = 33, M_4 = 15, M_2 = 15$	$F_x = 6, F_y = 6, F_z = 36$	0.823	99.97
	2	1		$M_6 = 10, M_5 = 24, M_4 = 21, M_3 = 8$	$F_x = F_y = F_z = 6$	0.666	> 99.99
	3	1		$M_6 = 18, M_4 = 45$	$F_x = F_y = F_z = 6$	0.591	100
	4	1/16		$M_6 = 1, M_5 = 2$	$F_x = 1, F_y = 6, F_z = 5$	0.293	< $10^{-3}$
	5	1/16		$M_6 = 3$	$F_x = F_y = F_z = 6$	0.293	< $10^{-6}$
7	1	1		$M_7 = 64, M_6 = 7, M_4 = 35, M_2 = 21$	$F_x = 7, F_y = 7, F_z = 49$	0.875	100
	2	1		$M_7 = 15, M_6 = 42, M_5 = 42, M_4 = 21, M_3 = 7$	$F_x = F_y = F_z = 7$	0.785	100
	3	1/2		$M_6 = 42, M_4 = 21$	$F_x = F_y = F_z = 7$	0.644	99.16

Table 1.5:  $k$ -uniform  $N$ -qubit states as defined in in Sec. 1.5: purity,  $W$  is a genuine multipartite entanglement monotone,  $M$  is the length of correlations,  $F$  is the quantum Fisher information,  $F_i = F(\rho, J_i)$ , where  $J_i$  is the collective angular momentum operator,  $f_{crit}$  is the white noise robustness, and  $p_v$  is the probability of violation of local realism.

## 1.10 Conclusions

In this chapter, we have discussed several aspects of  $k$ -uniform states of  $N$  qubits, for which it is known that the corresponding absolutely maximally entangled pure states do not exist. We find the  $k$ -uniform  $N$ -qubit states that are the  $N$ -qubit states with highest possible purity such that all its reduction to  $k$  subsystems become maximally mixed. The  $k$ -uniform states are distinguished by revealing the highest multipartite correlations among all quantum states of the same purity.

We present a general scheme to find such states which utilizes generators constructed using  $N$ -qubit Pauli operators to construct the  $k$ -uniform mixed states for this system. We provided several examples upto 6 qubits in the support of our scheme. Furthermore, we numerically verified that the states that are found using this generator scheme are indeed of the highest possible purity for that particular number of subsystems.

We also showed that particular mixed  $k$ -uniform states can be constructed with the help of orthogonal arrays, but in different way from the known scheme of utilizing the notion of OA for constructing pure AME states: in the case of mixed states the key role is played by the correlation tensor elements instead of ket vectors of the pure AME state itself. We investigated several characteristics of these states which provide strong evidence of non-classicality. We provided an example of quantum circuit that can be utilized to find such states. We also discussed the range of our scheme in higher dimensional systems. In this regard, we discussed some instances of  $k$ -uniform states of 3- and 4-qudit systems. Here, however, we observed that the dimensionality of the total system rises much faster with the number of qudits making the numerical analysis ineffective for high dimensions.

# Cooperation and dependencies in multipartite systems

Correlations are among the most elementary notions across all science. In recent years, the notion quantum correlation has emerged as topic of central importance, especially in the field of quantum information. In literature, several measures of correlation exist for bipartite systems among which many carry an operational meaning. The same ground remains relatively unexplored in the multipartite setting due to the complexity it yields, a consequence of the unclear notion of multipartite correlations. Natural postulates were formulated in Ref. [15, 24] in order to characterise the measures of genuinely multipartite correlations for both classical and quantum scenario. Attempts were made to resolve this postulates in terms of formulating correlation measures. But it was shown that to-date quantifiers have not been entirely successful in this matter. In this work, we attempt to address this problem at least partially and propose a quantifier which emerges from an operational standpoint, and quantify a certain notion of dependencies, even though it is not a measure of multipartite correlations par se.

In this chapter we introduce an quantifier that identifies and quantifies the mutual dependencies between distinct subsystems in multipartite systems. This quantifier, labeled as *multipartite dependence*, highlights the complex nature of multipartite systems from a different prospective.

Similar problem of dependence has been previously addressed by several communities, considering it for both classical and quantum systems. Among them a few are notable such as neuroscience and genetics where measures of multipartite synergy were put forward [74, 75, 76, 77, 78, 79]. Quantifiers of coordination were introduced in the field of quantitative sociology. In [80] an information-theoretic approach was taken in order to

model coordination in human-human interaction and also to measure coordination flows in a remote collaborative tracking task. The notion of redundancy was introduced in the generalized information theory to multiple variables in complex systems [81] in order to quantify the information that a set of sources can possess concerning a variable. Redundancy therefore quantifies the information that is encoded in a source concerning each possible outcome of a given variable, averaged over all possible outcomes.

In physics and information processing quantities aimed at characterizing genuine multiparty correlations were studied in depth [82, 83, 84, 15, 85, 24]. All these former quantifiers motivated mathematically, keeping the combinatorial aspects of complex systems in mind, e.g., the synergy is the difference in the information all subsystems have about an additional system as compared to the total information contained in any subset of the systems. In [82] a genuine multiparty correlation measure was introduced that can be used for a multiparty quantum system as the trace norm of the cumulant of the state. The multipartite measure was proven to be legitimate as satisfies the five basic conditions required for a correlation measure [86]. In [83] the author proposed a multipartite correlation measure that is able to obtain the degrees of irreducible multiparty correlations for the multipartite states without maximal rank. In [84] the authors show that genuine multiparty quantum correlations can exist in the systems where no genuine multiparty classical correlations was detected and proved it to be true even in macroscopic systems.

Three postulates for measures of genuine multipartite correlations were proposed in [15]. Many of these previously introduced quantifiers involve difficult optimizations and are therefore hard to compute. For example, in [15], in order to compute the extractable work used to define genuinely multipartite correlations one has to optimise over all protocols with local unitary operations, local dephasings and classical communication, which does not admit any computer-friendly parameterisation.

In this chapter, we introduce a quantity named *multipartite dependence* which is operationally defined, simple and easier to compute. It is defined in terms of information gain from cooperation when some of the parties cooperate with each other in order to gain information about some variables concerning to parties that are not involved. We also show that this quantifier fulfills several criteria for being a genuine multipartite correlation measure, which makes it a significant candidate in the ground of investigating and understanding multipartite systems. To compute multipartite dependence,  $\mathcal{D}_N$ , it is based on the consideration of the conditional mutual information between only two subsystems. With this regard, it is important to mention that the conditional mutual information is already a well established quantity in quantum information theory and broader physics and has numerous application in the field of quantum information and communications. For

example, in [87, 88, 89, 90], conditional mutual information has been used to capture the communication cost of quantum state redistribution. Importantly, it was proven in [90] that conditional mutual information provides an upper bound on the regularized relative entropy distance between a quantum state and its reconstructed version and in [88] an optimal “quantum state redistribution” protocol was introduced as the first ever operational interpretation to quantum conditional mutual information that quantifies the correlation between two parties from the prospective of a third party. In [91], the author used the structure of conditionally independent states to present a perturbative analysis of the stability of topological entanglement entropy [92, 93, 94] which was achieved by using conditional mutual information intuitively. An entanglement monotone was introduced in [95] for bipartite quantum states which is called squashed entanglement and was produced using the halved minimum quantum conditional mutual information over all tripartite state extensions. Multipartite dependence, however, present a completely different utilization of conditional mutual information.

Our quantifier is somewhat related to some other quantifiers. For example, a task conditional quantum one-time pad was introduced in [96] where it has been proved that the optimal rate of secret communication for the aforementioned task is equal to the conditional quantum mutual information. Similar quantifiers in this context are quantum discord [97, 98], intrinsic steerability [99], conditional erasure cost of a tripartite state [100, 101]. The quantity dependence that has been introduced here is a relevant quantity in all these problems if we symmetrize them and look for the worst case scenario.

## 2.1 Definition of multipartite Dependence

Let us first introduce the most common way to represent statistical independence, i.e., in terms of probabilities. Two classical variables  $\alpha_1$  and  $\alpha_2$  are statistically independent if their probabilities satisfy the following:

$$P(\alpha_1|\alpha_2) = P(\alpha_1), \quad \text{and} \quad (2.1)$$

$$P(\alpha_2|\alpha_1) = P(\alpha_2). \quad (2.2)$$

Alternatively, the statistical independence can also be defined using entropies.

When two classical variables  $\alpha_1$  and  $\alpha_2$  are dependent of each other, then mutual information quantifies the entropic difference of these two variables  $\alpha_1$  and  $\alpha_2$  [102] and hence can act as a measure of dependence among them.

$$I(\alpha_1 : \alpha_2) = H(\alpha_1) - H(\alpha_1|\alpha_2), \quad (2.3)$$

where  $H(\alpha)$  is the Shannon entropy and  $H(\alpha|\beta)$  is called the conditional entropy. Note that in this chapter, we take the logarithms that are used in defining these entropies considered to be of base  $d$ .

Similarly, for quantum subsystems as well where we use quantum mutual information [103] and  $\alpha$  and  $\beta$  represent the states of their respective subsystems of a given bipartite state  $\rho \equiv \rho^{\alpha\beta} =: \alpha\beta$ . By performing partial trace. The quantum mutual information is given by,

$$I(\alpha : \beta) = S(\alpha)_\rho - S(\alpha|\beta)_\rho, \quad (2.4)$$

where  $S(\rho)$  is called the von Neumann entropy and  $S(\alpha|\beta)$  is the conditional von Neumann entropy,

### 2.1.1 Tripartite dependence

While the two-variable case is pretty straight forward, complexity tends to increase with the increasing number of variables as they offer different levels of independence. For the three-variable case,  $\{X_1, X_2, X_3\}$ , provides us with two levels of independence. Firstly, the one of the variable, say  $X_1$ , can be completely independent, i.e.,

$$P(X_1|X_2X_3) = P(X_1). \quad (2.5)$$

The second option is that it is conditionally independent of one of the remaining variables, e.g.,

$$P(X_1|X_2X_3) = P(X_1|X_2). \quad (2.6)$$

The first kind of dependence can again be quantified using the mutual information  $I(X_1 : X_2X_3)$ . The latter, however, can be found by calculating the conditional mutual information.

$$I(X_1 : X_3|X_2) = H(X_1|X_2) - H(X_1|X_2X_3) \quad (2.7a)$$

$$= I(X_1 : X_2X_3) - I(X_1 : X_2). \quad (2.7b)$$

$I(X_1 : X_3|X_2)$  quantifies the difference between the information that is accessible about  $X_1$  when  $X_2$  and  $X_3$  considered together vs  $X_2$  alone. Therefore, it operationally quantity the amount of information that can be acquired by exchanging information, in other words, by cooperation among the remaining parties. More generally, a variable may also be dependent on all other variables and it is possible that different parties cooperate with each other in different degree. Hence the corresponding conditional mutual informations can differ from one another. In the case where each of these conditional mutual informations has a nonzero value, the probability distribution or the global state admits mutual dependencies

in all possible “cuts”. Then the lowest conditional mutual information value corresponds to the minimum dependence present in the system. Therefore, in the tripartite scenario, we define a *tripartite dependence* which can be quantified as the worst case conditional mutual information,

$$\mathcal{D}_3 \equiv \min[I(X_1 : X_2|X_3), I(X_1 : X_3|X_2), I(X_2 : X_3|X_1)]. \quad (2.8)$$

$\mathcal{D}_3$  expresses the least gain in information about the first subsystem that the second party can additionally acquire from *cooperating* with the third party. For example, in Tab.2.3, we have calculated tripartite dependence of the probability distributions  $\{P_{\text{same}}\}$ ,  $\{P_{\text{odd}}\}$  and states such GHZ and W. We will mention different examples through out the chapter in order to demonstrate different characteristics of this new quantifier.

Strong subadditivity [18] indicates that the conditional mutual information is non-negative. Hence,

$$\mathcal{D}_3 \geq 0. \quad (2.9)$$

The value of  $\mathcal{D}_3$  for a system can easily be calculated from either of the relations mentioned above Eq.(2.7). This above condition is also true for any variable that is not correlated with the rest of the system. The equality holds if and only if there exists a variable such that already a subset of the remaining parties contains all available information about it. For example, we assume that  $\mathcal{D}_3 = 0$  and the conditional mutual information corresponding to which it vanishes is  $I(X_1 : X_2|X_3)$ . Then, by definition, we have

$$\begin{aligned} I(X_1 : X_2|X_3) &= I(X_1 : X_2X_3) - I(X_1 : X_2) = 0 \\ \implies I(X_1 : X_2X_3) &= I(X_1 : X_2) \end{aligned} \quad (2.10)$$

Eq. (2.10) means that all accessible information about  $X_1$  is already available to  $X_2$  without any cooperation from  $X_3$ . On the other hand, if  $\mathcal{D}_3$  is positive then any two parties always gain through cooperation when accessing the knowledge about the remaining subsystem and  $\mathcal{D}_3$  gives us the minimal gain over the choice of parties.

For example, we here present  $\mathcal{D}_3$  of following classical probability distributions:

We take an equal mixture of three correlated binary random variables described by joint probability distribution,  $\{P_{\text{same}}\}$ , given by,

$$\begin{aligned} p(000) &= \frac{1}{2} \\ p(111) &= \frac{1}{2}. \end{aligned}$$

For this probability distribution, we have,

$$I(X_i : X_j | X_k) = H(X_i | X_k) - H(X_i | X_j X_k) = 0 \quad (2.11)$$

Therefore, this distribution admits  $\mathcal{D}_3 = 0$ . One should note that, all the variables here are however correlated with each other as for a given instance, if the first party's outcome is 0 (1), then the remaining parties must also produce the outcome 0(1).

Another interesting example in this context is  $\{P_{\text{even}}\}$  which corresponds to the following joint probability distribution:

$$\begin{aligned} p(000) &= \frac{1}{4} \\ p(001) &= 0 \\ p(010) &= 0 \\ p(011) &= \frac{1}{4} \\ p(100) &= 0 \\ p(101) &= \frac{1}{4} \\ p(110) &= \frac{1}{4} \\ p(111) &= 0. \end{aligned}$$

In this case, we have,

$$I(X_i : X_j | X_k) = H(X_i | X_k) - H(X_i | X_j X_k) = 1 \quad (2.12)$$

Therefore, we have  $\mathcal{D}_3 = 1$ . These examples will be important later in Subsec. 2.2.3.

### 2.1.2 Multipartite dependence ( $N > 3$ )

With increasing number of parties the conditions that needs to be considered increases. For example, in the case of four-partite scenario,  $\{X_1, X_2, X_3, X_4\}$ , we have three levels of dependence. Firstly, say,  $X_1$  can be independent of any other variables. Then  $P(X_1 | X_2, X_3, X_4) = P(X_1)$ . Next,  $X_1$  can be dependent to only one of the remaining variable, say  $X_2$ , giving  $P(X_1 | X_2, X_3, X_4) = P(X_1 | X_2)$ . Dependence can then stretch to two of the remaining parties, say  $X_2$  and  $X_3$ , yielding  $P(X_1 | X_2, X_3, X_4) = P(X_1 | X_2, X_3)$ . And finally,  $X_1$  can depend on all the remaining parties. In each case, the gain from cooperation can be quantified in terms of the respective mutual information. Therefore, the four-partite dependence, in analogy to the tripartite case, will then be the least information gained by cooperation among any three parties about the remaining party. Obviously, the four-partite dependence must be greater than any other kind of cooperation among a subset of the remaining parties, e.g.,  $I(X_1 : X_2 X_3 X_4) - I(X_1 : X_2 X_3) \geq 0$ . However, the cooperation between any pair brings information gain about the two remaining variables, e.g.,  $I(X_1 X_2 : X_3 X_4) - I(X_1 X_2 : X_3)$  must be positive. When these conditions hold, the system

exhibits mutual dependence in all possible scenario and for these conditions to be satisfied, we need, for the former,  $I(X_1 : X_4|X_2X_3) > 0$  and  $I(X_1X_2 : X_4|X_3) > 0$  for the latter. Hence,  $\mathcal{D}_4$  will simply be the minimum of these two conditional mutual informations over all permutations of subsystems.

$$\begin{aligned}\mathcal{D}_N &= \min_{\text{perm}} [I(X_2 : X_4|X_3), I(X_1 : X_4|X_2X_3)] \\ &= I(X_1 : X_4|X_2X_3),\end{aligned}\tag{2.13}$$

where we use the chain rule for mutual information and its non-negativity. And the minimum is taken over all permutations of the subsystems. Therefore, minimization over the conditional mutual information between two variables is sufficient to compute  $\mathcal{D}_4$ . And this step simplifies the computation of multipartite dependence significantly.

Following the similar lines, we can define the notion of multipartite dependence for arbitrary  $N$  number of parties which we will call  $N$ -partite dependence

$$\mathcal{D}_N = \min_{\text{perm}} I(X_1 : X_2|X_3 \dots X_N),\tag{2.14}$$

where the minimum is taken over all permutations of the subsystems.

Also, let us generalize the multipartite dependence for arbitrary  $N > 2$  in the quantum scenario. For an arbitrary  $N$ -partite state  $\rho$ , we have,

$$\mathcal{D}_N(\rho) = \min_{i,j} I(X_i : X_j|\underbrace{\{X_k\}}_{N-2}),\tag{2.15}$$

where,  $i, j = 1 \dots N$  and  $i \neq j$  and

$$\underbrace{\{X_k\}}_{N-2} = \{X_1, \dots, X_{i-1}, X_{i+1}, \dots, X_{j-1}, X_{j+1}, \dots, X_N\}.$$

and

$$\begin{aligned}& I(X_i : X_j|\underbrace{\{X_k\}}_{N-2}) \\ &= S(X_i|\underbrace{\{X_k\}}_{N-2}) + S(X_j|\underbrace{\{X_k\}}_{N-2}) - S(X_iX_j|\underbrace{\{X_k\}}_{N-2}) \\ &= S(\text{Tr}_i\rho) + S(\text{Tr}_j\rho) - S(\text{Tr}_{ij}\rho) - S(\rho).\end{aligned}\tag{2.16}$$

$\text{Tr}_i\rho$  denotes a partial trace over the subsystem  $i$ .

$\mathcal{D}_N$  can be calculated by computing and comparing  $\binom{N}{2}$  values, i.e., scales polynomially as  $N^2$ , whereas for permutationally invariant systems it is straightforward.

### 2.1.3 Pure states

Multipartite dependence can be significantly simplified when only pure states are considered. In this case, clearly,  $S(\rho) = 0$ . Moreover, from Schmidt theorem we know that, the non-zero eigenvalues of the reduced states are equal. Therefore, both the subsystems of a pure state have the same entropy:  $S(\text{Tr}_i \rho) = S(\rho_i)$  for  $\rho = |\Psi\rangle\langle\Psi|$ . Then for any pure quantum state  $|\Psi\rangle$ , the dependence can be simplified as

$$\mathcal{D}_N(|\Psi\rangle) = \min_{i,j} [S(\rho_i) + S(\rho_j) - S(\rho_{ij})], \quad (2.17)$$

where

$$\rho_i = \text{Tr}_{1\dots(i-1)(i+1)\dots N} \rho \quad (2.18)$$

is the state of the system after removing all but the  $i$ -th particle. Hence,  $\mathcal{D}_N(|\Psi\rangle)$  is given by the smallest quantum mutual information of the two-partite subsystems,

$$\mathcal{D}_N(|\Psi\rangle) = \min_{i,j} I(\rho_i : \rho_j). \quad (2.19)$$

Its there the trade-off relation between the quantum mutual information for different two-particle subsystems of a pure global state and the definition of  $\mathcal{D}_N$  where the smallest conditional mutual information is chosen.

### 2.1.4 Relevant Examples

#### 2.1.4.1 Dependence of GHZ state

The bound for the dependence of pure states can be achieved by the  $N$ -qudit GHZ state,

$$|\psi\rangle_{GHZ}^N = \frac{1}{\sqrt{d}}(|0\dots 0\rangle + \dots + |d-1\dots d-1\rangle). \quad (2.20)$$

The value can easily be calculated using Eq. (2.17). The two-particle subsystems of the GHZ state are of the form  $\rho_{12} = \sum_{j=0}^{d-1} \frac{1}{d} |jj\rangle\langle jj|$  and their mutual information equals 1. Because separable states have non-negative quantum conditional entropy  $S_{i|j}(\rho_{ij}) \geq 0$  [104], the quantum mutual information is bounded by 1 whenever the state  $\rho_{ij}$  is separable. Therefore, their mutual information will also be bounded as,

$$\begin{aligned} I_{i:j}(\rho_{ij}) &= S(\rho_i) - S_{i|j}(\rho_{ij}) \\ &\leq S(\rho_i) \\ &\leq 1 \end{aligned} \quad (2.21)$$

### 2.1.4.2 Dependence of Dicke states

Dicke states [105] are key resources in the regime of combinatorial optimization quantum algorithms and also have a widespread application in quantum networking [106], quantum game theory [107], multiparty quantum communication [108, 109, 110], and quantum metrology [111, 112, 113].

The  $N$ -partite Dicke state  $|D_N^e\rangle$  is an equal-weight superposition of all  $N$  qubit states with  $e$  excitations and can be expressed in the following form,

$$|D_N^e\rangle = \binom{N}{e}^{-\frac{1}{2}} \sum_l |1\rangle^{\otimes e} \otimes |0\rangle^{\otimes (N-e)}, \quad (2.22)$$

where  $|0\rangle$  is the ground state while  $|1\rangle$  is the excited state and  $l$  denotes the sum over all possible permutations. Any one-partite reduced density matrix  $\rho_i$  of the state  $|D_N^e\rangle$  has the following form,

$$\rho_i = \binom{N}{e}^{-1} (e|1\rangle\langle 1| + (N-e)|0\rangle\langle 0|). \quad (2.23)$$

Therefore, all one-partite reduced density matrices  $\rho_i$  have the two non-zero eigenvalues given by,

$$e/N, \quad (2.24a)$$

$$(N-e)/N. \quad (2.24b)$$

And on the other hand, all two-partite reduced states  $\rho_{ij}$  also have a symmetry and reduces to the following state,

$$\rho_{ij} = \binom{N}{e}^{-1} (|00\rangle\langle 00| + \sum_{m,t=0}^1 |mt\rangle\langle mt|) \quad \text{for } e = 1, \quad (2.25)$$

$$\rho_{ij} = \binom{N}{e}^{-1} (|11\rangle\langle 11| + \sum_{m,t=0}^1 |mt\rangle\langle mt|) \quad \text{for } e > 1. \quad (2.26)$$

and therefore have only at most three non-vanishing eigenvalues,

$$e(e-1)/N(N-1), \quad (2.27a)$$

$$2e(N-e)/N(N-1), \quad (2.27b)$$

$$(N-e-1)(N-e)/N(N-1). \quad (2.27c)$$

Therefore,  $\mathcal{D}_N$  for a Dicke state is given by

$$\begin{aligned}
\mathcal{D}_N(D_N^e) &= S(\rho_i) + S(\rho_j) - S(\rho_{ij}) \\
&= \binom{N}{e}^{-1} \left[ -\frac{2(N-1)! \log\left(\frac{e}{N}\right)}{(e-1)!(N-e)!} - 2 \binom{N-1}{e} \log\left(1 - \frac{e}{N}\right) \right. \\
&\quad + \binom{N-2}{e-2} \log\left(\frac{\binom{N-2}{e-2}}{\binom{N}{e}}\right) + 2 \binom{N-2}{e-1} \log\left(\frac{2\binom{N-2}{e-1}}{\binom{N}{e}}\right) \\
&\quad \left. + \binom{N-2}{e} \log\left(\frac{\binom{N-2}{e}}{\binom{N}{e}}\right) \right]. \tag{2.28}
\end{aligned}$$

We can alternatively represent  $e$  as a function of the number of parties,  $e = N/k$  where  $k \in \mathbb{R}$ . In the limit of  $N \rightarrow \infty$ , the  $N$ -dependence then converges to a finite value,

$$\lim_{N \rightarrow \infty} \mathcal{D}_N(D_N^e) = 2(k-1)/k^2. \tag{2.29}$$

The maximally achievable dependence of  $1/2$  is reached for  $e = N/2$ . For an arbitrarily chosen constant  $e$  (e.g., for the W state,  $e = 1$ ),  $\mathcal{D}_N(D_N^e)$  vanishes for  $N \rightarrow \infty$ .

A comprehensive list of dependencies within standard classes of quantum states is given in Tab. 2.3.

### 2.1.5 $k$ -partite $N$ -Dependence

$\mathcal{D}_N$  is defined operationally with respect to the information gain from cooperation when  $N-1$  parties are divided into two different sets and their goal is to predict the value of the  $N^{\text{th}}$  party. Within the  $N$ -partite system, there is also a possibility to exclude one or more parties, and define a similar cooperation scenario within the remaining subsystems. Hence we extend the definition of  $\mathcal{D}_N$  further to  $k$ -partite dependencies,  $\mathcal{D}_N^k$ , within an  $N$ -partite system for all  $1 \geq k \geq N-3$ .  $\mathcal{D}_N^k$  therefore quantifies the dependency among any  $k$ -parties and the definition of  $\mathcal{D}_N^k$  is driven from the fact that it is  $\mathcal{D}_N$  for any  $k$ -partite subsystem.  $\mathcal{D}_N^k$  can be expressed as

$$\mathcal{D}_N^k = \min_{\Pi} \min_{\text{perm}(i_1, \dots, i_k)} I(X_{i_1} : X_{i_2} | X_{i_3} \dots X_{i_k}) \tag{2.30}$$

where the  $\Pi$  is the set of all the strings  $\{i_1, \dots, i_k\}$ , of length  $k$  for  $k \leq N-3$  by choosing  $k$  out of  $N$  parties in every possible combination. We call  $k$ , the *rank of multipartite dependence*.

It turns out that  $\mathcal{D}_N^k$  can be non-zero even for the states whose  $\mathcal{D}_N$  vanishes (and also vice versa). In other words, there are states for which one can not gain any information about one party by cooperating among all other parties. However, they can gain some

information if they cooperate in groups of  $k$  subsystems. In fact  $\mathcal{D}_N^k$  is the same as  $\mathcal{D}_N$  given that  $N - k$  number of parties are traced out from the initial  $N$ -partite states, of course considering different permutations over sites that are traced out, and then calculated for  $N = k$ . In Tab. 2.1 we present such examples where  $\mathcal{D}_N$  for the states are zero but  $\mathcal{D}_N^k$  are not necessarily so. Such examples are the so called linear cluster and the ring cluster states and some of the AME states, i.e., the absolutely maximally entangled states which are the  $\lfloor n/2 \rfloor$ -uniform states of  $d$  dimensions [114]. In Tab.2.3 presents all the examples for which  $\mathcal{D}_N$  and  $\mathcal{D}_N^k$  were calculated.

$N$	state	$\mathcal{D}_3$	$\mathcal{D}_4$	$\mathcal{D}_5$	$\mathcal{D}_6$
4	$L_4$	1	0	-	-
5	$R_5$	1	1	0	-
5	AME(5,2)	1	1	0	-
6	AME(6,2)	0	2	0	0

Table 2.1: Values of the dependence for several quantum states for which  $\mathcal{D}_N$  do not exist.  $L_k$  and  $R_k$  stands for the linear cluster and the ring cluster states of  $k$  qubits (in general, the graph states are defined by the elements of the stabilizer group for a particular linear or ring graphs, as shown in [115]), and AME(n,k) states are Absolutely Maximally Entangled states.

## 2.2 General Properties

### 2.2.1 Extremal values of dependence

#### 2.2.1.1 Classical Distribution

In this section we present the bounds for  $\mathcal{D}_N$  considering various scenario. First we consider the classical distributions. In tripartite case,  $I(X_1 : X_2|X_3)$  has the form,

$$\begin{aligned}
I(X_1 : X_2|X_3) &= H(X_1|X_2) - H(X_1|X_2X_3) \\
&\leq H(X_1|X_2) \\
&= H(X_1X_2) - H(X_2) \\
&\leq H(X_1) + H(X_2) - H(X_2) \\
&\leq H(X_1) \\
&\leq 1
\end{aligned} \tag{2.31}$$

Here we have used the fact that  $H(X_1X_2) \leq H(X_1) + H(X_2)$ . As  $I(X_1 : X_2|X_3) \leq H(X_1)$ , the classical mutual information cannot exceed the value of entropy of each variable and therefore, additional conditioning do not change it. Therefore, the maximum value that can

be achieved by  $\mathcal{D}$  is also unity. The same is true for any number of parties and one can think of  $X_3$  as a collection of  $N$  parties. Therefore, for classical distributions,

$$\mathcal{D}_N^{classical} \leq 1. \quad (2.32)$$

The bound presented here is tight and in Tab. 2.3 we present examples where it is shown that this bound holds for both odd and even distribution.

### 2.2.1.2 Bounds on mutual $N$ -partite dependence for quantum states

Now we will look at the case of quantum states and derive a bound for  $\mathcal{D}_N$ . We will begin with pure state and move to mixed states. Interestingly, we will show that the mixed states' bound exceeds the pure states' bound.

### 2.2.1.3 Bounds for pure states

We know,

$$\begin{aligned} \mathcal{D}_N(|\psi\rangle) &= \min_{i,j,k} I(X_i : X_j | \underbrace{X_k}_{N-2}) \\ &= \min_{i,j} S(\rho_i) + S(\rho_j) - S(\rho_{ij}). \end{aligned} \quad (2.33)$$

Therefore, to find the bound, we need to find the smallest mutual information  $I(\rho_i : \rho_j)$ , where  $\rho_i, \rho_j$  are subsystems of the pure state  $\rho$ . The sum of such two above-mentioned mutual informations that have one common subsystem satisfies the following:

$$\begin{aligned} I(\rho_i : \rho_j) + I(\rho_j : \rho_k) &= S(\rho_i) + S(\rho_j) - S(\rho_{ij}) + S(\rho_j) + S(\rho_k) - S(\rho_{jk}) \\ &\leq 2S(\rho_j) \\ &\leq 2, \end{aligned} \quad (2.34)$$

where the first inequality follows from the strong subadditivity of entropy

$$S(\rho_i) + S(\rho_k) \leq S(\rho_{ij}) + S(\rho_{jk}). \quad (2.35)$$

Hence, we find a monogamy relation with respect to mutual information,

$$I(\rho_i : \rho_j) + I(\rho_j : \rho_k) \leq 2 \quad (2.36)$$

From this relation we can clearly see that minimum of two different mutual information is bounded by 2 and then the smaller one will necessarily be bounded by 1. As  $\mathcal{D}_N$  is the

minimum of the mutual information, we have the value of  $\mathcal{D}_N$  for pure states bounded by,

$$\mathcal{D}_N^{pure} \leq 1. \quad (2.37)$$

Having this bound, we may ask the following question what happens if a state for which  $\mathcal{D}_N \leq 1$ ? Are there any local measurements on the subsystems with classical outcomes having conditional mutual information equal to  $\mathcal{D}_N$ ? The answer to this question is negative. We have optimized the conditional informations over local measurements for Dicke states which do not attain the upper bound to  $\mathcal{D}_N^{pure}$  with  $N = 3, 4$  and  $0 < e < N$ , and observed that the values obtained are always smaller than  $\mathcal{D}_N$ .

#### 2.2.1.4 Bound on mixed states

In order to find the bound of  $\mathcal{D}_N$  for mixed states we first consider subadditivity relation of quantum entropy for the reduced quantum states. From this we get

$$S(\text{Tr}_j \rho) \leq S(\text{Tr}_{ij} \rho) + S(\rho_i), \quad (2.38)$$

$$S(\text{Tr}_i \rho) - S(\rho_i) \leq S(\rho), \quad (2.39)$$

where  $\rho_i$  is again the reduced state of the  $i$ -th particle. Therefore, we can use the above inequalities to write the following form of  $\mathcal{D}_N$

$$\begin{aligned} \mathcal{D}_N(\rho) &\leq S(\text{Tr}_i \rho) - S(\rho) + S(\text{Tr}_j \rho) - S(\text{Tr}_{ij} \rho) \\ &\leq S(\rho_i) + S(\rho_i) \\ &\leq 2. \end{aligned} \quad (2.40)$$

Therefore,

$$\mathcal{D}_N^{mixed} \leq 2. \quad (2.41)$$

After finding this bound, we can say that, overall, the  $\mathcal{D}_N$  for quantum states is bounded by,

$$\mathcal{D}_N^{quantum} \leq 2. \quad (2.42)$$

This bound is tight and can be achieved by mixed states mentioned in the next subsection. It is then worth investigating that for which mixed states does  $\mathcal{D}_N$  attains its quantum bound. Interestingly enough, we find that the states for which this maximal bound is achievable are the so-called  $(N - 1)$ -uniform states. We will prove this statement bellow.

#### 2.2.1.5 Qudit state maximizing $\mathcal{D}_N$

We start with the simplest case of  $d = 2$  to determine the optimal states that provides us with the bound given in Eq. 2.42. The maximum  $\mathcal{D}_N$  is given by the so-called  $k$ -uniform

states, in particular for  $k = N - 1$ . Entropy of an  $N$ -qubit  $N - 1$ -uniform state with even  $N$ ,  $\rho_N^{(2)}$ , is given by,

$$\begin{aligned} S(\rho_N^{(2)}) &= -\sum_{j=1}^{2^N} \eta_j \log_2 \eta_j \\ &= -2^{N-2} \cdot \frac{1}{2^{N-2}} \cdot \log_2 \frac{1}{2^{N-2}} \\ &= N - 2. \end{aligned} \quad (2.43)$$

For an  $(N - 1)$ -uniform state, all reduced density matrices are proportional to identity matrices. Therefore,

$$S(\text{Tr}_i \rho_N^{(2)}) = N - 1, \quad (2.44a)$$

$$S(\text{Tr}_{i,j} \rho_N^{(2)}) = N - 2. \quad (2.44b)$$

Therefore, for  $N$  even

$$\mathcal{D}_N(\rho_N^{(2)}) = S(\text{Tr}_i \rho_N^{(2)}) + S(\text{Tr}_j \rho_N^{(2)}) - S(\text{Tr}_{i,j} \rho_N^{(2)}) - S(\rho_N^{(2)}) = 2. \quad (2.45)$$

The same argument can be extended to the qudit case. Therefore, to find the maximal  $\mathcal{D}_N$  for arbitrary  $d$ , we consider the  $N - 1$ -uniform quantum state of  $N$  qudits. For  $N \geq 3$  and also being a multiple of  $d$ , such a state can be defined in terms of common eigenstates of the following generators,

$$G_1^{(d)} = \bigotimes_{i=1}^N X^{(d)}, \quad (2.46)$$

$$G_2^{(d)} = \bigotimes_{i=1}^N Z^{(d)}. \quad (2.47)$$

Here, the generators are comprised of the so-called  $d$ -dimensional Weyl-Heisenberg matrices given by,

$$X^{(d)} = \sum_{j=0}^{d-1} |j\rangle \langle j+1|, \quad (2.48)$$

$$Z^{(d)} = \sum_{j=0}^{d-1} \omega^j |j\rangle \langle j|, \quad (2.49)$$

where  $\omega = e^{i2\pi/d}$ . And the state can then be written as,

$$\rho_N^{(d)} = \frac{1}{d^N} \sum_{i,j=0}^{d-1} (G_1^{(d)})^i (G_2^{(d)})^j. \quad (2.50)$$

The above mentioned states belong to a special class of states which has been thoroughly discussed in the previous chapter, i.e., the class of  $k$ -uniform mixed states defined in chapter 1, where  $k = N - 1$ .

For even  $N$ , the state  $\rho_N^{(d)}$  has  $d^{N-2}$  eigenvalues equal to  $\frac{1}{d^{N-2}}$ . Therefore the entropy  $S(\rho_N^{(d)})$  is equal to

$$\begin{aligned} S(\rho_N^{(d)}) &= - \sum_{j=1}^{d^N} \eta_j \log_d \eta_j \\ &= -d^{N-2} \cdot \frac{1}{d^{N-2}} \cdot \log_d \frac{1}{d^{N-2}} \\ &= N - 2. \end{aligned} \quad (2.51)$$

Also, for the states being  $(N - 1)$ -uniform, all reduced density matrices are proportional to identity matrices giving

$$S(\text{Tr}_i \rho_N^{(d)}) = N - 1, \quad (2.52a)$$

$$S(\text{Tr}_{i,j} \rho_N^{(d)}) = N - 2. \quad (2.52b)$$

Therefore, for  $N$  even

$$\mathcal{D}_N(\rho_N^{(d)}) = S(\text{Tr}_i \rho_N^{(d)}) + S(\text{Tr}_j \rho_N^{(d)}) - S(\text{Tr}_{i,j} \rho_N^{(d)}) - S(\rho_N^{(d)}) = 2. \quad (2.53)$$

In the case of  $N$  odd, however, the state  $\rho_N^{(d)}$  has  $d^{N-1}$  eigenvalues equal to  $\frac{1}{d^{N-1}}$ . Therefore,

$$\begin{aligned} S(\rho_N^{(d)}) &= - \sum_{j=1}^{d^N} \eta_j \log_d \eta_j \\ &= -d^{N-1} \cdot \frac{1}{d^{N-1}} \cdot \log_d \frac{1}{d^{N-1}} \\ &= N - 1. \end{aligned} \quad (2.54)$$

And using the values from Eq. (2.52) we get  $\mathcal{D}_N$  for  $(N - 1)$ -uniform states with odd  $N$ ,

$$\begin{aligned} \mathcal{D}_N(\rho_N^{(d)}) &= S(\text{Tr}_i \rho_N^{(d)}) + S(\text{Tr}_j \rho_N^{(d)}) \\ &\quad - S(\text{Tr}_{i,j} \rho_N^{(d)}) - S(\rho_N^{(d)}) = 1. \end{aligned} \quad (2.55)$$

We will now show that *the states achieving the bound for  $\mathcal{D}_N$  must necessarily be of a class of  $(N - 1)$ -uniform states.*

To do so, let us recall that the requirement for  $\mathcal{D}_N$  to attain this maximum value is the following,

$$\begin{aligned}\mathcal{D}_N &= I(X_1 : X_2 | X_3 \dots X_N) \\ &= I(X_1 : X_2 X_3 \dots X_N) - I(X_1 : X_3 \dots X_N) \\ &= 2,\end{aligned}\tag{2.56}$$

The definition of  $\mathcal{D}_N$  states that we minimize over all permutations. Therefore, the same equation holds for all permutations of subsystems.

Due to subadditivity, the only way to satisfy (2.56) is to have zero mutual information corresponding to a  $N - 1$ -qudit reduced state, say after reducing the  $j^{\text{th}}$  subsystem. Then we have,

$$I(X_i : X_1 \dots X_{i-1} X_{i+1} \dots X_{j-1} X_{j+1} \dots X_N) = 0,\tag{2.57a}$$

$$I(X_i : X_j X_1 \dots X_{i-1} X_{i+1} \dots X_{j-1} X_{j+1} \dots X_N) = 2.\tag{2.57b}$$

From Eq. (2.57a) we can conclude that the state  $\rho_N^{(d)}$  is biseparable when the  $j^{\text{th}}$  party is removed i.e.,

$$\rho_{1\dots N-1} = \rho_{1\dots X_{j-1}} \otimes \rho_{X_{j+1}\dots N},\tag{2.58}$$

which also holds for all permutation of indices. After tracing out all but the  $j - 1^{\text{th}}$  and  $j + 1^{\text{th}}$  subsystem, we get,

$$\rho_{red} = \rho_{j-1} \otimes \rho_{j+1},\tag{2.59}$$

which implies that the bipartite reduced state is a product of the corresponding 1-partite reduced states. It follows that any  $N - 1$  particle subsystem is described by a simple tensor product, e.g.,

$$\rho_{13\dots N} = \rho_1 \otimes \dots \otimes \rho_{j-1} \otimes \rho_{j+1} \otimes \dots \otimes \rho_N.\tag{2.60}$$

Now, using Eq. (2.57b) we can write

$$S(X_i) - S(X_i | X_1 \dots X_{i-1} X_{i+1} \dots X_N) = 2.\tag{2.61}$$

Since for the quantum conditional entropy we have

$$-S(X_i | X_1 \dots X_{i-1} X_{i+1} \dots X_N) \leq S(X_i),\tag{2.62}$$

the bound Eq. (2.42) is achieved if

$$\begin{aligned} 2 &= S(X_i) - S(X_i|X_1 \dots X_{i-1} X_{i+1} \dots X_N) \\ &\leq S(X_i) + S(X_i), \end{aligned}$$

i.e., for  $S(X_i) = 1$ . Hence, taking into account (2.60), all  $N - 1$  particle subsystems are maximally mixed, i.e., the total state is  $(N - 1)$ -uniform. Therefore quantum mutual information is bounded by 2 and this also serves as the bound on  $\mathcal{D}_N$  optimized over quantum states which is achieved by the  $N - 1$ -uniform states with even  $N$ . The optimal states have the following form:

$$\rho_{\max} = \frac{1}{2^N} \left( \sigma_0^{\otimes N} + (-1)^{N/2} \sum_{j=1}^3 \sigma_j^{\otimes N} \right), \quad (2.63)$$

where  $\sigma_j$  are the Pauli matrices and  $\sigma_0$  is the  $2 \times 2$  identity matrix.  $\rho_{\max}$  is permutationally invariant and therefore gives rise to perfect correlations or anti-correlations when all observers measure locally the same Pauli observable. Such states are often called as the generalized bound entangled Smolin states [116, 117]. These states are useful quantum resource for multiparty communication schemes [118] and were experimentally demonstrated in Refs. [119, 120, 121, 122, 123, 124].

### 2.2.2 Key properties of $\mathcal{D}_N$

We will now show what aspects of correlations and mutual dependencies are grasped by  $\mathcal{D}_N$ . We recall the natural postulates that were formulated in Ref. [15, 24] in order to characterise the measures of genuinely multipartite correlations for both classical and quantum scenario. We will investigate how  $\mathcal{D}_N$  corresponds to those postulates.

The first postulates corresponds to the question that what happens if an auxiliary systems is added to the  $N$ -partite state under consideration. In case of multipartite correlations, such addition of an auxiliary party in a product state that resulting in an  $N + 1$  partite state does not have genuine  $n$ -partite correlations either. The same is true for  $\mathcal{D}_N$ .

**Property 1:** *If  $\mathcal{D}_N = 0$  and one adds a party in a product state then the resulting  $(N + 1)$ -party state has  $\mathcal{D}_N = 0$ .*

*Proof.* The definition of  $\mathcal{D}_N$  states that we are minimizing the conditional mutual information over all  $N$ -partite subsystems of the total  $(N + 1)$ -party state. By assumption,  $\mathcal{D}_N$  is zero that implies that the minimum value of the conditional mutual information is zero as well. Therefore, the dependence after adding an auxiliary system also remains zero. In other words, if the cooperation among  $N - 1$  parties within the  $N$ -partite system does not

help in gaining additional knowledge about any other remaining party, then the cooperation with any additional independent system which was uncorrelated with all of them, will not add up to the knowledge either.  $\square$

Next we consider the scenario of splitting one party into two and send one part of the system to a new party who is not correlated with the remainder of the system.

**Property 2:** *If  $\mathcal{D}_N = 0$  for an  $N$ -partite state and one subsystem is split with two of its parts placed in different laboratories then the resulting  $(N + 1)$ -party state has  $\mathcal{D}_{N+1} = 0$ .*

*Proof.* First of all, we consider a tripartite case where  $\mathcal{D}_3 = 0$ . Specifying  $\mathcal{D}_3 = 0$  however does not indicate which conditional mutual information in Eq. (2.8) vanishes. Now we assume that the third party are divided in two parts labeled as  $X_3$  and  $X_4$ , producing a four-partite system and one of them is sent to a spatially separated laboratory. Now, if the mutual information that vanishes is where the variables  $X_3$  and  $X_4$  of the third party enter in the condition, then this mutual information is also minimizing  $\mathcal{D}_4$ , and hence the latter vanishes.

$$\begin{aligned} I(X_1 : X_2 | X_3) &= 0 \\ \implies I(X_1 : X_2 | X_3 X_4) &= 0 \end{aligned}$$

Another possibility is that the variables of the third party enter outside the condition, e.g., the vanishing conditional mutual information could be  $I(X_1 : X_3 X_4 | X_2)$ . From the chain rule for mutual information we get,

$$I(X_1 : X_4 | X_2 X_3) \leq I(X_1 : X_3 X_4 | X_2) = 0 \quad (2.64)$$

This rule can easily be followed from the strong subadditivity of quantum entropy:

$$\begin{aligned} I(X_1 : X_4 | X_2 X_3) &\leq I(X_1 : X_3 X_4 | X_2) \\ \implies S(X_1 X_2 X_3) + S(X_4 X_2 X_3) &- S(X_1 X_2 X_3 X_4) - S(X_2 X_3) \\ &\leq S(X_1 X_2) + S(X_3 X_4 X_2) - S(X_1 X_2 X_3 X_4) - S(X_2) \\ \implies S(X_1 X_2 X_3) - S(X_2 X_3) &\leq S(X_1 X_2) - S(X_2) \\ \implies S(X_1 X_2 X_3) + S(X_2) &\leq S(X_1 X_2) + S(X_2 X_3) \end{aligned}$$

As conditional mutual information is always non-negative, we therefore conclude  $\mathcal{D}_4 = 0$ . For the  $N$ -partite case, same proof is applicable with increasing number of variables in the conditions.  $\square$

Lastly, we investigate the property of  $\mathcal{D}_N$  under local operations. In the case of genuine multipartite correlations, local operations and unanimous postselection cannot gener-

ate any genuine  $N$ -partite correlations that was not present in the initial state. We will see that this monotonicity property does not hold for  $\mathcal{D}_N$ , making it distinctive from a measure of genuine multipartite correlations. This also has a clear interpretation: local operations that uncorrelate a given subsystem from the others may lead to information gain when the less correlated party cooperates with other parties

**Property 3:**  $\mathcal{D}_N$  can increase under local operations. We denote the quantities computed after local operations with a bar, e.g.,  $\overline{\mathcal{D}}_N, \overline{X}_i$  etc. Then the  $N$ -partite dependence,  $\overline{\mathcal{D}}_N$ , is bounded by,

$$\overline{\mathcal{D}}_N \leq \mathcal{D}_N + I(X_1 X_2 : X_3 \dots X_N) - I(X_1 X_2 : \overline{X}_3 \dots \overline{X}_N), \quad (2.65)$$

where systems  $X_1$  and  $X_2$  are the ones minimizing  $\mathcal{D}_N$  before the operations were applied, i.e.,

$$\mathcal{D}_N = I(X_1 : X_2 | X_3 \dots X_N).$$

*Proof.* We consider a  $N$ -partite state  $\rho$ . Then general local operations (CPTP maps) is performed on the state and the resultant state is  $\overline{\rho}$ . After that we consider the lemma characterizing the lack of monotonicity of conditional mutual information under local operations. It states the following:

**Lemma 1:** *The following inequality holds:*

$$\begin{aligned} I(\overline{X}_1 : \overline{X}_2 | \overline{X}_3 \dots \overline{X}_N) &\leq I(X_1 : X_2 | X_3 \dots X_N) \\ + I(X_1 X_2 : X_3 \dots X_N) - I(X_1 X_2 : \overline{X}_3 \dots \overline{X}_N), \end{aligned} \quad (2.66)$$

where bars denote subsystems transformed by arbitrary local CPTP maps. The conditional mutual information is monotonic under operations on systems not in the condition [125], i.e.,

$$I(\overline{X}_1 : \overline{X}_2 | \overline{X}_3 \dots \overline{X}_N) \leq I(X_1 : X_2 | \overline{X}_3 \dots \overline{X}_N) \quad (2.67)$$

Now we continue as follows:

$$\begin{aligned} &I(X_1 : X_2 | \overline{X}_3 \dots \overline{X}_N) + I(X_1 X_2 : \overline{X}_3 \dots \overline{X}_N) \\ &= I(X_1 : X_2 \overline{X}_3 \dots \overline{X}_N) + I(X_2 : X_1 \overline{X}_3 \dots \overline{X}_N) - I(X_1 : X_2) \\ &\leq I(X_1 : X_2 X_3 \dots X_N) + I(X_2 : X_1 X_3 \dots X_N) - I(X_1 : X_2) \\ &= I(X_1 : X_2 | X_3 \dots X_N) + I(X_1 X_2 : X_3 \dots X_N), \end{aligned}$$

where the first equation is obtained by manipulating entropies such that the mutual informations containing barred subsystems come with positive sign, next we used the data processing inequality and in the last step we reversed the manipulations on entropies. The data processing inequality states that for a given set of variable  $\{X, Y, Z\}$  that form a Markov

Chain given by  $X \rightarrow Y \rightarrow Z$ , we have

$$I(X : Y) \geq I(X : Z). \quad (2.68)$$

Therefore the above lemma is proved.

Coming back to the proof of property 3 we now rewrite  $\mathcal{D}_N$

$$\begin{aligned} \mathcal{D}_N &= I(X_1 : X_2 | X_3 \dots X_N) \\ &\geq I(\bar{X}_1 : \bar{X}_2 | \bar{X}_3 \dots \bar{X}_N) - I(X_1 X_2 : X_3 \dots X_N) + I(X_1 X_2 : \bar{X}_3 \dots \bar{X}_N) \\ &\geq \bar{\mathcal{D}}_N - I(X_1 X_2 : X_3 \dots X_N) + I(X_1 X_2 : \bar{X}_3 \dots \bar{X}_N). \end{aligned}$$

Here in the first line we denote the subsystems such that the conditional mutual information  $I(X_1 : X_2 | X_3 \dots X_N)$  gives  $\mathcal{D}_N$ . Then, the first inequality follows from Lemma 2.2.2. Finally the second inequality comes from the fact that  $I(\bar{X}_1 : \bar{X}_2 | \bar{X}_3 \dots \bar{X}_N)$  is bounded by  $\bar{\mathcal{D}}_N$ . We also provide an example in Sec. 2.3.1 where given a three-qubit state there exist local measurements with outcomes producing  $\mathcal{D}_3$  higher than that of the corresponding initial quantum states.

### 2.2.3 Partial extension of classical interpretations

In classical information theory  $I(X_i : X_j | \underbrace{\{X_k\}}_{N-2})$  is interpreted as the expected gain in information about the outcome of a random variable  $X_i$  by another party when rest of  $(N-2)$  number of parties are cooperating with the latter. The agents could measure their subsystems obtaining some particular outcomes and by analysing both outcomes together they may infer the outcome of the third agent better than what they would have done individually (and this information gain is quantified by  $\mathcal{D}_N$ ). This interpretation can be extended to quantum systems where the  $\mathcal{D}_N$  values do not exceed unity, i.e., for the pure states.

We have also considered to provide an comparison between the classical and quantum distributions. To do so, we take the example of the joint probability distribution,  $\{P_{\text{same}}\}$  given in Subsec.2.1.1. As we know, this distribution admits  $\mathcal{D}_3 = 0$ , however, all the variables here are correlated with each other. In analogy, we take an example in a quantum scenario, the so-called GHZ state,

$$|\psi\rangle_{GHZ}^3 = \frac{1}{\sqrt{2}}(|000\rangle + |111\rangle). \quad (2.69)$$

We calculate,

$$\begin{aligned}
S(|\psi\rangle_{GHZ}^3) &= 0, \\
S(\text{Tr}_i[|\psi\rangle_{GHZ}^3]) &= 1 \quad \text{for } i \in \{1, 2, 3\}, \\
S(\text{Tr}_{ij}[|\psi\rangle_{GHZ}^3]) &= 1 \quad \text{for } \{i, j\} \in \{1, 2, 3\}. \\
\implies \mathcal{D}_3 &= 1
\end{aligned}$$

The value of dependence is improved here due to quantum coherence. This is because of the fact that we can measure the GHZ state in a different basis and the classical dataset that we obtain will give rise to  $\mathcal{D}_3 = 1$ . The relevant basis is to measure each qubit along  $\frac{1}{\sqrt{2}}(|0\rangle \pm |1\rangle)$  directions. By doing the measurement in the appropriate basis, we find the classical dataset,  $\{P_{\text{even}}\}$  (defined in Subsec. 2.1.1) which indeed leads to  $\mathcal{D}_3 = 1$ .

As another example can be constructed from the classical distribution,

$$\begin{aligned}
p(100) &= \frac{1}{3} \\
p(010) &= \frac{1}{3} \\
p(001) &= \frac{1}{3}.
\end{aligned}$$

This distribution gives rise to  $\mathcal{D}_3 = \frac{2}{3}$ . However, if we consider the quantum counterpart, i.e., the quantum superposition  $|W\rangle = \frac{1}{\sqrt{3}}(|100\rangle + |010\rangle + |001\rangle)$ , then  $\mathcal{D}_N$  has a rather non-trivial value which is given by  $\mathcal{D}_3 = 0.9183$ . It is important to remark that this result doesn't necessarily imply that there exists a set of local measurements on  $|W\rangle$  which yields a classical distribution with higher dependence. In fact, by optimising the dependence of local measurement results:

$$\sum_{i,j,k} P_i^1 \otimes P_j^2 \otimes P_k^3 |W\rangle \langle W| P_i^1 \otimes P_j^2 \otimes P_k^3, \quad (2.70)$$

where,  $P_i^k = \frac{1}{2}(\mathbb{1} + \vec{v} \cdot \vec{\sigma})$  is a single qubit projective measurement, the  $\mathcal{D}_3$  is found to be equal to the classical value  $\frac{2}{3}$ . It is therefore natural to also consider joint measurements on two parties. Hence, we have therefore computed the post-measurement state

$$\sum_{j,k} \Pi_j^{12} \otimes \Pi_k^3 |W\rangle \langle W| \Pi_j^{12} \otimes \Pi_k^3, \quad (2.71)$$

where  $\Pi_j^{12}$  are the rank-one projectors on the first two particles and correspondingly  $\Pi_k^3$  are for the last qubit. Indeed, when we optimise over these projectors the dependence of the post-measurement state precisely matches the value computed for the  $W$  state, i.e.  $\mathcal{D}_3 = 0.9183$ . All these dependence values are summarized in Tab. 2.2. These examples may suggest that perhaps the interpretation of the value of  $\mathcal{D}_N$  for quantum states (whenever

$N$	state	$\mathcal{D}_3$	$\mathcal{D}_4$	$\mathcal{D}_5$	$\mathcal{D}_6$
3	$\{P_{\text{same}}\}$	0	-	-	-
3	$\{P_{\text{even}}\}$	1	-	-	-
3	GHZ	1	-	-	-
3	W	0.9183	-	-	-

Table 2.2:  $\mathcal{D}_N$  values for different probability distributions and corresponding quantum states.  $\{P_{\text{same}}\}$  stands for  $P(000) = P(111) = \frac{1}{2}$  and  $\{P_{\text{even}}\}$  for  $P(000) = P(110) = P(101) = P(011) = \frac{1}{4}$ .

not exceeding unity) can be interpreted as the highest dependence of the classical dataset that can be obtained by performing measurements on the quantum state that include single party measurements as well as joint party measurements. However, it turns out that this is not the case. We have found evidences where we show that given a four-qubit state there exist local measurements with outcomes producing  $\mathcal{D}_4$  higher than that of the corresponding quantum states.

## 2.3 Comparison with other quantifiers of correlations

### 2.3.1 $N$ -dependence versus $N$ -partite correlations

We will now compare between multipartite dependence and a typical measure of multipartite correlations. Making a continuation from Subsec. 2.2.3, we provide a simple example that provides us enough intuition in support to the aforementioned fact. We consider three classical binary random variables that are described by the joint probability distribution  $\{P_{\text{same}}\}$ . As we have pointed out previously, these variables are correlated. This can be proved by using the quantifiers introduced in Refs. [85, 24]. However, the knowledge of, say, the first party about the third party does not increase if the first observer is allowed to cooperate with the second one. By examining her data, the first observer knows the variables of both remaining parties and any cooperation with one of them does not change this. There is no information gain and hence this distribution has vanishing tripartite dependence.

Another such example can be considered which follows the joint probability distribution  $\{P_{\text{even}}\}$ . In this case, any two variables in this distribution are completely uncorrelated in a sense that for a given value of one variable, the other variable can acquire its value at random. However, any two parties can also perfectly decode the value of the remaining variable as we notice, given the value of any two variable to be known, we can guess the value of the third variable with certainty. If two variable has the same outcome, then the

third variable's outcome is always 0, whereas if the two variable get two different outcome, then the third variable will have outcome 1 with certainty. Therefore, the gain from cooperation is 1 and so is the value of  $\mathcal{D}_3$ . This quantifier is thus very good for identifying the suitability of a system for secret sharing, where the secret could be at any party.

In the previous section, we have discussed the general properties of multipartite dependence. Here we show how do they relate to the postulates that any genuine multipartite correlation measure [15, 24] must satisfy. We will show contradiction to one of postulates indicating that despite of being a quantifier of certain multipartite feature of a system,  $\mathcal{D}_N$  in fact does not quantify the multipartite correlation that is defined in terms of the postulates given in Refs. [15, 24]. Therefore  $\mathcal{D}_N$  cannot be termed as a measure of multipartite correlations. The set of postulates that a quantifier of genuinely  $N$ -partite correlation should satisfy are as follows:

*Postulate 1.* If an  $N$ -partite state does not have genuine  $N$ -partite correlations and one adds a party in a product state, then the resulting  $N + 1$  partite state does not have genuine  $N$ -partite correlations.

*Postulate 2.* If an  $N$ -partite state does not have genuine  $N$ -partite correlations, then local operations and unanimous post-selection (which mathematically correspond to the operation  $\Lambda_1 \otimes \Lambda_2 \otimes \dots \otimes \Lambda_N$ , where  $N$  is the number of parties and each  $i$  is a trace non-increasing operation acting on the  $i^{\text{th}}$  party's subsystem) cannot generate genuine  $N$ -partite correlations.

*Postulate 3.* If an  $N$ -partite state does not have genuine  $N$ -partite correlations, then if one party splits his subsystem into two parts, keeping one part for himself and using the other to create a new  $N + 1^{\text{st}}$  subsystem, then the resulting  $N + 1$ -partite state does not have genuine  $N + 1$ -partite correlations.

In Subsec. 2.2.2, we show that  $\mathcal{D}_N$  satisfies the first and third postulates as they are clearly satisfied for having properties (i) and (ii) respectively.

However,  $\mathcal{D}_N$  evidently deviates from postulate 2. The measures of multipartite correlations are additionally expected to be monotonic under local operations. However this condition is often relaxed in practice, e.g., for quantum discord [103, 126, 127]). For  $\mathcal{D}_N$ , the monotonicity property does not hold in general. Although, property (iii) puts a bound on its maximal violation. For this postulate to hold, we must have  $\mathcal{D}_N(\bar{\rho}) \leq \mathcal{D}_N(\rho)$  where

$$\bar{\rho} = \Lambda_1 \otimes \Lambda_2 \otimes \dots \otimes \Lambda_N \rho.$$

For this constraint to hold, it is necessarily required to be translated to the conditional mutual information, i.e.,  $\min I(\bar{\rho}) \leq \min I(\rho)$ . This is not true in general and here we provide an example where  $\mathcal{D}_3$  increases under local operation on the system in the condition.

We consider a classical state,

$$\rho = \frac{1}{2}|000\rangle\langle 000| + \frac{1}{8}|101\rangle\langle 101| + \frac{1}{8}|110\rangle\langle 110| + \frac{1}{4}|111\rangle\langle 111| \quad (2.72)$$

has its 3-dependence equals  $\mathcal{D}_3(\rho) = I(X_2 : X_3|X_1) = 0.06$ . This result also implies that the conditioning on  $X_1$  gives the smallest conditional mutual information. Now we pass this state through an amplitude-damping channel. The channel can be represented in terms of the Kraus operators [18] given by,

$$\begin{aligned} K_0 &= \begin{pmatrix} 0 & 1/\sqrt{2} \\ 0 & 0 \end{pmatrix}, \\ K_1 &= \begin{pmatrix} 1 & 0 \\ 0 & 1/\sqrt{2} \end{pmatrix} \end{aligned} \quad (2.73)$$

which applies on subsystem  $X_1$  and produces some state denoted by  $\bar{\rho}$ . We then computed  $\mathcal{D}_3$  for this state. After passing through the channel, the state has  $\mathcal{D}_3(\bar{\rho}) = I(\bar{X}_1 : X_2|X_3) = I(\bar{X}_1 : X_3|X_2) = 0.19$  which, in turns, proves that in this case,

$$\mathcal{D}_N(\bar{\rho}) \geq \mathcal{D}_N(\rho).$$

Therefore, it is proved that postulate 2 does not hold for multipartite dependence in general. Moreover, it also changes in the conditioned subsystem that minimizes the dependence. Therefore, it is evident that local operation on  $X_1$  has increased the information  $I(X_2 : X_3|\bar{X}_1)$  above the other two conditional mutual informations. Also, from property (iii) we see that,

$$\bar{\mathcal{D}}_N \leq \mathcal{D}_N + I(X_2X_3 : X_1) - I(X_2X_3 : \bar{X}_1). \quad (2.74)$$

This inequality must hold and the value of the right hand side is  $\frac{3}{4}$ . Therefore this example also proves the validity of the bound provided in property (iii). Moreover, it also has a clear interpretation that the local operations that uncorrelate a given subsystem from the others may lead to information gain when the less correlated party cooperates with other parties.

The conditional mutual information between variables  $X_1$  and  $X_2$  is monotonic under local operations on subsystems not in the condition [125]. But we have proved that the following inequality is satisfied under local operations on arbitrary subsystem (being the

origin of property (iii)):

$$I(\bar{X}_1 : \bar{X}_2 | \bar{X}_3 \dots \bar{X}_N) \leq I(X_1 : X_2 | X_3 \dots X_N) + I(X_1 X_2 : X_3 \dots X_N) - I(X_1 X_2 : \bar{X}_3 \dots \bar{X}_N). \quad (2.75)$$

The last two terms is non-negative all together due to the data processing inequality and it quantifies how much the local operations have uncorrelated the variables in the condition  $X_3 \dots X_N$  from the variables  $X_1 X_2$ . This sets the upper bound to the lack of monotonicity of the conditional mutual information. This lack of monotonicity under local operations has been discussed in the context of complexity measures for multipartite systems [128, 129, 130]. The measures introduced in the above mentioned references involve a different concept of correlation. Such correlations are interpreted in terms of the number of particles that have to be coupled in the Hamiltonian for which the discussed state is a thermal state. However, these measures are of similar spirit to the dependence as they capture the improvement in approximating a given distribution when more and more particles are coupled in the Hamiltonian.

### 2.3.2 Dependence without correlations

We now investigate the relationship between multipartite dependence and multipartite correlations and it turns out that multipartite dependence can exist in absence of multipartite correlations and vice versa. The cluster states is one such example where the state give rise to non-vanishing  $N$ -partite correlations which is defined by non-zero  $N$ -partite correlation tensor, while  $\mathcal{D}_N$  vanishes. Therefore  $N$ -partite correlations can exist without  $N$ -partite dependence.

Conversely, the dependence can also be non-zero even in states with no  $N$ -partite correlations. To demonstrate this, we consider the state,

$$\rho_{\text{nc}} = \frac{1}{2} |D_N^1\rangle\langle D_N^1| + \frac{1}{2} |D_N^{N-1}\rangle\langle D_N^{N-1}|, \quad (2.76)$$

where,  $D_N^k$  is the  $N$ -partite Dicke state with  $k$ - excitations. This state has a non-vanishing  $\mathcal{D}_N$  value that has been provided in Tab. 2.3. Interestingly, this state, despite of being genuinely entangled, has no  $N$ -partite correlations [84]. This is a proof that multipartite dependence is distinct from multipartite correlations as quantified by the correlation tensor of the highest rank.

### 2.3.3 Entanglement without dependence

An intriguing question in the theory of multipartite entanglement is whether entanglement can exist without classical multipartite correlations. It is important to note that

these classical multipartite correlations may not refer to the genuine multipartite correlations that are defined with respect to the postulates in [15]. There are several such examples of  $N$ -party entangled states having vanishing  $N$ -party classical correlations in the literature [131, 132, 133, 134, 135]. However, the corresponding notions of classical correlations do not satisfy all the postulates of Refs. [15, 24]. In this subsection we address the question whether there are genuinely multipartite entangled states with no multipartite dependence or not. The answer to this question is affirmative. Examples can be found even for pure genuinely multipartite entangled states which have vanishing multipartite dependence.

For example, any  $N$ -qudit cluster state including linear, ring, and 2D, which have been mentioned in the previous chapter with  $N \geq 4$  have vanishing dependence value. In other words, cooperating among the subsystems does not have any role in gaining information about the subsystem under consideration (for  $k$ -partite independence when  $k = N$ , see Subsec. 2.1.5). In Ref. [115] it has been shown that all single-particle subsystems are completely mixed and there exists at least one pair of subsystems in the bipartite completely mixed state. The corresponding entropies are equal to  $S(\rho_i) = 1$  and  $S(\rho_{ij}) = 2$ , and lead to  $\mathcal{D}_N = 0$ , due to Eq. (2.17). Therefore, the information about the subsystem under consideration cannot be increased by bringing the other subsystems together. This fact also explains the impossibility of the corresponding secret sharing task [136, 137, 138]. It is also important to note that there exist other subsets of observers who can successfully run secret sharing using a cluster state.

### 2.3.4 Connections to the costs of merging and Markov Chains

We know that conditional mutual information can be represented as,

$$I(X_1 : X_3|X_2) = S(X_1|X_2) + S(X_3|X_2) - S(X_1X_3|X_2), \quad (2.77)$$

where  $S(X_i|X_j)$  is defined as the entanglement cost of merging a state  $X_i$  with  $X_j$  [139]. Therefore conditional mutual information can be interpreted as the extra cost of merging states one by one ( $X_1$  with  $X_2$  and  $X_3$  with  $X_2$ ) instead of altogether ( $X_1X_3$  with  $X_2$ ). In such a scenario,  $\mathcal{D}_3$  can then be seen as the minimum extra cost of merging parties individually instead of all together.

Quantum conditional mutual information also appears in the definition of Markov chains and for a tripartite state  $\rho_{123}$ , vanishing  $I(X_1 : X_3|X_2) = 0$  means that there exists a recovery map  $\mathcal{R}_{X_2 \rightarrow X_2X_3}$ , such that  $\rho_{123} = \mathcal{R}_{X_2 \rightarrow X_2X_3}(\rho_{12})$ . In other words, the global state can be recovered by applying map from  $X_2$  to  $X_2X_3$  on marginal  $X_1X_2$  and the global state is then called a quantum Markov chain. The state  $\mathcal{R}_{X_2 \rightarrow X_2X_3}(\rho_{12})$  also has a high fidelity with  $\rho_{123}$  for all states with a small  $I(X_1 : X_3|X_2)$  [140]. Therefore, a small value of  $\mathcal{D}_3$  implies

that there exists a subsystem from which the global state can be recovered whereas a large value of  $\mathcal{D}_3$  indicates that there is no such subsystem. However, our quantity is designed to be sensitive to genuinely multipartite properties of the state only.

## 2.4 Applications

### 2.4.1 Quantum secret sharing

Quantum secret sharing (QSS) [25, 26, 27, 28] is a fundamental primitive in the field of cryptography for creating highly secured multipartite quantum protocols. Hence it has an important role to play in quantum information theory. In secret sharing protocol, a message is being split into several parts such that the message cannot be retrieved by any subset of the parts unless the entire set is accessible. One of the parties initially possess the entire message which he or she then breaks into parts and shares to the remaining parties. The parties must collaborate with each other afterwards, in order to retrieve the message.

Multipartite dependence can have an intuitive application in such protocol.  $\mathcal{D}_N$  becomes useful when an additional constrain is imposed over the parties that the secret could be shared by any of them. This situation can be called as the *symmetric secret sharing*.

In the tripartite scenario, the protocol demands collaboration among two parties to read out the message conveyed by the sender party. For classical secret sharing, this message can be interpret as a random variable, e.g., the measurement outcome of, say, the first party, shared by the sender party, say  $X_1$ . It is thus required that both the receiving parties has only little or no information about the secret individually, i.e.,  $I(X_1 : X_2)$  and  $I(X_1 : X_3)$  are small. However, by collaborating with each other, the receiver parties can reveal the secret message, i.e.,  $I(X_1 : X_2X_3)$  is large or unity. Therefore,  $\mathcal{D}_3$  is clearly the relevant figure of merit as it is a minimization of conditional mutual information over all permutation as described in Eq.(2.8). For  $\mathcal{D}_3$  being significantly greater than zero, the conditional mutual information  $I(X_i : X_j|X_k)$  is large for any permutation of parties. Now, given the chain rule

$$I(X_i : X_jX_k) = I(X_i : X_k) + I(X_i : X_j|X_k),$$

we can conclude that  $I(X_i : X_jX_k)$  is also large or unity. Therefore, the secret can be generated by any of the parties.

In the quantum version of this protocol, the state  $\rho_{\max}$  in Eq. (2.63) happens to be a good choice to perform the task. By sharing this state, the parties admit perfect correlations along

complementary local measurements. And by following the protocol in [27], the quantum solution to the secret sharing problem offers additionally security against eavesdropping. In [96] such security has been quantified in terms of the conditional mutual information.

To demonstrate the relevance of multipartite dependence in a slightly altered scenario which we now formally define the QSS task below.

We assume that the sender party Alice has a quantum state  $\rho$  which contains the secret message. Alice wants to split the state into  $n$  shares in such a way that the secret message can only be recovered if all the  $n$  shares are accessible by one of the receiver party. Then a QSS scheme in [28] states that there exists a map  $\mathcal{E}_n : A \rightarrow X^{\otimes n}$  such that,

$$C_Q(\text{Tr}_k \circ \mathcal{E}_n) = 0 \quad (2.78)$$

where  $\text{Tr}_k$  is the partial trace over an arbitrary set of subsystems and  $C_Q(\Lambda)$  is the quantum capacity of the channel  $\Lambda$ . In the theory of quantum communication, this quantity quantifies the highest rate at which quantum information can be communicated over many independent uses of a noisy quantum channel from a sender to a receiver. Eq. (2.78) implies that if the map is performed over a state, then the rate at which quantum information can be communicated is zero when a subset of subsystems is traced out. In other words, this condition ensures that the message is not recoverable by any subset of the shared parts and hence only possible when all parts are together. Asymptotically, a scheme with rate  $R$  allows sharing quantum secrets of size  $nR$  using  $n$  copies of the channel.

Now we show that  $\rho_{\max}$  is likely to be the most suitable choice for the QSS scheme, i.e, to read out the secret of the sender party which was initially encoded into a state and distributed among the parties after dividing the state into subsystems, by collaborating among the remaining two parties. Let us assume that in this protocol a single qubit quantum secret  $\rho$  needs to be shared. Alice then use the teleportation protocol with postselection such that there is no need to perform any correcting measurement on her side with state  $\rho$  and one subsystem of  $\rho_{\max}$  in her possession. By doing so she performs the encoding map  $\mathcal{E}_{N-1}$  to her qubit which results in the following state for the rest of the parties.

$$\mathcal{E}_{N-1}(\rho) = \frac{1}{2^{N-1}} \left( \sigma_0^{\otimes N-1} + (-1)^{N/2} \sum_{j=1}^3 \sigma_j^{\otimes N-1} \text{Tr}(\sigma_j^T \rho) \right). \quad (2.79)$$

In this way Alice prepares  $n = N - 1$  shares of the secret. Let us denote the resultant state as  $\rho_{N-1}$ . Since  $\rho_{\max}$  is an  $N - 1$ -uniform state, tracing out any one or more of the parties results in a maximally mixed reduced state. Interestingly, the state  $\rho_{N-1}$  is also  $N - 2$ -uniform. This implies that the secret cannot be retrieved unless we have all shares,

because

$$(\text{Tr}_k \circ \mathcal{E}_{N-1})(\rho) \propto \mathbb{1}, \quad \text{for any } \rho, \quad (2.80)$$

and the condition in Eq. 2.78 is satisfied.

In the next step, we will show that all the receiver parties can recover the message by the following “reverse” teleportation scheme. We take an  $(N - 1)$ -uniform state  $\rho_{\max}$  as a resource and conduct a joint measurement in the basis  $\{(\mathbb{1} \otimes \cdots \otimes \mathbb{1} \otimes \sigma_{\mu_1} \otimes \cdots \otimes \sigma_{\mu_{N-1}})|\Psi\rangle\}$ , where  $\mu_n = 0, 1, 2, 3$  and

$$|\Psi\rangle = \frac{1}{\sqrt{2^{N-1}}} \sum_{j_1 \dots j_{N-1}=0,1} |j_1 \dots j_{N-1}\rangle \otimes |j_1 \dots j_{N-1}\rangle. \quad (2.81)$$

This state is a maximally entangled state. We will now perform measurement on the shares  $\rho_{N-1}$  and  $N - 1$  subsystems of  $\rho_{\max}$ . If the outcome corresponds to the projection  $|\Psi\rangle\langle\Psi|$ , then the remaining qubit in  $\rho_{\max}$  is in the state  $\rho$ , otherwise there always exists a unitary depending on the outcome that transform the single qubit to  $\rho$ . Therefore, the state  $\rho_{\max}$  enables a perfect QSS protocol among an arbitrary number of parties.

We can now show that any  $N$ -partite state  $\rho_c$  with maximally mixed marginals and non-classical dependence  $\mathcal{D}_N(\rho_c) > 1$  is always useful for QSS. We consider the encoding map  $\mathcal{E}_c : A \rightarrow X^{\otimes N-1}$  with the Choi state given by  $\rho_c$  [141], i.e.,  $(\mathbb{1} \otimes \mathcal{E}_c)(|\Phi\rangle\langle\Phi|) = \rho_c$ , where  $|\Phi\rangle$  is the maximally entangled state. The rate of quantum secret sharing admits the lower bound

$$R = C_Q(\mathcal{E}_c) \quad (2.82a)$$

$$\geq \sup_{\phi_{A'A}} -S_{A'|X_1 \dots X_{N-1}}((\mathbb{1} \otimes \mathcal{E}_c)(\phi_{A'A})) \quad (2.82b)$$

$$\geq -S_{A'|X_1 \dots X_{N-1}}(\rho_c) \quad (2.82c)$$

$$= I(A' : X_1 | X_2 \dots X_{N-1}) - S(A' | X_2 \dots X_{N-1}) \quad (2.82d)$$

$$= I(A' : X_1 | X_2 \dots X_{N-1}) - 1 \quad (2.82e)$$

$$\geq \mathcal{D}_N(\rho_c) - 1. \quad (2.82f)$$

Above, the first ineq. (2.82b) is the result of computing the quantum capacity of a channel [142, 143, 144, 145, 146, 87] with system  $A'$  being of the same dimension as system  $A$  and where  $S_{A'|X_1 \dots X_{N-1}}(\rho)$  is the quantum conditional entropy of state  $\rho$ . The second ineq. (2.82c) follows because the maximally entangled state is a particular choice of  $\phi_{A'A}$ , and from the definition of  $\rho_c$ . Eq. (2.82d) follows from the properties of entropy, and lastly eq. (2.82e) follows from the assumption that the state has maximally mixed marginals for being a  $N - 1$ -uniform state. Finally, the dependence bounds conditional mutual in-

formation from bellow. Similar to the marginals of  $\rho_c$ , the marginals of the encoded state  $\rho_{N-1} = \mathcal{E}_c(\rho)$  are maximally mixed. Therefore, no subset of parties can recover the quantum message alone, yet for all of them together  $R > 0$  holds for  $\mathcal{D}_N(\rho_c) > 1$ . This lower bound is tight and can be achieved by using the  $(N - 1)$ -uniform states [114]. Therefore, dependence of the Choi state corresponding to the QSS map bounds the rate of the QSS protocol. Also, we should note that  $\rho_{max}$  gives us the highest possible dependence. Therefore, the dependence of the state shared among the parties also serves as a figure of merit for this protocol. As a matter of fact, all degradable channels give rise to the equality in (2.82b) and all symmetric states admit the equality in (2.82f). For pure states, the lower bound for the rate of QSS scheme is zero. On the other hand, by using GHZ state, one can achieve a unit rate [27]. As GHZ state gives classically correlated marginals rather than the maximally mixed state, the conditional entropy in Eq. (2.82d) vanishes and the rate is lower bounded by the dependence alone, which is 1 for the GHZ state.

From a more practical prospective, we consider the scenario where a subset of  $k$  parties is required to read the message. Analogous to the previous argument, it can be shown that the dependence  $\mathcal{D}_k$  can be considered as the figure of merit for sharing the secret among any  $k$ -partite subsystem of  $N$ -party state where anyone could be the sender.

## 2.4.2 Witnessing entanglement

Using the constraint  $\mathcal{D}_N > 1$ , we will now prove that  $\mathcal{D}_N$  can be utilized as an witness of quantum entanglement. For  $\mathcal{D}_N > 1$ , we know that,

$$I(X_1 : X_2 X_3 \dots X_N) > 1, \quad (2.83)$$

for all possible permutations of indices. Here, without any loss of generality we have assumed that the smallest difference of mutual informations, i.e., the value of  $\mathcal{D}_N$ , is found for an arrangement of subsystems such that  $\mathcal{D}_N = I(X_1 : X_2 X_3 \dots X_N) - I(X_1 : X_3 \dots X_N)$  yields the minimum value. Now, we write  $I(X_1 : X_2 X_3 \dots X_N)$  using quantum conditional entropies.

$$\begin{aligned} I(X_1 : X_2 X_3 \dots X_N) &= S(\rho_{X_1}) - S_{X_1|X_2 X_3 \dots X_N}(\rho) > 1 \\ \implies S_{X_1|X_2 X_3 \dots X_N}(\rho) &< -1 + S(\rho_{X_1}), \end{aligned} \quad (2.84)$$

for the subsystems who have equal dimensions  $S(\rho_1) \leq 1$ . This implies that quantum conditional entropy is necessarily negative in the above equation. Now, according to [104], a negative quantum conditional entropy is possible only when the state is entangled. However, this entanglement need not to be necessarily genuinely multipartite. For a negative value of conditional entropy in a particular cut, e.g.,  $S_{X_1|X_2 X_3 \dots X_N}$ , we know that entan-

gement is present in the cut  $X_1|X_2X_3 \dots X_N$ . Eq. (2.63) is an example of a particular state which violates the bound of 1. This state can be written as a mixture of correlated Bell states [116], also known as the Smolin state, and can have the form,

$$\rho_s = \sum_{i=1}^4 \alpha_i |\psi_i\rangle\langle\psi_i|^{\otimes N/2}, \quad (2.85)$$

where,  $|\psi_i\rangle$  are the four Bell states. and therefore is biseparable which demonstrates the fact that entanglements that are not genuine can be detected by this bound. Furthermore, similar proof can be given for arbitrary number of subsystems  $k$ , i.e. whether  $\mathcal{D}_k > 1$  any  $k$ -party subsystem is entangled or not. An example of such detection is provided in Tab. 2.3 for the four-party subsystems of absolutely maximally entangled state of 6 qubits.

### 2.4.3 Data science

Multipartite dependence is also expected to find its applications outside physics. As an example, we sketch how it can be useful in data science. To do so, we consider the problem of feature selection. It is concerned with finding a subset or reduced version of an original features of a dataset, such that the predictions made on the basis of the subset would be the same as based on the entire set. In other words, we would like to eliminate variables that are not essential. Such variables can be identified from the conditions of extremal dependence. This follows from the fact that variables that minimizes the conditional mutual information and hence provides the dependence value can be ignored because they produce the least information about the other party. Some other functions of conditional mutual information were also considered in feature selection [147, 148].

We first analyze the case where  $\mathcal{D}_N \approx 0$ . Let us assume that the minimizing conditional information is

$$I(X_1 : X_2|X_3 \dots X_N) \approx 0. \quad (2.86)$$

Therefore either variable  $X_1$  or  $X_2$  can be eliminated as it does not improve the information between the remaining variables, e.g.,  $I(X_1 : X_2X_3 \dots X_N) \approx I(X_1 : X_3 \dots X_N)$ . Now, the  $\mathcal{D}_N \approx 1$  corresponds to the situation where each variable is independent of the rest, e.g.,  $I(X_1 : X_3 \dots X_N) \approx 0$ . And hence at first sight one would have to keep track of all of them, but from  $N - 1$  variables one can predict the remaining one, e.g.  $I(X_1 : X_2X_3 \dots X_N) \approx 1$ . Accordingly, one variable can be eliminated. Therefore,  $\mathcal{D}_N$  can be useful in performing such tasks.

$N$	state	$\mathcal{D}_3$	$\mathcal{D}_4$	$\mathcal{D}_5$	$\mathcal{D}_6$
3	$\{P_{\text{same}}\}$	0	-	-	-
3	$\{P_{\text{even}}\}$	1	-	-	-
3	GHZ	1	-	-	-
3	$D_3^1$	0.9183	-	-	-
3	$D_3^2$	0.9183	-	-	-
3	$\rho_{\text{nc},3}$	0.5033	-	-	-
4	GHZ	0	1	-	-
4	$D_4^1$	0.3774	0.62256	-	-
4	$D_4^2$	0.5033	0.7484	-	-
4	$\Psi_4$	0.4150	0.4150	-	-
4	$L_4$	1	0	-	-
4	3-uniform	0	2	-	-
5	GHZ	0	0	1	-
5	$D_5^1$	0.2490	0.2490	0.4729	-
5	$D_5^2$	0.3245	0.3245	0.6464	-
5	$D_5^3$	0.3245	0.3245	0.6464	-
5	$\rho_{\text{nc},5}$	0.1710	0.6490	0.4729	-
5	$L_5$	0	0	0	-
5	$R_5$	1	1	0	-
5	AME(5,2)	1	1	0	-
6	GHZ	0	0	0	1
6	$D_6^1$	0.1866	0.1634	0.1866	0.3818
6	$D_6^2$	0.2566	0.1961	0.2566	0.5637
6	$D_6^3$	0.2729	0.1961	0.2729	0.6291
6	$L_6$	0	0	0	0
6	$R_6$	0	0	0	0
6	AME(6,2)	0	2	0	0
6	5-uniform	0	0	0	2

Table 2.3:  $\mathcal{D}_N$  values for different quantum states and probability distributions.

## 2.5 Conclusions

In this chapter we have introduced multipartite dependence  $\mathcal{D}_N$  as a new tool for the characterisation of quantum states as well as the classical joint probability distributions. Multipartite dependence can be seen as the method of choice to determine whether and by what amount cooperation between any subsystems brings additional information about the remaining subsystems. We have investigated its characteristics in details and provided key properties in support. We have discussed these properties in details and we have compared them with the postulates that need to be satisfied for a quantifier to quantify multipartite correlations. It turns out that despite of sharing many traits with multipartite correlation quantifier, multipartite dependence is evidently distinct from them.

We have also provided evidence of the fact that non-vanishing dependence value can exist where there is no multipartite correlation. In other words This strengthen the argument of dependence being an unique quantifier of multipartite characteristics. The dependence is directly calculable and has a clear interpretation. We have investigated several aspects of this quantity. Importantly, we have seen that entanglement in multipartite systems can exist despite of having zero  $\mathcal{D}_N$  value. While pure states can only attain the classical bound 1, we have shown that multipartite dependence attains highest values for mixed states. This can be highlighted as an interesting feature of mixed states. We also found the  $n$ -qudit state that maximizes multipartite dependence. Interestingly, these states are the  $(N - 1)$ -uniform states.

Finally, several applications of multipartite dependence have also been identified here such as quantum secret sharing, entanglement witness and data science which clearly indicating its relevance for future studies in quantum communication and elsewhere.

## Simultaneous multiphase estimation with Heisenberg scaling

The principal aim of *quantum metrology* [149, 150, 151, 152, 153, 154, 155, 156] is to make high precision measurements of given parameters exploiting quantum systems and quantum resources which are not attainable using classical approaches. In recent years, quantum metrology has gained attention due to its wide spread applications in fields such as the gravitational wavedetection [157], quantum imaging [158, 159], quantum spectroscopy [160].

Attaining the highest possible precision limit for a given parameter is seemingly a difficult task when the number of measurements is limited. Lack of sufficient prior information about the parameter makes the problem "global" in a sense that it requires the cost function to be minimized over a certain region. Such a situation is usually resolved by minimizing the mean of the cost function or minimizing the worst case over the region [161, 162, 163]. The problem, however, becomes asymptotically "local" when the number of measurements is asymptotically large. In that case, a well-behaved cost function can be approximated by the variance [164] and precision limit can be quantified by the quantum Cramér-Rao bound [165, 166].

A standard estimation protocol typically includes four major steps as follows:

- (1) preparation of the probe state;
- (2) encoding of the parameters via evolution;
- (3) measurement;
- (4) classical estimation.

We further discuss these steps in Subsec.3.1.1 with more details. One of the problem of *simultaneous estimation of multiple parameters* is the possibility of the occurrence of correlations between the estimators corresponding to different parameters. This complication can result in decrease in the overall precision of joint estimation [151]. Also, it has been shown in [167] that the number of simultaneously estimable parameters reduces when an external reference mode is absent. This is because the absence of external mode causes the immeasurability of global phases.

Another difficulty arises from the inability of utilizing the most important tool of parameter estimation, i.e., the quantum Cramér-Rao bound (QCRB). This bound utilizes the inverse of Quantum Fisher Information (QFI) to provide an upper limit to the variance of any unbiased estimator of a deterministic parameter. However, for estimating multiple parameters at a time with utmost precision, one need to incorporate the generalized form of QFI [168], i.e., the Quantum Fisher Information Matrix (QFIM) [153]. In QFIM, the diagonal entries simply produce the QFI. Despite of sharing similar significance in quantum theory as QFI, QFIM happens to reflect very different properties and behaviors compared to QFI [150]. For sufficiently uncorrelated parameters, QFIM is non-singular and the inverse of it bounds the covariance matrix of the estimated parameters from below. This bound is known to be the multiparameter version of QCRB. The elements of QFIM depend on the size of the initial probe state. However, in our setup, having highly correlated phases prevents us from having a QFIM that is invertible and hence making QCRB directly inapplicable.

In this chapter we discuss the simultaneous estimation of multiple phases scenario for 3- and 4-port generalised Mach-Zehnder interferometer [169]. Extensive works can be found in literature concerning multiphase estimation with symmetric multiports [170, 171, 172, 173, 174]. In this estimation scheme the number of parameters to estimate is  $d - 1$ , given the total number of modes to be  $d$ . The remaining phase is known and acts as a reference.

In this work, we take a different approach to estimate multiple phases. We take the following measures that are described in details in this chapter,

- We assume that the phases are placed in each mode of the  $d$ -mode interferometer. We show that there is a possibility of obtaining a precision of order  $1/N^2$ , which is the so-called Heisenberg-like (HL) scaling of precision [175, 176, 177, 178, 179, 180, 181, 182, 183, 184] for simultaneous estimation of any  $(d - 1)$ -element subset of the phases in a completely fixed interferometric setup for  $d = 3, 4$ .
- we are not using the methods of QCRB, which in our case would not guarantee

achievability of the Heisenberg-like scaling with the same fixed setup; instead we use directly the method of classical Fisher-information-based analysis on the basis of output probabilities, which does not raise the questions of achievability, as no implicit optimisation over measurement procedure is included.

- We also assume the input state with arbitrary number of photons which allows directly for asymptotic scaling discussions.

Besides the primary objective of presenting estimation scheme for 3- and 4-port generalised Mach-Zehnder interferometer, we also show that it is possible to construct a 5-mode fully symmetric multipoint which can be generated by a symmetric Hamiltonian. This result disproves the previous claims by Zeilinger et. al [185] in this scenario.

## 3.1 Prerequisites and the Setup

### 3.1.1 General introduction to multiphase estimation

The description of a standard approach to multiparameter estimation can be found widely discussed in literature [150, 152, 151]. In this subsection we describe the fundamental steps of the estimation process in details that we have mentioned in the introduction.

The first step is to prepare a *probe state* for the estimation setup. Keeping in mind that the aim is to optimize the setup such that the precision is maximized, we prepare a  $N$ -partite state that is optimal and we introduce this as the initial probe state,  $\rho_{in}$ . In the next stage, called as *parametrization*, the probe state undergoes an evolution which is characterized by a quantum channel  $\Lambda_{\vec{\alpha}}$  and is a CPTP map in general. This evolution is characterized in terms of a vector of unknown parameters  $\vec{\alpha} = (\alpha_1, \dots, \alpha_d)$  whose elements are the key ingredients to estimate the phases. In other words, this evolution encodes necessary information in the state  $\rho_{in}$  that are essential for the estimation. After the evolution, in the third step, single-particle projective measurements  $\{\Pi\}_k$  are performed. We label the outcomes as  $k$ 's with the use of which we determine the final probability distribution. Therefore the probability distribution will have the form,

$$p(k|\vec{\alpha}) = \text{Tr}(\Lambda_{\vec{\alpha}}(\rho_{in})\Pi_k). \quad (3.1)$$

After determining the parameter-dependent probability distribution  $p(k|\vec{\alpha})$ , the final task is to construct a set of estimators,  $\vec{A} = \{A_i\}$ , to determine the unknown parameters  $\vec{\alpha} = \{\alpha_i\}$ .

### 3.1.1.1 Cramer-Rao bound

As we are estimating a number of parameters at the same time, we need to estimate the joint accuracy of these estimators. In order to do so, we introduce a joint measure of sensitivity of the distribution  $p(k|\vec{\alpha})$  on the parameters  $\{\alpha_i\}$ . In classical estimation theory such a measure is provided by the Fisher Information Matrix (FIM). FIM is well-established in the field of statistics and is often considered as a function of sensitivities. It is represented in terms of the partial derivatives of outputs with respect to faults and uncertainty which, in turns, indeed quantify the sensitivity of the probability distribution over the parameters. In the most simple terms, it can be said that FIM is a way of quantifying the information that a realisation of a random variable carries about an unknown phase. FIM is defined as:

$$\mathcal{F}_{ij}(\vec{\alpha}) = \sum_k \frac{\partial_{\alpha_i} p(k|\vec{\alpha}) \partial_{\alpha_j} p(k|\vec{\alpha})}{p(k|\vec{\alpha})}. \quad (3.2)$$

As evident from the above expression, FIM is a matrix that is constructed in terms of the partial derivatives of the probability distribution with respect to the parameters that we are supposed to estimate. Now,  $p(k|\vec{\alpha})$  carries the information about the parameters. The greater value of the derivative, the more precise is the estimation.

The estimators,  $\{A_i\}$ , are called unbiased if their mean values equal to  $\{\alpha_i\}$  for the entire range of  $\alpha$ 's. In such a scenario, the  $\mathcal{F}$  matrix is often invertible [186] which is essential to formulate the *original* Cramer-Rao bound. However, one should note that we can have biased estimators and can still formulate the bound, which is slightly more complicated than the original bound [187]. Moreover there also exists constrained Cramér–Rao Bound With a singular FIM [188]. When the parameters are sufficiently uncorrelated, the FIM is invertible the quality of estimation of  $\{\alpha_i\}$  based on distribution  $p(k|\vec{\alpha})$  is described by the *Cramer-Rao bound* [186]:

$$\text{Cov}(\vec{A}) \geq \frac{\mathcal{F}^{-1}}{\nu}, \quad (3.3)$$

where  $\text{Cov}(\vec{A})$  is the covariance matrix for the estimators given by

$$\text{Cov}(\vec{A})_{mn} = \text{Cov}(A_m, A_n) = \langle (A_m - \langle A_m \rangle)(A_n - \langle A_n \rangle) \rangle, \quad (3.4)$$

and  $\nu$  is the number of repetitions of the experiment. The quantity covariance is a measure of the joint variability or sensitivity of two random variables. Hence the covariance is a  $d \times d$  matrix each element of which gives the covariance between estimators corresponding to each pair of parameters in  $\vec{\alpha}$ . Covariance matrix is symmetric and positive semi-definite. By knowing this quantity, we can then calculate the efficiency of the estimators.

### 3.1.1.2 Quantum Cramer-Rao bound

In the case of quantum estimation theory, we are now interested in description of efficiency of estimation of  $\alpha$ 's from an evolved quantum state  $\rho_{out}(\vec{\alpha}) = \Lambda_{\vec{\alpha}}(\rho_{in})$  in a way which assumes optimisation over all possible measurements. Analogous to its classical counterpart, we will now consider quantum fisher information matrix (QFIM) to bound the joint measure of sensitivity. QFIM, defined in an operator-based way, has the following form:

$$\mathcal{F}_{ij}^Q = \frac{1}{2} \text{Tr}[\rho_{out}(\vec{\alpha})\{L_i, L_j\}], \quad (3.5)$$

where  $\{L_i, L_j\}$  denotes anticommutator of operators between  $L_i$  and  $L_j$  and the operators  $L_i$  are defined implicitly by the equation:

$$\frac{1}{2}\{L_i, \rho_{out}(\vec{\alpha})\} = \partial_{\alpha_i}\rho_{out}(\vec{\alpha}). \quad (3.6)$$

In the case of pure input state  $|\psi\rangle$  and the unitary evolution of the form  $U = e^{-iH_i\alpha_i}$  the QFIM can be expressed in an explicit and neater form:

$$\mathcal{F}_{ij}^Q = 4\langle \text{cov}H \rangle_{\psi} = 4(\langle H_i H_j \rangle_{\psi} - \langle H_i \rangle_{\psi} \langle H_j \rangle_{\psi}). \quad (3.7)$$

Similar to FIM, QFIM is also invertible when the parameters are sufficiently uncorrelated. Then the covariance matrix of the estimated parameters is bounded from below by the inverse of the QFIM and is given by a multiparameter version of the *Quantum Cramer-Rao bound* (QCRB) [151],

$$\text{Cov}(\vec{A}) \geq \frac{(\mathcal{F}^Q)^{-1}}{\nu}. \quad (3.8)$$

Given an  $N$ -partite state, the elements of QFIM can depend at most quadratically on  $N$ , i.e., upto the HL scaling. This precision of multiparameter estimation can be attained using an entangled state as probe and some measurement strategy, which in principle demands the use of arbitrary multiports [189, 149, 190, 191, 192, 152]. HL scaling is achievable in the asymptotic limit for large  $N$ . Given a new "quantum" bound on the covariance matrix, similar to the classical case, we can again estimate the achievable precision of the given setup.

A relevant bound that concerns multiphase estimation which is also considered as another version of the Quantum Cramer-Rao bound and does not utilise the QFIM, is known as the *Holevo bound* [193, 151, 194]. This bound provides an upper bound on the information contained in a quantum system that uses a fixed initial state and is expressed using the notion of a cost matrix, denoted as  $\mathcal{C}$ .  $\mathcal{C}$  is a positive matrix providing weights to the uncertainties related with different parameters. The Holevo bound has the following

form [151]:

$$\mathrm{Tr}(\mathcal{C} \mathrm{Cov}(\{A_i\})) \geq \min_{\mathcal{X}_i} \left( \mathrm{Tr}(\mathcal{C} \mathrm{Re}(\mathcal{V})) + \|\sqrt{\mathcal{C}} \mathrm{Im}(\mathcal{V}) \sqrt{\mathcal{C}}\| \right), \quad (3.9)$$

where the norm in the RHS of (3.9) is the trace norm and the matrix  $\mathcal{V}$  is defined element-wise by the relation

$$\mathcal{V}_{ij} = \mathrm{Tr}(\mathcal{X}_i \mathcal{X}_j \rho_{out}(\vec{\alpha})). \quad (3.10)$$

$\mathcal{X}_i$ 's are Hermitian matrices constrained by,

$$\mathrm{Tr}(\{\mathcal{X}_i, L_j\} \rho_{out}(\vec{\alpha})) = 2\delta_{ij}, \quad (3.11)$$

where the operators  $L_i$  are defined in (3.6).

### 3.1.1.3 Multiparameter Cramer-Rao bound with additional parameters

In the literature, attempts have been made to show whether the bounds (3.8) and (3.9) can be saturated by experimentally accessible measurement schemes in order to maximize the sensitivity of quantum sensors.

We particularly focus on investigating the multiphase estimation process within a *fixed* interferometer and a simple *fixed* measurement scheme consisting of single output mode measurements that is convenient for our setup as described in 3.1.2. Our approach to evaluate the precision of estimation would be based on basic tools in classical estimation theory, namely on the classical Fisher information matrix techniques. To our advantage, we also do not need to assume optimisation over all possible measurement strategies (required only for QFIM). Given that, our concern comes down to estimate the phases that depend on all the parameters that are also responsible for the characteristics of the final probability distribution. These multiple phases include both the phases that need to be estimated as well as the reference phase that is fixed and known. Such a situation in estimation theory has been discussed extensively in [195, 196].

To estimate multiple phases in our setup we divide the set of phase in two parts,  $d - 1$  number of unknown phases and the reference phase. Given that, two kind of approaches can be taken: either (i) the additional parameters are fixed and known, or, (ii) the additional parameters are fixed but unknown (and are called in this context the *nuisance parameters*). We consider our reference phase to be fixed and known.

In a general scenario, we assume that all unknown parameters and the additional known (nuisance) reference parameters are given by a vector  $(\vec{\alpha}_{\mathcal{I}}, \vec{\alpha}_{\mathcal{O}})$  ( $(\vec{\alpha}_{\mathcal{I}}, \vec{\alpha}_{\mathcal{N}})$ ). Then the Fisher Information Matrix and its inverse can be expressed in a block form with respect to the fixed partition of parameters  $(\vec{\alpha}_{\mathcal{I}}, \vec{\alpha}_{\mathcal{O}})$  and  $(\vec{\alpha}_{\mathcal{I}}, \vec{\alpha}_{\mathcal{N}})$  [196] and can be written

respectively as:

$$\mathcal{F}(\vec{\alpha}) = \begin{pmatrix} \mathcal{F}(\vec{\alpha})_{\mathcal{I},\mathcal{I}} & \mathcal{F}(\vec{\alpha})_{\mathcal{I},\mathcal{O}} \\ \mathcal{F}(\vec{\alpha})_{\mathcal{O},\mathcal{I}} & \mathcal{F}(\vec{\alpha})_{\mathcal{O},\mathcal{O}} \end{pmatrix} \quad (3.12)$$

$$(\mathcal{F}(\vec{\alpha}))^{-1} = \begin{pmatrix} \mathcal{G}(\vec{\alpha})_{\mathcal{I},\mathcal{I}} & \mathcal{G}(\vec{\alpha})_{\mathcal{I},\mathcal{N}} \\ \mathcal{G}(\vec{\alpha})_{\mathcal{N},\mathcal{I}} & \mathcal{G}(\vec{\alpha})_{\mathcal{N},\mathcal{N}} \end{pmatrix}, \quad (3.13)$$

where we use the notation  $\mathcal{G}(\vec{\alpha})$  for block of inverse of the FIM with nuisance parameters. Therefore, the Cramer-Rao bound will have the following form for the unknown set of parameters, for the case in which the additional parameters are fixed and known,

$$\text{Cov}(\{A_{\mathcal{I}}\}) \geq \frac{(\mathcal{F}(\vec{\alpha})_{\mathcal{I},\mathcal{I}})^{-1}}{\nu}. \quad (3.14)$$

In this case, the bounds are reduced to a form concerning only *inverse of the submatrix* of the FIM. Whereas for the case where the additional parameters are nuisance parameters it will be given by,

$$\text{Cov}(\{A_{\mathcal{I}}\}) \geq \frac{\mathcal{G}(\vec{\alpha})_{\mathcal{I},\mathcal{I}}}{\nu}. \quad (3.15)$$

This bound demands calculating firstly the inverse of the entire FIM and then taking blocks of the inverse matrix.

### 3.1.2 Setup for the estimation procedure

In this subsection, we describe the setup that has been considered for our simultaneous estimation scheme. The schematic of the setup is presented in Fig [3.1(a)]. Here we consider a scenario where phases are placed in between each of the internal ports of the  $d$ -mode interferometer and are represented by  $\{\alpha_1, \dots, \alpha_d\}$ . The unitary part *before* these phaseshifts is considered as the preparation procedure of the initial state and the part *after* them is treated as an implementation of the measurement. Our aim is to simultaneously estimate any  $(d - 1)$ -element subset of the set  $\{\alpha_1, \dots, \alpha_d\}$ , whereas the remaining one is known, and serves as a reference phase.

We, however, approach the scenario as a fixed single unitary operation where the goal is to investigate the metrological properties of a generalised Mach-Zehnder interferometer as a whole. *Our aim of this project is to show that with the help of having one known phase as reference, a fixed initial entangled probe state and a fixed interferometer, Heisenberg-like scaling of precision of simultaneous estimation of any  $(d - 1)$ -element subset of the phases can be attained without making any changes in the setup.*

We calibrate our setup in such a way that a fixed symmetric multiports and an  $N$ -partite entangled *probe* state is equivalent to feeding a GHZ state [197] each of whose subsystems are  $d$ -level systems through identical local unitary transformation on each site and the unitary transformation can be implemented by an additional symmetric multiport. After achieving the probe state, the standard procedure follows. Finally, we perform detailed analysis of the precision of our estimation scheme as well as develop a description of a generalised 3- and 4-mode Mach-Zehnder (MZ) interferometer [169]. Such interferometers can be realized by intertwining two symmetric multiports with single-mode phase shifters using the Heisenberg-Weyl operators.

Our setup can be presented in terms of two different configurations such that they are equivalent from the estimation perspective. Firstly, we can think of our setup in a star-like configuration as presented in Fig [3.1(b)] consisting of  $N$  local MZ interferometers. However, we can opt for a more experimentally feasible configuration with a single-interferometer version of the setup Fig [3.1(a)], which uses the so-called NOON states [198] as the initial probe states.

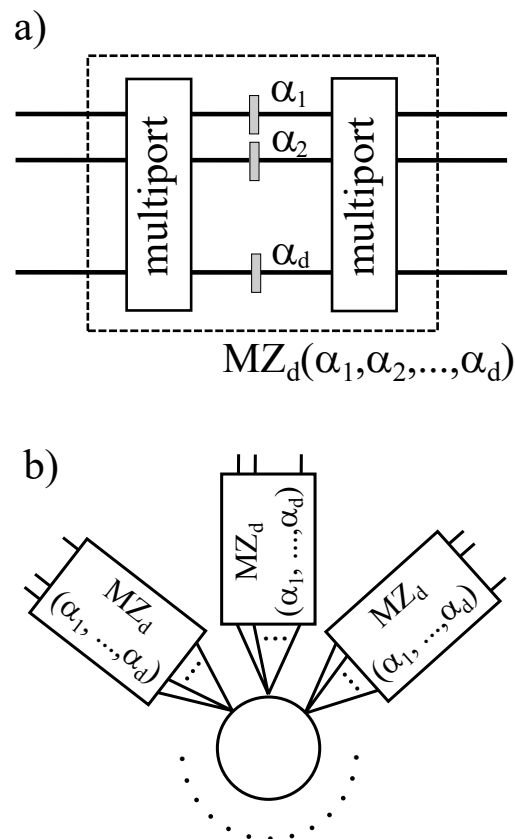


Figure 3.1: a) Schematic of a generalised  $d$ -mode Mach-Zehnder (MZ) interferometer consisting of symmetric multiports intertwined with  $d$  phaseshifts to be estimated. b) An  $N$ -party configuration of the estimation setup, which consists of a central source of GHZ-path-entangled photons and  $N$  local stations consisting of generalised MZ interferometers from Figure 1a).

## 3.2 Main Results

In this section we illustrate the main results that has been obtained. We give a detailed description of the analytical interpretation of the multiphase generalised Mach-Zehnder interferometer that has been considered for the course of our setup. Next we narrate the precision that has been attained. These results pertain to 2-, 3-, 4-mode Mach-Zehnder interferometer respectively. We make separate subsections for the single mode and five mode Mach-Zehnder interferometer for the uniqueness of their results.

### 3.2.1 Generalised Mach-Zehnder interferometer

In this section, we will provide the analytical description of our experimental setup. The setup is described in 3.1.2 and the schematic given in Figure (3.1b). It starts with a source that is producing a  $N$ -partite GHZ state of  $d$ -level subsystems. In their respective stations, each party undergoes to the same unitary evolution which is referred as the preparation symmetric multiport  $U_d$ . After this procedure, we get our probe state.

$$\begin{aligned} |\Psi^d\rangle_N &= U_d^{\otimes N} |\text{GHZ}^d\rangle_N \\ &= \frac{1}{\sqrt{d}} U_d^{\otimes N} (|\underbrace{0\dots 0}_N\rangle + |\underbrace{1\dots 1}_N\rangle + \dots + |\underbrace{d-1\dots d-1}_N\rangle). \end{aligned} \quad (3.16)$$

We will specify  $U_d$  later that are specific for each cases. Thereafter, in the next step, the probe state passes through the next stage of the  $N$  measurement stations, each of which consists of a  $d$ -mode interferometer, which is a generalised Mach-Zehnder interferometer involving  $d$  phases. Here, we should remind ourselves that only  $d - 1$  out of the total  $d$  number of phases can be estimated during this process. In this whole process, the probe state gets encoded with the information about the phases that we want to estimate and also gets measured in order to determine the probability distribution  $p(k|\vec{\alpha})$ . The generalised Mach-Zehnder interferometer [169] consists of two symmetric multiports intertwined with a series of phaseshifts on each of the  $d$  modes linking the multiports that has been described in Figure (3.1a). Such a symmetric  $d$ -mode multiport is a generalized version of balanced beam splitters where we have  $d$  inputs and  $d$  outputs. Therefore, it is a  $d$ -mode multiport with the property that a single photon entering by any of the  $d$  input modes has a uniform probability  $\frac{1}{d}$  to be detected in any of the  $d$  output modes. The entire procedure can then be represented by the unitary operator of the following form

$$U_d = SF(\alpha)S^\dagger, \quad (3.17)$$

where  $S$  is the discrete Fourier Transform that represents the role of the symmetric multi-

ports and  $F(\alpha)$  is the phase-imprinting operator.

While dealing with the current problem, it is convenient to describe the interferometer in the Hamiltonian-like form  $U = e^{-ih_i\alpha_i}$ , with an explicit form of generators corresponding to phaseshifts. The typical choice for the operator basis in order to find such generators  $h_i$  is the set of so called Gell-Mann matrices. In this work and for the particular choice of setup, we, however, found that it is much more convenient to describe the interferometers based on symmetric multiports is the Heisenberg-Weyl operator basis given by,

$$\begin{aligned} X &= \sum_{i=0}^{d-1} |i\rangle\langle i+1|, \\ Z &= \sum_{i=0}^{d-1} \omega^i |i\rangle\langle i|, \\ Y &= XZ, \end{aligned} \tag{3.18}$$

where  $\omega = \exp(2i\pi/d)$ . At this point, we are ready to present explicit form of the generator scheme that we use to describe the entire estimation procedure to estimate  $d - 1$  number of phases using  $d$ -mode MZ interferometers. We describe the scheme for  $d = 2, 3, 4$  respectively.

### 3.2.1.1 Two-mode case

For the two-mode case the Heisenberg-Weyl operators (3.18) are equivalent to the basis comprised of standard Pauli matrices. The operator representing the symmetric two-port can be expressed in the following form:

$$S_2 = \exp\left[\frac{1}{4}i\pi X\right]. \tag{3.19}$$

Next the phase-imprinting part of the interferometer has the following representation:

$$F_2(\vec{\alpha}) = \exp\left[\frac{1}{2}(\mathbb{1} + Z)i\alpha_1 + \frac{1}{2}(\mathbb{1} - Z)i\alpha_2\right]. \tag{3.20}$$

Therefore, the evolution of the entire interferometer can be expressed in the following con-

cise way where we only need the  $Y$  operators:

$$\begin{aligned}
\mathcal{U}_2 &= S_2 F_2(\vec{\alpha})(S_2)^\dagger \\
&= \exp\left[\frac{1}{4}i\pi X\right] \cdot \exp\left[\frac{1}{2}(\mathbb{1} + Z)i\alpha_1 + \frac{1}{2}(\mathbb{1} - Z)i\alpha_2\right] \cdot \exp\left[-\frac{1}{4}i\pi X\right] \\
&= \exp\left[\frac{1}{2}(\mathbb{1} + Y)i\alpha_1 + \frac{1}{2}(\mathbb{1} - Y)i\alpha_2\right].
\end{aligned} \tag{3.21}$$

This evolution,  $\mathcal{U}_2$ , is generated by the following two Hamiltonians,

$$(\alpha_1 \text{ angle}) \quad h_1 = \frac{1}{2}(\mathbb{1} + Y), \tag{3.22}$$

$$(\alpha_2 \text{ angle}) \quad h_2 = \frac{1}{2}(\mathbb{1} - Y). \tag{3.23}$$

Clearly, the eigenvalues of these generators are given by,  $\{0, 1\}$ . Hence,  $\mathcal{U}_2$  can alternatively be represented as,

$$\mathcal{U}_2 = \exp\left[h_1 i\alpha_1 + h_2 i\alpha_2\right]. \tag{3.24}$$

### 3.2.1.2 Three-mode case

The analytical description of the 3-mode multiphase Mach-Zehnder interferometer in the Heisenberg-Weyl basis is completely analogous to its 2-mode case. We start with the 3-port symmetric multiport which we represent in the following form using generalised  $X$  operators:

$$S_3 = \exp\left[\frac{2}{9}i\pi(X + X^2)\right]. \tag{3.25}$$

Next we represent the phase-imprinting part in the similar fashion,

$$F_3(\vec{\alpha}) = \exp\left[\frac{1}{3}i\pi\left(\alpha_1(Z + Z^2) + \alpha_2(\omega^2 Z + \omega Z^2) + \alpha_3(\omega Z + \omega^2 Z^2)\right)\right]. \tag{3.26}$$

Then the entire evolution is again represented in the concise form where it is generated solely by the generalised  $Y$  matrices:

$$\begin{aligned}
\mathcal{U}_3 &= S_3 F_3(\vec{\alpha})(S_3)^\dagger \\
&= \exp\left[\frac{1}{3}i\left(\alpha_1(\omega Y + \omega^2 Y^2) + \alpha_2(Y + Y^2) + \alpha_3(\omega^2 Y + \omega Y^2)\right)\right].
\end{aligned} \tag{3.27}$$

Then we go forward and construct generators for  $\mathcal{U}_3$  that are given by the three following

Hamiltonians:

$$\begin{aligned}
(\alpha_1 \text{ angle}) \quad h_1 &= \frac{1}{3}(\omega Y + \omega^2 Y^2), \\
(\alpha_2 \text{ angle}) \quad h_2 &= \frac{1}{3}(Y + Y^2), \\
(\alpha_3 \text{ angle}) \quad h_3 &= \frac{1}{3}(\omega^2 Y + \omega Y^2).
\end{aligned} \tag{3.28}$$

The above Hamiltonians fulfill  $h_1 + h_2 + h_3 = 0$ , and their eigenvalues are given by  $\{2/3, -1/3, -1/3\}$ . It is interesting to note that despite the fact that in the three-mode case the Heisenberg-Weyl operators (3.18) are no longer Hermitian, their appropriate combinations give rise to a proper Hermitian Hamiltonians (3.28). Again  $\mathcal{U}_3$  can alternatively be represented as,

$$\mathcal{U}_3 = \exp \left[ h_1 i \alpha_1 + h_2 i \alpha_2 + h_3 i \alpha_3 \right]. \tag{3.29}$$

### 3.2.1.3 Four-mode case

Unlike the previous two cases, the description of a 4-mode case is rather complicated. However, the 4-mode symmetric multipoint still has an analogous and simple form in terms of a generalised  $X$  operator given by,

$$S_4 = \exp \left[ \frac{1}{4} i \pi (X + X^2 + X^3) \right], \tag{3.30}$$

Again, the phase-imprinting part can be presented in terms of  $Z$  operators,

$$F_4(\vec{\alpha}) = \exp[i\vec{\alpha} \cdot \vec{z}], \tag{3.31}$$

where  $\vec{z}$  has the following form,

$$\begin{pmatrix} z_1 \\ z_2 \\ z_3 \\ z_4 \end{pmatrix} = K \begin{pmatrix} 1 \\ Z \\ Z^2 \\ Z^3 \end{pmatrix}, \tag{3.32}$$

where  $K_{mn} = \omega^{(m-1)(n-1)}$ .

The entire evolution is then generated by 4 Hamiltonians:

$$\mathcal{U}_4 = S_4 F_4(\vec{\alpha}) (S_4)^\dagger = \exp [i(h_1 + h_2 + h_3 + h_4)], \tag{3.33}$$

where,

$$\begin{aligned}
h_1 &= \frac{1}{4}\omega (Y - Y^2 + Y^3 - \eta \operatorname{Re}Y - \theta \operatorname{Re}Y^3), \\
h_2 &= \frac{1}{4}\omega (-Y + Y^2 - Y^3 + \eta \operatorname{Re}Y + \eta \operatorname{Re}Y^3), \\
h_3 &= \frac{1}{4}\omega (Y^\dagger + (Y^3)^* - Y^2 - \mu \operatorname{Re}Y + \nu \operatorname{Re}Y^3), \\
h_4 &= \frac{1}{4}\omega (Y + Y^3 - (Y^2)^* - \mu \operatorname{Re}Y + \nu \operatorname{Re}Y^3),
\end{aligned} \tag{3.34}$$

where the star  $*$  denotes complex conjugation and for clarity we introduced constants:

$$\begin{aligned}
\eta &= \sqrt{\frac{2}{\omega}}, \\
\theta &= \sqrt{2\omega}, \\
\mu &= 2\omega \left(1 - \frac{i}{\sqrt{2\omega}}\right), \\
\nu &= 2\omega \left(1 - \frac{1}{\sqrt{2\omega}}\right).
\end{aligned} \tag{3.35}$$

Although the generators still depend only on generalised  $Y$  matrices, they have much more complicated forms compared to the previous cases. The eigenvalues of  $h_i$  are  $\{3/4, -1/4, -1/4, -1/4\}$ . In this case also, despite having a non-Hermitian basis, properly defined functions give rise to the desired Hermitian Hamiltonians.

### 3.2.2 Precision of the multiphase estimation scheme

In this section we investigate the estimation precision of our proposed scheme. We particularly consider  $N$ -partite initial state for  $d = 3$  and  $d = 4$ . We could use QFIM approach to the setup with the reference phase being known, but we do not do it to avoid the necessity for finding optimal measurements. As we do not allow for tunable measurements, we cannot utilise the Quantum Cramer-Rao Bound for our joint estimation since we couldn't prove its attainability with our fixed measurements.

First, the precision of joint estimation of several parameters in the presence of fixed and known additional parameters is specified by the Cramer-Rao bound based on the inverse of the Fisher Information Submatrix corresponding to the parameters of interest (3.14). Therefore, to describe the precision of estimation by a single quantity we take the trace of both sides of the Cramer-Rao bound (3.14) [173]:

$$\operatorname{Tr}(\operatorname{Cov}(\{A_{\mathcal{I}}\})) \geq \frac{\operatorname{Tr}\left((\mathcal{F}(\vec{\alpha})_{\mathcal{I},\mathcal{I}})^{-1}\right)}{\nu}, \tag{3.36}$$

where the matrix  $\mathcal{F}(\vec{\alpha})_{\mathcal{I},\mathcal{I}}$  is a Fisher Information submatrix corresponding to the subset of jointly estimated phases as defined in 3.1.1.3.

The next task is to analyse the behaviour of the quantity  $\text{Tr} \left( (\mathcal{F}(\vec{\alpha})_{\mathcal{I},\mathcal{I}})^{-1} \right)$  as a function of the number of photons  $N$ . In this way we will find asymptotic scaling of precision.

Luckily in our setup, we can use a pre-optimized initial state. We should note that this pre-optimisation has nothing to do with our final precision analysis. It is rather an ad-hoc procedure which fits to our estimation scheme. The characteristics of the state is that it is only dependent on the dimension of the local multiport. To get this optimization, we maximized the mean QFI per parameter. To do so we consider the following inequality:

$$\frac{1}{d} \text{Tr} \mathcal{F}^Q \leq \frac{4}{d} \sum_{i=1}^d \langle H_i^2 \rangle_\psi, \quad (3.37)$$

This can be easily derived from (3.7).

$$\begin{aligned} \text{Tr} \mathcal{F}^Q &= \sum_{i=1}^d \mathcal{F}_{ii}^Q \\ &= 4 \sum_{i=1}^d (\langle H_i^2 \rangle_\psi - \langle H_i \rangle_\psi^2) \\ &\leq 4 \sum_{i=1}^d \langle H_i^2 \rangle_\psi \\ \implies \frac{1}{d} \text{Tr} \mathcal{F}^Q &\leq \frac{4}{d} \sum_{i=1}^d \langle H_i^2 \rangle_\psi. \end{aligned}$$

The LHS of Ineq.[3.37] refers to the mean QFI per parameter. This quantity is treated as an approximate measure of average estimation performance per parameter. The total collective Hamiltonian corresponding to the action of  $N$  local interferometers is given by,

$$H_i = h_i \otimes \mathbb{1} \otimes \dots \otimes \mathbb{1} + \mathbb{1} \otimes h_i \otimes \mathbb{1} \otimes \dots \otimes \mathbb{1} + \dots + \mathbb{1} \otimes \dots \otimes \mathbb{1} \otimes h_i, \quad (3.38)$$

where  $\mathbb{1}$  is the identity operator and  $h_i$  denotes any of the local Hamiltonians from formulas (3.28) and (3.34). The inequality (3.37) implies that the optimal state can be achieved when the initial state is an eigenstate of the operator  $\sum_i H_i^2$ .

### 3.2.2.1 Three-mode case

In this subsection we explicitly investigate the  $d = 3$  mode case.

***Optimal state.***

The  $N$ -qutrit optimal state that maximizes the trace of the QFIM  $\mathcal{F}^Q$  is given by:

$$|\Psi_3\rangle_N = \frac{1}{\sqrt{3}} U_3^{\otimes N} (|0\dots 0\rangle + |1\dots 1\rangle + |2\dots 2\rangle), \quad (3.39)$$

where

$$U_3 = \frac{1}{\sqrt{3}} \begin{pmatrix} 1 & 1 & 1 \\ \omega^2 & 1 & \omega \\ 1 & \omega^2 & \omega \end{pmatrix}. \quad (3.40)$$

We can now easily prove that the operator  $U_3$  simultaneously diagonalises the local Hamiltonians in Eq.[(3.28)] which will be essential to validate the fact that our initial state is indeed the optimal one. We know that the operators in Eq[(3.28)] are completely expressible by the operators  $Y$  and  $Y^2$ . Moreover, we have,

$$\begin{aligned} U_3^\dagger Y U_3 &= Z, \\ U_3^\dagger Y^2 U_3 &= Z^2. \end{aligned}$$

Finally,  $Z$  and  $Z^2$  are diagonal by definition. Consequently, following the action of the collective unitary operation  $U_3^{\otimes N}$ , the total collective Hamiltonians  $H_i$  (3.38) are diagonal with the eigenstates  $|0\dots 0\rangle$ ,  $|1\dots 1\rangle$  and  $|2\dots 2\rangle$ . This implies that the operator  $\sum_i H_i^2$  is also diagonal with the same set of eigenstates.

***Achievable Precision.***

We will now calculate the precision of our estimation method using classical Fisher Information matrix (3.2). In order to do so, we first need to determine the parameter-dependent probability distribution for measurement outcomes  $p(k|\vec{\alpha})$ . The outcomes are labeled by the numbers  $i_k \in \{0, 1, 2\}$  that denote detector clicks in local modes  $i_k$  in measurement stations  $k$ . Therefore the distribution has the form  $p(i_1, \dots, i_N|\vec{\alpha})$ .

Now we are set to calculate the final probability distribution. Let  $i_k \in \{0, 1, 2\}$  be the measurement outcome at  $k$ -th station corresponding to detector click in  $i_k$ -th local mode. Then the conditional probability distribution for the outcomes conditioned on the values of the phase shifts is given by

$$\begin{aligned}
& p(i_1, i_2, \dots, i_N | \alpha_1, \alpha_2, \alpha_3) \\
&= |\langle i_1 \dots i_N | \mathcal{U}_3(\alpha_1, \alpha_2, \alpha_3)^{\otimes N} U_3^{\otimes N} |GHZ\rangle_N|^2 \\
&= \frac{1}{3} \left| \sum_{j=0}^2 \langle i_1 \dots i_N | \mathcal{U}_3(\alpha_1, \alpha_2, \alpha_3)^{\otimes N} U_3^{\otimes N} | \underbrace{j \dots j}_N \rangle \right|^2 \\
&= \frac{1}{3} \left| \sum_{j=0}^2 \langle i_1 \dots i_N | \mathcal{U}_3(\alpha_1, \alpha_2, \alpha_3) U_3 | j \rangle^N \right|^2 \\
&= \frac{1}{3} \left| \sum_{j=0}^2 \prod_{k=1}^N \langle i_k | \mathcal{U}_3(\alpha_1, \alpha_2, \alpha_3) U_3 | j \rangle \right|^2 \tag{3.41}
\end{aligned}$$

The first simplification that can be made is that the entire local evolution operator  $\mathcal{U}_3(\alpha_1, \alpha_2, \alpha_3)U_3$  can be presented in the following compact matrix form by direct use of the defining formulas (3.27) and (3.40):

$$\mathcal{U}_3(\alpha_1, \alpha_2, \alpha_3)U_3 = \frac{1}{\sqrt{3}} \begin{pmatrix} e^{i\alpha_2} & e^{i\alpha_3} & e^{i\alpha_1} \\ \omega^2 e^{i\alpha_2} & e^{i\alpha_3} & \omega e^{i\alpha_1} \\ e^{i\alpha_2} & \omega^2 e^{i\alpha_3} & \omega e^{i\alpha_1} \end{pmatrix} e^{-\frac{1}{3}i(\alpha_1+\alpha_2+\alpha_3)}. \tag{3.42}$$

Next, we can observe a symmetry in the probability distribution (3.41) that we calculated. We observe that the probability distribution depends only on the total number of local clicks in local modes  $\{0, 1, 2\}$ , which we denote by  $z, j, d$  respectively. Using this property, we derive the final form of the probability distribution,

$$\begin{aligned}
p(\underbrace{0, \dots, 0}_z, \underbrace{1, \dots, 1}_j, \underbrace{2, \dots, 2}_d | \alpha_1, \alpha_2, \alpha_3) &= \frac{1}{3^{N+1}} \left( 3 + 2 \cos \left[ \frac{2\pi}{3}(d-j) + N(\alpha_1 - \alpha_2) \right] \right. \\
&+ 2 \cos \left[ \frac{2\pi}{3}(j-d) + N(\alpha_1 - \alpha_3) \right] \\
&+ \left. 2 \cos \left[ \frac{4\pi}{3}(j-d) + N(\alpha_2 - \alpha_3) \right] \right). \tag{3.43}
\end{aligned}$$

Therefore we have  $p(i_1, \dots, i_N | \vec{\alpha}) = p(z, j, d | \vec{\alpha})$ . Using this final form of the probability distribution (3.43) we can now directly derive the compact forms of the elements of the  $2 \times 2$  Fisher Information submatrix (3.2) that corresponds to joint estimation of two of the three phases  $\{\alpha_1, \alpha_2\} = \mathcal{I}$ , whereas the third phase is set to zero as a reference mode,

$$[\mathcal{F}(\alpha_1, \alpha_2)_{\mathcal{I}, \mathcal{I}}]_{ij} = \sum_{z, j, d=0}^N \binom{N}{z, j, d} \frac{\partial_{\alpha_i} p(z, j, d | \alpha_1, \alpha_2, 0) \partial_{\alpha_j} p(z, j, d | \alpha_1, \alpha_2, 0)}{p(z, j, d | \alpha_1, \alpha_2, 0)}, \tag{3.44}$$

where the multinomial coefficient counts the number of separate detection situations giving rise to the total of  $z, j, d$  clicks in modes  $\{0, 1, 2\}$ .

However, it is evident that the above Fisher information submatrix does not depend on the choice of the reference mode due to its symmetry in the final probability distribution (3.43) with respect to the parameters  $\alpha_i$ . Therefore the following analysis holds for estimation of subset any two of the 3-mode interferometer.

However, the exact analytical expression for the above defined Fisher information submatrix for arbitrary values of  $\alpha$ 's is somewhat complicated. But it is possible to calculate its inverse and therefore to find the optimal scaling of the following quantity  $\text{Tr} \left( (\mathcal{F}(\vec{\alpha})_{\mathcal{I},\mathcal{I}})^{-1} \right)$  as a function of the number of photons  $N$ ,

$$\text{Tr} \left( (\mathcal{F}(\alpha_1^{\text{opt}}, \alpha_2^{\text{opt}})_{\mathcal{I},\mathcal{I}})^{-1} \right) = \frac{6 + \sqrt{3}}{2N^2}, \quad (3.45)$$

and for the optimal values of estimated phases are given by

$$\alpha_1^{\text{opt}} = \alpha_2^{\text{opt}} = \pi - \arctan \left( \sqrt{6 + 4\sqrt{3}} \right) \approx 35.2^\circ. \quad (3.46)$$

If we take the estimated phases to be equal, i.e.,  $\alpha_1 = \alpha_2 = \alpha$ , then the trace of the inverse Fisher information submatrix has the following form,

$$\text{Tr} \left( (\mathcal{F}(\alpha)_{\mathcal{I},\mathcal{I}})^{-1} \right) = \frac{1}{N^2} (3 + \cos(N\alpha) - \cos(2N\alpha)) (\csc(N\alpha))^2. \quad (3.47)$$

Next, we plot of the right-hand-side of the Cramer-Rao bound (3.36), i.e.,  $\text{Tr} \left( (\mathcal{F}(\alpha_1, \alpha_2)_{\mathcal{I},\mathcal{I}})^{-1} \right)$ , as a function of the jointly estimated phases  $\alpha_1$  and  $\alpha_2$  for the 3-mode Mach-Zehnder interferometer case considering the number of photons in the initial state set to be  $N = 8$ . It shows the minimal value of  $\text{Tr} \left( (\mathcal{F}(\alpha_1, \alpha_2)_{\mathcal{I},\mathcal{I}})^{-1} \right)$  for the optimal values of the estimated phases reads  $\frac{6+\sqrt{3}}{128} \approx 0.06$ , whereas the Monte-Carlo-estimated median, where both the phases were drawn uniformly, reads 0.65. Therefore it gives us a clear picture of the robustness of our strategy for estimation of arbitrary values of the phases. The precision is highly dependent on the values of the estimated phases themselves as witnessed by the complexity of the plot. Therefore in realistic applications one needs to obtain some prior knowledge of the phases in order to tune the interferometer in a way that the unknown phases are close to the optimal values for which the error is the lowest. Even though we do not allow for optimization of final measurements, we still obtain the Heisenberg-like scaling of precision of joint estimation for each of the parameters around its optimal values.

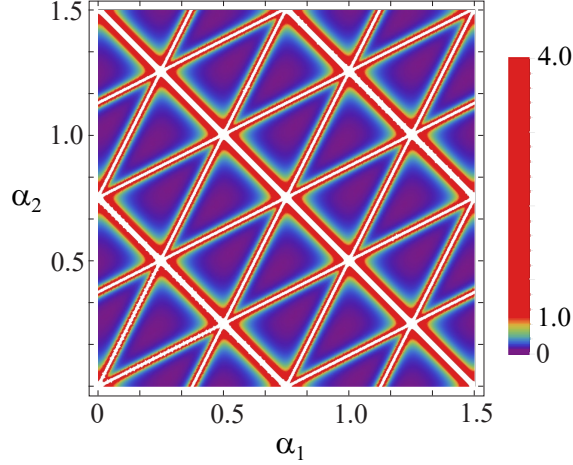


Figure 3.2: Contour plot of  $\text{Tr} \left( (\mathcal{F}(\alpha_1, \alpha_2)_{\mathcal{I}, \mathcal{I}})^{-1} \right)$  vs  $\alpha_1$  vs  $\alpha_2$  in a 3-mode Mach-Zehnder setting for  $N = 8$ .

#### Four-mode case

##### *Optimal state.*

Next, in analogy to the three-mode case, we analyse the four mode case using the  $N$ -quart state. In this case, using the same logic as (3.39), we obtain the state for which the trace of QFIM attains the maximal value,

$$|\Psi_4\rangle_N = \frac{1}{2} U_4^{\otimes N} (|0\dots 0\rangle + |1\dots 1\rangle + |2\dots 2\rangle + |3\dots 3\rangle), \quad (3.48)$$

where:

$$U_4 = \frac{1}{2} \begin{pmatrix} -1 & -1 & 1 & 1 \\ 1 & -1 & 1 & -1 \\ 1 & -1 & -1 & 1 \\ 1 & 1 & 1 & 1 \end{pmatrix}. \quad (3.49)$$

Similar to the three-mode case,  $U_4$  simultaneously diagonalizes local Hamiltonians  $h_i$  (3.34) with the eigenstates being the standard basis  $|0\rangle, |1\rangle, |2\rangle$ , and  $|3\rangle$ . Consequently, following the action of the unitary operation  $U_4^{\otimes N}$ , the total collective Hamiltonians  $H_i$  (3.38) are diagonal with the eigenstates  $|0\dots 0\rangle, |1\dots 1\rangle, |2\dots 2\rangle$ , and  $|3\dots 3\rangle$ , which implies that the operator  $\sum_i H_i^2$  is also diagonal with the same set of eigenstates.

##### *Achievable Precision.*

The estimation of the achievable precision for this case is again analogous to the 3-mode case. We start by determining the final probability distribution  $p(k|\vec{\alpha})$  that we write as

$p(i_1, \dots, i_N | \vec{\alpha})$ . It has the following form for  $d = 4$ ,

$$\begin{aligned}
p(i_1, i_2, \dots, i_N | \alpha_1, \alpha_2, \alpha_3, \alpha_4) &= |\langle i_1 \dots i_N | \mathcal{U}_4(\alpha_1, \alpha_2, \alpha_3, \alpha_4)^{\otimes N} U_4^{\otimes N} |GHZ\rangle_N|^2 \\
&= \frac{1}{4} \left| \sum_{j=0}^3 \langle i_1 \dots i_N | \mathcal{U}_4(\alpha_1, \alpha_2, \alpha_3, \alpha_4)^{\otimes N} U_4^{\otimes N} | \underbrace{j \dots j}_N \rangle \right|^2 \\
&= \frac{1}{4} \left| \sum_{j=0}^3 \langle i_1 \dots i_N | \mathcal{U}_4(\alpha_1, \alpha_2, \alpha_3, \alpha_4) U_4 | j \rangle^N \right|^2 \\
&= \frac{1}{4} \left| \sum_{j=0}^3 \prod_{k=1}^N \langle i_k | \mathcal{U}_4(\alpha_1, \alpha_2, \alpha_3, \alpha_4) U_4 | j \rangle \right|^2 \tag{3.50}
\end{aligned}$$

The local evolution operator  $\mathcal{U}_4(\alpha_1, \alpha_2, \alpha_3, \alpha_4) U_4$  can be expressed as,

$$\mathcal{U}_4(\alpha_1, \alpha_2, \alpha_3, \alpha_4) U_4 = \frac{1}{2} \begin{pmatrix} -e^{i\alpha_1} & -e^{i\alpha_2} & e^{i\alpha_3} & e^{i\alpha_4} \\ e^{i\alpha_1} & -e^{i\alpha_2} & e^{i\alpha_3} & -e^{i\alpha_4} \\ e^{i\alpha_1} & -e^{i\alpha_2} & -e^{i\alpha_3} & e^{i\alpha_4} \\ e^{i\alpha_1} & e^{i\alpha_2} & e^{i\alpha_3} & e^{i\alpha_4} \end{pmatrix} e^{-\frac{i}{4}(\alpha_1 + \alpha_2 + \alpha_3 + \alpha_4)}. \tag{3.51}$$

$p(k | \vec{\alpha})$  depends only on the total number of clicks in local modes  $\{0, 1, 2, 3\}$  that are denoted respectively as  $z, j, d, t$  and we can write  $p(i_1, \dots, i_N | \vec{\alpha}) = p(z, j, d, t | \vec{\alpha})$ .

$$\begin{aligned}
&p(\underbrace{0, \dots, 0}_z, \underbrace{1, \dots, 1}_j, \underbrace{2, \dots, 2}_d, \underbrace{3, \dots, 3}_t | \alpha_1, \alpha_2, \alpha_3, \alpha_4) \\
&= \frac{1}{4^{N+1}} \left( 4 + 2 \cos [(d+j)\pi + N(\alpha_2 - \alpha_1)] + 2 \cos [(d-z)\pi + N(\alpha_3 - \alpha_1)] \right. \\
&\quad + 2 \cos [(j-z)\pi + N(\alpha_4 - \alpha_1)] + 2 \cos [(j+z)\pi + N(\alpha_2 - \alpha_3)] \\
&\quad \left. + 2 \cos [(d+z)\pi + N(\alpha_2 - \alpha_4)] + 2 \cos [(d-j)\pi + N(\alpha_3 - \alpha_4)] \right). \tag{3.52}
\end{aligned}$$

We will now use  $p(i_1, \dots, i_N | \vec{\alpha})$  to the classical  $3 \times 3$  Fisher Information submatrix corresponding to joint estimation of the three phases  $\{\alpha_1, \alpha_2, \alpha_3\} = \mathcal{I}$  while assuming that the fourth phase is the reference mode and is set to zero without any loss of generality. The fisher information matrix will then have the form,

$$[\mathcal{F}(\alpha_1, \alpha_2, \alpha_3)_{\mathcal{I}, \mathcal{I}}]_{ij} = \sum_{z, j, d, t=0}^N \binom{N}{z, j, d, t} \frac{\partial_{\alpha_i} p(z, j, d, t | \alpha_1, \alpha_2, \alpha_3, 0) \partial_{\alpha_j} p(z, j, d, t | \alpha_1, \alpha_2, \alpha_3, 0)}{p(z, j, d, t | \alpha_1, \alpha_2, \alpha_3, 0)}, \tag{3.53}$$

where the multinomial coefficient counts the number of separate detection situations giving rise to the total of  $z, j, d, t$  clicks in modes  $\{0, 1, 2, 3\}$ .

Here also, the form of the Fisher information submatrix is independent of choice of the

reference mode and hence the following analysis of precision of estimation holds for estimating any triple of phases chosen from all the four ones.

Analogous to the mode-three case we calculated the optimal scaling of the quantity  $\text{Tr} \left( (\mathcal{F}(\vec{\alpha})_{\mathcal{I},\mathcal{I}})^{-1} \right)$  as a function of the number of photons  $N$  and we get,

$$\text{Tr} \left( \left( \mathcal{F}(\alpha_1^{\text{opt}}, \alpha_2^{\text{opt}}, \alpha_3^{\text{opt}})_{\mathcal{I},\mathcal{I}} \right)^{-1} \right) = \frac{6}{N^2}, \quad (3.54)$$

and this is attained for the following optimal values of estimated phases,

$$\alpha_1^{\text{opt}} = \alpha_2^{\text{opt}} = \alpha_3^{\text{opt}} = 0. \quad (3.55)$$

Assuming that all the estimated phases are equal,  $\alpha_1 = \alpha_2 = \alpha_3 = \alpha$ , the trace of the inverse Fisher information submatrix scales with the number of photons  $N$  as follows,

$$\text{Tr} \left( (\mathcal{F}(\alpha)_{\mathcal{I},\mathcal{I}})^{-1} \right) = \frac{3}{2N^2} (3 + \cos(N\alpha)) \left( \sec \left( \frac{N\alpha}{2} \right) \right)^2. \quad (3.56)$$

Here we also obtain the Heisenberg-like scaling of precision of joint estimation of any triple of the phases around their optimal values.

### 3.2.3 Optical implementation of Single-interferometer

In this section we discuss the practicality of our proposed scheme. The main difficulty of implementation of this scheme is to produce the multiphoton  $d$ -level GHZ state which remains an experimental challenge for higher number of subsystems. With a feasible fix for this problem, we can directly implement the scheme using optical interferometry. In order to resolve our problem, we simplify our scheme in the following way which is then absolutely feasible within current optical technology. To do so we perform a second quantization of the scheme. We recall that the final states in our setup are symmetric states of photons which are distinguishable by path degree of freedom given by,

$$\begin{aligned} |\Psi_{out}^3\rangle_N &= \mathcal{U}_3^{\otimes N} U_3^{\otimes N} |\text{GHZ}^3\rangle_N \\ |\Psi_{out}^4\rangle_N &= \mathcal{U}_4^{\otimes N} U_4^{\otimes N} |\text{GHZ}^4\rangle_N. \end{aligned} \quad (3.57)$$

We can write a second-quantized version of the above states by assuming that a state of  $N$  indistinguishable photons is sent to a single  $d$ -mode interferometer. Then the states can be expressed in the following form,

$$\begin{aligned} |\Psi_{out}^3\rangle &= \mathcal{U}_3 U_3 |\text{NOON}^3\rangle_N \\ |\Psi_{out}^4\rangle &= \mathcal{U}_4 U_4 |\text{NOON}^4\rangle_N, \end{aligned} \quad (3.58)$$

where the  $|\text{NOON}^d\rangle_N$  states are given by,

$$|\text{NOON}^d\rangle_N = \frac{1}{\sqrt{d}}(|\underbrace{N0\dots 0}_d\rangle + |\underbrace{0N\dots 0}_d\rangle + \dots + |\underbrace{0\dots 0N}_d\rangle). \quad (3.59)$$

The new detection probabilities for the this simplified scheme are identical to the ones for the original scheme (3.43), (3.52) with a minor change incorporated. In this new detection scheme, the meaning of the detection events is now the numbers  $z, j, d, t$  denoting the photon counts in modes  $\{0, 1, 2, 3\}$  for their respective case. The probability distribution found in this method is completely equivalent to the probability distribution associated with the original scheme as at the level of probabilities in (3.43) and (3.52), we do not distinguish in which of the  $N$  stations there was a click in a given mode. Therefore the quantity solely depends on the total number of clicks in given modes across all the labs.

This experiment can now be realized in terms of a *single* interferometer consisting of the initial-state-correcting multiports  $U_3$  (3.40) (or  $U_4$  (3.49)) and the generalised Mach-Zehnder interferometer  $\mathcal{U}_3$  (3.27) (or  $\mathcal{U}_4$  (3.33)) that uses a NOON state as an input which is a feasible experiment for higher values of  $N$  [198]. Several other interesting experimental advancements can be found in literature in this regard [170, 171, 172, 174, 173].

### 3.2.4 Symmetric 5-mode multiport

In this final subsection of our results, we investigate symmetric multiports with  $d = 5, 6$ . Analogous to the previous cases, these multiports can also be represented in terms of the powers of generalised  $X$  and are given by,

$$S_5 = \exp \left[ \frac{4\sqrt{5}}{25} i\pi (X - X^2 - X^3 + X^4) \right], \quad (3.60)$$

$$S_6 = \exp \left[ i\pi \left( \frac{1}{3}X + \frac{1}{9}X^2 + \frac{1}{12}X^3 + \frac{1}{9}X^4 + \frac{1}{3}X^5 \right) \right]. \quad (3.61)$$

We now try to analyse the optical multiports from the Hamiltonian perspective [185]. In the second quantisation description, the symmetric Hamiltonian for  $d$ -mode optical instrument can be represented in the following form:

$$H_{sym} = \sum_{i < j} e^{i\varphi_{ij}} (a_i^\dagger a_j + a_j^\dagger a_i), \quad (3.62)$$

This is a generalized version of the Hamiltonian that is provided in [185] that additionally incorporates phases. The Hamiltonian of the form (3.62) cannot generate evolution of a symmetric multiport for  $d > 4$  [185]. However, it can be easily seen that the evolution

(3.60) of a symmetric 5-port is in fact generated by such a Hamiltonian. We know that the Hamiltonian of the symmetric multiport in (3.60) reads up to the following constant factor,

$$H_5 = X - X^2 - X^3 + X^4. \quad (3.63)$$

Here we utilize the Jordan–Schwinger map that maps a set of matrices  $\mathbf{M}$  in  $\mathbb{C}^d$  into second-quantised operators on  $d$ -mode Fock space. This map can be represented in the following way,

$$\mathbf{M} \mapsto M \equiv \sum_{i,j=1}^d a_i^\dagger M_{ij} a_j, \quad (3.64)$$

This map is a Lie algebra isomorphism, ensuring that the operators  $M$  satisfy the same commutation relations as the matrices  $\mathbf{M}$ . We obtain that  $H_5$  has the symmetric representation (3.62) with the following phases:

$$\begin{aligned} \varphi_{12} &= \varphi_{15} = \varphi_{23} = \varphi_{34} = \varphi_{45} = 2\pi \\ \varphi_{13} &= \varphi_{14} = \varphi_{24} = \varphi_{25} = \varphi_{35} = \pi. \end{aligned} \quad (3.65)$$

On the other hand the Hamiltonian for the 6-mode symmetric multiport has the following form,

$$H_6 = \frac{1}{3}X + \frac{1}{9}X^2 + \frac{1}{12}X^3 + \frac{1}{9}X^4 + \frac{1}{3}X^5 \quad (3.66)$$

Unfortunately, generating the evolution of the 6-mode symmetric multiport (3.61) does not have symmetric representation as (3.62). Instead it has the following form,

$$H_6 = \sum_{i<j} \alpha_{ij} (a_i^\dagger a_j + a_j^\dagger a_i), \quad (3.67)$$

and the amplitudes are given by,

$$\begin{aligned} \alpha_{12} &= \alpha_{16} = \alpha_{23} = \alpha_{34} = \alpha_{45} = \alpha_{56} = \frac{1}{3} \\ \alpha_{13} &= \alpha_{15} = \alpha_{24} = \alpha_{26} = \alpha_{35} = \alpha_{46} = \frac{1}{9}, \\ \alpha_{14} &= \alpha_{25} = \alpha_{36} = \frac{1}{12}. \end{aligned} \quad (3.68)$$

### 3.3 Conclusion

In this chapter we investigated metrological properties of multimode generalized Mach-Zehnder interferometer and its importance in simultaneous multiphase estimation task. We thoroughly discussed our finding for  $m = 2, 3$ , and 4. We discussed our setup in details which comprises of a  $N$ -qdit state generator source that produces an initial state, a setup to perform identical local unitary evolution on the initial state to provide the probe state, and finally the standard and fixed measurement setup to generate the probability distribution. Using this setup we investigated possibilities to estimate  $d - 1$  out of  $d$  phases that are placed in arbitrary configuration across the modes where one remaining phase is known and acts as an reference mode. We calculated the achievable precision of our estimation setup and compare it with the so called Heisenberg-limit. We represented our setup of generalised Mach-Zehnder interferometer using a generator scheme constructed in terms of the Heisenberg-Weyl operators. Using this approach, we were able to calculate the inverse of the submatrix of a FIM related with each of the subsets of parameters of interest, which, in contrast to methods implicitly involving optimisation over measurement strategies based on Quantum Cramer-Rao or Holevo bounds, provides a *factual* limit for the efficiency of estimation within assumed concrete measurement setup. We therefore showed that even though we used the same initial state and the same measurement for estimation of all the subsets of phases, we were still able to obtain the Heisenberg-like scaling of precision of estimation of each of the subset. In the final section we investigated symmetric multiports with  $d = 5, 6$  and showed that while the 5-mode symmetric multiport can be expressed in terms of the symmetric Hamiltonian, the same is, however, not true for 6-mode symmetric multiport.

# Optimal tests of genuine multipartite nonlocality

One of the most important signature of non-classicality exhibited by quantum system is the notion of *Bell nonlocality*. Nonlocal correlations can be interpreted as correlations that arise from the outcomes of measurements performed on sub-parts of a bipartite system which are situated in spatially separated labs and cannot be explained by classical theory. One can detect such correlations by violating suitable Bell inequality [199, 200, 201, 202]. Besides entanglement, nonlocal correlations also proven to be a crucial resource, "alternative to entanglement and necessary for device-independent quantum information protocols" [203]. However, it can be inferred that these two concepts are intimately related. Despite that, it has been proved that nonlocality and entanglement are indeed two distinct concepts and two inequivalent resources [204] given the facts such as there exist entangled state which are locally realisable [205, 206, 207] and a maximally nonlocal states are not maximally entangled in general [208].

A natural extension to this study is to investigate the structure of nonlocality in the composite quantum systems, referred as *multipartite nonlocality*. Analogous to multipartite entanglement, in this generalized scenario, nonlocality can be shared between all or a subset of parties. Characterizing such correlations, however, is an increasingly demanding task given that the complexity of the possible states and sets of correlations grow exponentially with increasing number of parties. Among all nonlocal multipartite correlations, genuine multipartite nonlocality (GMNL) is considered to be the most fundamental non-classical feature. GMNL is the subclass of multipartite nonlocality that requires all the parties to be correlated with each other non-classically. In fact, different "genuine" non-classical correlations, namely, genuine multipartite total correlations (GMT), genuine multipartite discord (GMD), genuine multipartite entanglement (GME), genuine multipartite steering (GMS)

and GMNL form the following hierarchy [209, 210, 211, 207, 212, 213]:

$$\text{GMT} \supseteq \text{GMD} \supseteq \text{GME} \supseteq \text{GMS} \supseteq \text{GMNL}. \quad (4.1)$$

GMNL is a strongly non-classical correlation in a sense that it is distinct from the correlations that are local to some bipartition. The very first tool to detect GMNL, the Svetlichny inequality, was introduced in [214] for three parties. It was then generalized in [215] by constructing  $N$ -particle Bell-type inequalities under the assumption of partial separability and later for the most general separability condition [216]. Svetlichny's approach to detect is however inconsistent with more recently introduced operational framework [203]. Further relevant works can be found in Refs. [216, 217, 218, 219].

Therefore, classification of states in terms of GMNL is an appealing task and has been carried out extensively in literature. Notably, it was found that any one-way entanglement distillable state [220] is a nonlocal resource [221]. Interestingly, it was proved that multipartite entangled pure states are never fully local [222, 223] and all pure  $N$ -qubit states that are GME, are also GMNL [224]. However, in the case of mixed states, it was found that there exist several examples of genuinely entangled  $N$ -partite states [204, 225] that are not genuinely nonlocal with respect to the Svetlichny and the recent operational definitions of nonlocality [203, 226] and some of which are even fully local [227]. It was also shown that local operators applied prior to measurements can activate "hidden nonlocality" in the states that are initially entangled but local [227, 228, 229, 230, 231, 232]. This was later exploited in [233] to extend the equivalence of GME and GMNL for three parties beyond qubits. Also, the violations of local realism by families of multipartite quantum states has been analysed numerically in [234] and it has been proven that the probability of violation can also serve as a witness of genuine multipartite entanglement that increases with the number of parties or settings.

Multipartite correlations are commonly tested and assigned to models that concern to different physical resources such as classical, quantum or post-quantum correlations [214, 203, 219, 226]. Ref. [226] provides us with an operational definition of genuine multipartite nonlocality. Here, models of non-classical correlation resources are considered that are hybrids of classical and non-classical correlations such that a subset of parties share non-classical correlation while the remaining parties only share classical correlation with each other. This family of models, equipped with a series of Bell-type inequalities, range from completely classical to genuinely multipartite, providing us with a rich structure of the multipartite scenario. [226] gives us two alternative definitions of genuine  $n$ -partite nonlocality that are strictly weaker than the Svetlichny's version.

## 4.1 Definitions and Methodology

### 4.1.1 Bell nonlocality

In the simplest Bell scenario, we consider that a bipartite state is shared between two observers, Alice and Bob, located in spatially separated labs. The observers perform local measurements and Alice obtain the outcome  $a$  and Bob obtain the obtain  $b$ . We represent the joint probability of the outcome as  $P(a, b|x, y)$  where  $x$  is the measurement conducted by Alice and  $y$  is the measurement conducted by Bob. According to *Local causality* statement, spatially separated events are independent of each other regardless of their past interaction. Then, there exists a more complete description  $\lambda$  for the global system and we refer to  $\lambda$  as a *hidden variable*. Then we have,

$$P_\lambda(a, b|x, y) = P_\lambda(a|x)P_\lambda(b|y). \quad (4.2)$$

A correlation that satisfy the above equation is said to be a *local state* and there always exists a local hidden variable model that will reproduce this correlations. The joint probability of the outcomes are then represented as:

$$P(a, b|x, y) = \sum_\lambda q_\lambda P_\lambda(a|x)P_\lambda(b|y), \quad (4.3)$$

where  $q_\lambda \geq 0$ ,  $\sum_\lambda q_\lambda = 1$ , and  $P_\lambda(a|x)$  and  $P_\lambda(b|y)$  are referred as the marginal probabilities for Alice to obtain outcome  $a$  corresponding to the measurement setting  $x$  and Bob to obtain outcome  $b$  corresponding to the measurement setting  $y$ . However, if some correlations  $P(a, b|x, y)$  violate a suitable Bell inequality, then they cannot be realized using a local hidden variable model given in the form of Eq. (4.3) and such correlations are referred as *nonlocal correlations*.

### 4.1.2 Tripartite nonlocality

With increasing number of parties, i.e., for three or more subsystems, nonlocal correlations can be qualitatively different. We begin with a tripartite Bell-type scenario. Three observers, assumed to be in their spatially separated labs, share a quantum state  $\rho$ . The observers act locally on their shared part of the system and there is no communication is allowed between them during the course of the experiment. We label each of the observers as  $i = \{1, 2, 3\}$ . The observers have access to  $m$  number of local measurement choices, i.e.,  $m$  measurement settings which are labeled as  $\{M_i^j\}_{j=1}^m$ . Then the probability distribution

arising from the correlations between measurement outcomes can be expressed as,

$$p(r_1, r_2, r_3 | M_1^{i_1}, M_2^{i_2}, M_3^{i_3}) = \text{Tr}(\Pi_{M_1^{i_1}}^{r_1} \otimes \Pi_{M_2^{i_2}}^{r_2} \otimes \Pi_{M_3^{i_3}}^{r_3} \rho), \quad (4.4)$$

where,  $\Pi_{M_j^{i_j}}^{r_j}$  is the projection operator corresponding to the outcome  $r_j$ .

As discussed earlier, the correlations that the three subsystems share can now be distinguished at a qualitative level. Here we introduce different notions of multipartite nonlocal correlations for a tripartite system. In particular, we investigate correlations belong to the following three sets, namely, Bell local ( $\mathcal{L}$ ), Svetlichny-local ( $\mathcal{S}_2$ ) and No-signaling bilocal ( $\mathcal{NS}_2$ ). We should note that the inclusion relations between these sets [226] are the following:

$$\mathcal{L} \subsetneq \mathcal{NS}_2 \subsetneq \mathcal{S}_2. \quad (4.5)$$

In this work, we consider the operational framework presented in Refs. [226, 203] and show that given correlation point,  $\mathbf{p} = \{P(a, b, c | x, y, z)\}$ , determining whether this correlation lies in one of the above mentioned sets is computationally feasible problem using linear programming. We use the notation  $r_1 = a, r_2 = b, r_3 = c$  and  $M_1^{i_1} = x, M_2^{i_2} = y, M_3^{i_3} = z$  in Eq. (4.4). In other words, three observers, Alice, Bob and Charlie performs dichotomic measurements corresponding to measurement settings  $x, y, z$  and obtain outcomes  $a, b, c$ . Given the total number of measurement settings  $m$ , we have  $x = (1, 2, \dots, m)$ ,  $y = (1, 2, \dots, m)$  and  $z = (1, 2, \dots, m)$  while the outcomes are  $a = (0, 1)$ ,  $b = (0, 1)$  and  $c = (0, 1)$ .

### Bell local ( $\mathcal{L}$ )

Analogous to the bipartite scenario, if the joint probability distribution can be written in the following form,

$$P(a, b, c | x, y, z) = \sum_{\lambda} q_{\lambda} P_{\lambda}(a | x) P_{\lambda}(b | y) P_{\lambda}(c | z), \quad (4.6)$$

with  $0 \leq q_{\lambda} \leq 1$  and  $\sum_{\lambda} q_{\lambda} = 1$ , then  $\mathbf{p}$  is inside the set  $\mathcal{L}$  and is referred as Bell local or classical. If the probability distribution does not admit the decomposition Eq. (4.6), then the correlation  $\mathbf{p}$  is *Bell nonlocal* or non-classical. We refer to the non-classicality of such correlations as *standard nonlocality* ( $\mathcal{NL}$ ) in our work.

### Svetlichny-local ( $\mathcal{S}_2$ )

Next, we consider the correlations for which a locally causal theory is not attainable. In [214], some correlations that  $\mathbf{p} \notin \mathcal{L}$ , can be defined in a hybrid local-nonlocal form. Such

correlation has the following joint probability distribution,

$$\begin{aligned}
P(a, b, c|x, y, z) = & \sum_{\lambda_1} q_{\lambda_1} P_{\lambda_1}(a, b|x, y) P_{\lambda_1}(c|z) + \sum_{\lambda_2} q_{\lambda_2} P_{\lambda_2}(a, c|x, z) P_{\lambda_2}(b|y) \\
& + \sum_{\lambda_3} q_{\lambda_3} P_{\lambda_3}(b, c|y, z) P_{\lambda_3}(a|x),
\end{aligned} \tag{4.7}$$

where  $0 \leq q_{\lambda_i} \leq 1$  for  $i = 1, 2, 3$  and

$$\sum_{\lambda_1} q_{\lambda_1} + \sum_{\lambda_2} q_{\lambda_2} + \sum_{\lambda_3} q_{\lambda_3} = 1.$$

Correlations satisfying Eq. (4.7) will be referred as *Svetlichny-local* or  $S_2$  correlations and will belong to set  $\mathcal{S}_2$ . Each of the terms in the corresponding joint probability distribution can be factorized such that they comprises of a probability concerning one of the three parties' outcome alone, and a joint probability concerning the two remaining parties. No restrictions are imposed on the joint probability distributions, i.e., they can be either local or nonlocal. Moreover, they can also allow signaling, in principle. If correlations  $P(a, b, c|x, y, z)$  cannot be written in the above mentioned form, then it must appear in the decomposition which indicates the presence *genuine tripartite nonlocality*.

### No-signaling bilocal ( $\mathcal{NS}_2$ )

The last set of correlation that we consider, are referred as *no-signaling bilocal* ( $\mathcal{NS}_2$ ). It is yet another example of a case where the hidden state  $\lambda$  is not local. In this case, tripartite correlation that resides in  $\mathcal{NS}_2$  admits the following decomposition:

$$\begin{aligned}
P(a, b, c|x, y, z) = & \sum_{\lambda_1} q_{\lambda_1} P_{\lambda_1}^{\text{NS}}(a, b|x, y) P_{\lambda_1}(c|z) \\
& + \sum_{\lambda_2} q_{\lambda_2} P_{\lambda_2}^{\text{NS}}(a, c|x, z) P_{\lambda_2}(b|y) \\
& + \sum_{\lambda_3} q_{\lambda_3} P_{\lambda_3}^{\text{NS}}(b, c|y, z) P_{\lambda_3}(a|x),
\end{aligned} \tag{4.8}$$

where the bipartite correlations,  $P_{\lambda_1}^{\text{NS}}(a, b|x, y)$  for instance, obeys the no-signaling condition, i.e., the observers gains no information about a spatially separated party's measurement choice by observing his/her own outcome. In other words, the marginal probabilities corresponding to a certain outcome of Alice is independent of Bob or Charlie's measure-

ment choices. Hence, we can write,

$$\sum_a P_{\lambda_1}^{\text{NS}}(a, b|x, y) = \sum_a P_{\lambda_1}^{\text{NS}}(a, b|x', y) \quad \forall x, x', y, b, \lambda_1 \quad (4.9a)$$

$$\sum_b P_{\lambda_1}^{\text{NS}}(a, b|x, y) = \sum_b P_{\lambda_1}^{\text{NS}}(a, b|x, y') \quad \forall y, y', x, a, \lambda_1. \quad (4.9b)$$

The same is applicable for every bipartite correlations obtained from different permutations of the parties. Violating any of the no-signaling constraints implies signaling allowed between the corresponding observers and each of their outcomes carries non-vanishing information about the other observer's measurement choice.

Considering the scenario concerning Eq. (4.9), say, if Eq. (4.9a) is satisfied but Eq. (4.9b) is violated, then Alice can signal superluminally to Bob. This signalling refers to instantaneous change of the one's outcome just by changing measurement choice of the other. This is the scenario where  $\lambda_1$  is *one-way signaling* and for both Eqs. (4.9a) and (4.9b) violating,  $\lambda_1$  is said to be *two-way signaling*. All these no-signaling constraints are linear function of the probabilities.

### 4.1.3 Indicators of genuine multipartite nonlocality

In our work, we consider two indicators of genuine multiparticle nonlocality, namely, the strength of nonlocality and probability of violation of local realism [235].

#### The maximal strength of nonlocality

The strength of nonlocality  $\mathcal{S}$ , considered to be good candidate for measuring nonlocal correlations, is defined in terms of the robustness with respect to the effects of admixing white noise.

$\mathcal{S}$  can be quantified in terms of the amount of white noise that is required to be added in a convex mixture with a state  $\rho$  that is initially non-classical, in order to completely suppress the non-classicality it possesses. The resultant state can be expressed as

$$\rho(v) = v\rho + (1 - v)\frac{\mathbb{1}}{d^N}, \quad (4.10)$$

where  $v$  is called the visibility of the state,  $d$  is the dimension of each subsystem and  $N$  is the total number of systems. For a given state corresponding to a particular choice of observables, there always exists a critical visibility  $v_{crit}$  such that for any visibility value lower than  $v_{crit}$  results in a state that is realizable using a local hidden variable model. In

other words,  $v_{crit}$  quantifies the noise resistance of a given quantum state. The strength of nonlocality,  $\mathcal{S}$ , is then defined as the smallest admixture of white noise for which the state becomes local for a fixed set of observables,

$$\mathcal{S} = 1 - v_{crit}. \quad (4.11)$$

We optimize the value  $v_{crit}$  over all possible measurement settings to determine the minimal critical visibility required for a given state, referred as  $v_{crit}^{min}$ . Then the maximal strength of nonlocality is given by,

$$\mathcal{S}^{max} = 1 - v_{crit}^{min}. \quad (4.12)$$

### Probability of violation

The second quantifier under consideration is referred as the probability of violation, denoted by  $\mathcal{P}_V$ , tells us how many sets of measurements settings lead to violation of the models prescribed above.  $\mathcal{P}_V$ , while not providing any information about the strength of nonlocality, allows us to investigate the non-classical correlations under random measurements [235]. As in the case of maximum strength of nonlocality, the probability of violation was successfully used to quantify the standard nonlocality [236], and we will now use it to describe the genuine multiparticle nonlocality ( $\mathcal{S}_2, \mathcal{NS}_2$ ).

$\mathcal{P}_V$  is defined as

$$\mathcal{P}_V(\rho) = \int f(\rho, \Omega) d\Omega, \quad (4.13)$$

where the integration is over all parameters that vary within the Bell scenario and

$$f(\rho, \Omega) = \begin{cases} 1, & \text{if settings lead to violations} \\ & \text{of } \mathcal{L}/\mathcal{S}_2/\mathcal{NS}_2 \text{ model,} \\ 0, & \text{otherwise.} \end{cases} \quad (4.14)$$

#### 4.1.4 Linear Programming for tripartite nonlocality

The quantities mentioned above can be obtained by employing linear programming methods. The method, despite being numerical, can give us results that are equivalent of using a complete set of Bell-type inequalities, i.e., the Bell-Pitovsky polytope [237]. Therefore it is reasonable to call our method an optimal GMNL test. We now formulate the corresponding linear programming (LP) task. For a given correlation point  $\mathbf{p}$ , we will present LP algorithm to detect whether the point  $\mathbf{p}$  is inside the sets  $\mathcal{L}$ ,  $\mathcal{NS}_2$ , and  $\mathcal{S}_2$  or not.

We first present a standard structure of a linear optimization program. This is comprised of a linear objective function that is subjected to linear equality and/or inequality constraints. The algorithm then finds an optimal point in the feasible region which forms a convex polytope. The algorithm has the following structure:

$$\begin{aligned} & \text{maximize} && \mathbf{c}^T \mathbf{x} \\ & \text{subject to} && A\mathbf{x} \geq \mathbf{b} \\ & \text{and} && \mathbf{x} \geq 0, \end{aligned}$$

where the  $\mathbf{x}$  is the variable to be determined for a given  $\mathbf{c}$ ,  $\mathbf{b}$  and matrix  $A$ .

For the optimization scheme specific to our problem, we first take into account the fact that any randomness present in either the two-party or one-party probabilities, namely  $P_\lambda$ ,  $P_{\lambda_i}$ ,  $P_{\lambda_i}^{\text{NS}}$  for  $i = 1, 2, 3$  in Eqs. (4.6,4.7,4.8), acting as *response functions*, can always be incorporated in the shared random variables  $\lambda$  and  $\lambda_i$ ,  $i = 1, 2, 3$  as these response functions are mathematical functions of those shared random variables and plays defining role in constructing the criterion to evaluate a numerical solution to the problem. Given the aforementioned fact, we then assume that these functions can be realized as deterministic functions of the inputs  $x$ ,  $y$  and  $z$ . In other words, each shared random variable  $\lambda$ ,  $\lambda_i$  for  $i = 1, 2, 3$  refers to the assignment of one of the possible outputs to each input. There is only a finite number of such assignments. We name them as  $D_\lambda^L(a|x)$ ,  $D_{\lambda_i}^S(a, b|x, y)$ ,  $D_{\lambda_i}^{\text{NS}}(a, b|x, y)$  for  $i = 1, 2, 3$ . Similar functions that are deterministic with respect to the inputs, are defined for the other two possible bipartitions:  $(AC|B)$  and  $(BC|A)$ . Therefore, without any loss of generality, we can assume that in Eqs. (4.6,4.7,4.8) the functions are the above deterministic functions. For instance, equation (4.6) can now be equivalently written in terms of these deterministic functions,

$$P(a, b, c|x, y, z) = \sum_{\lambda} q_{\lambda} D_{\lambda}^L(a|x) D_{\lambda}^L(b|y) D_{\lambda}^L(c|z). \quad (4.15)$$

For simplicity, let  $\mathbf{d}_{\lambda}$  be a product of these deterministic functions. For example, in Eq. (4.15), we have

$$\mathbf{d}_{\lambda}^L = D_{\lambda}^L(a|x) D_{\lambda}^L(b|y) D_{\lambda}^L(c|z). \quad (4.16)$$

Then a correlation point  $\mathbf{p} \in \mathcal{L}$  if it can be written as a convex combination of deterministic functions  $\mathbf{d}_{\lambda}$ , that is

$$\mathbf{p} = \sum_{\lambda} q_{\lambda} \mathbf{d}_{\lambda}^L, \quad (4.17)$$

where  $q_{\lambda} \geq 0$  and

$$\sum_{\lambda} q_{\lambda} = 1.$$

Similarly, for Svetlichny-local correlations  $S_2$  we will have

$$\mathbf{p} = \sum_{\lambda_1} q_{\lambda_1} \mathbf{d}_{\lambda_1}^S + \sum_{\lambda_2} q_{\lambda_2} \mathbf{d}_{\lambda_2}^S + \sum_{\lambda_3} q_{\lambda_3} \mathbf{d}_{\lambda_3}^S \quad (4.18)$$

where  $q_{\lambda_1}, q_{\lambda_2}, q_{\lambda_3} \geq 0$ ,

$$\mathbf{d}_{\lambda_1}^S = P_{\lambda_1}(a, b|x, y)P_{\lambda_1}(c|z), \quad (4.19)$$

$$\mathbf{d}_{\lambda_2}^S = P_{\lambda_2}(a, c|x, z)P_{\lambda_1}(b|y), \quad (4.20)$$

$$\mathbf{d}_{\lambda_3}^S = P_{\lambda_3}(b, c|y, z)P_{\lambda_3}(a|x), \quad (4.21)$$

and

$$\sum_{\lambda} q_{\lambda_1} + \sum_{\lambda} q_{\lambda_2} + \sum_{\lambda} q_{\lambda_3} = 1.$$

Lastly, for no-signaling bilocal correlations  $NS_2$  we will have

$$\mathbf{p} = \sum_{\lambda_1} q_{\lambda_1} \mathbf{d}_{\lambda_1}^{NS} + \sum_{\lambda_2} q_{\lambda_2} \mathbf{d}_{\lambda_2}^{NS} + \sum_{\lambda_3} q_{\lambda_3} \mathbf{d}_{\lambda_3}^{NS} \quad (4.22)$$

where  $q_{\lambda_1}, q_{\lambda_2}, q_{\lambda_3} \geq 0$ ,

$$\mathbf{d}_{\lambda_1}^{NS} = P_{\lambda_1}^{NS}(a, b|x, y)P_{\lambda_1}^{NS}(c|z), \quad (4.23)$$

$$\mathbf{d}_{\lambda_2}^{NS} = P_{\lambda_2}^{NS}(a, c|x, z)P_{\lambda_1}^{NS}(b|y), \quad (4.24)$$

$$\mathbf{d}_{\lambda_3}^{NS} = P_{\lambda_3}^{NS}(b, c|y, z)P_{\lambda_3}^{NS}(a|x), \quad (4.25)$$

and

$$\sum_{\lambda} q_{\lambda_1} + \sum_{\lambda} q_{\lambda_2} + \sum_{\lambda} q_{\lambda_3} = 1.$$

After introducing all our inequalities in this simpler representation, the next step is to determine whether there exist weights  $\lambda$  in Eq. (4.17) and weights  $\lambda_i, i = 1, 2, 3$  in Eq. (4.22) which satisfy the given linear constraints. From here, we are able to frame the task as a linear programming problem. There are several efficient solvers to run such linear programming which run in polynomial time in the number of variables [238].

We now turn the feasibility problems presented in (4.17) and (4.22) into a task of finding the critical visibility of a correlation point  $\mathbf{p}$  such that the noisy distribution has the form,

$$\mathbf{p}_v = v\mathbf{p} + (1 - v)\mathbf{p}_{\text{iso}}, \quad (4.26)$$

where  $\mathbf{p}_{\text{iso}}$  is the isotropic distribution defined by  $P_{\text{iso}}(a, b, c|x, y, z) = 1/2^3$  for all  $a, b, c$  and  $x, y, z$ . This noisy distribution is such that it can be still be described within the respective sets of  $\mathcal{L}$ ,  $\mathcal{S}_2$  and  $\mathcal{NS}_2$ . Then finding  $v_{\text{crit}}$  is a membership problem.

For the Bell local set  $\mathcal{L}$ , this problem translates to the following LP task:

$$\begin{aligned}
v_{\text{crit}} &= \max v \\
\text{s. t. } \mathbf{p}_v &= \sum_{q_\lambda} q_\lambda \mathbf{d}_\lambda^{\mathcal{L}} \\
&\text{with } q_\lambda \geq 0, \\
&\text{and } \sum_{\lambda} q_\lambda = 1.
\end{aligned} \tag{4.27}$$

For the Svetlichny-local set  $\mathcal{S}_2$  we have,

$$\begin{aligned}
v_{\text{crit}} &= \max v \\
\text{s. t. } \mathbf{p}_v &= \sum_{i=1,2,3} \sum_{q_{\lambda_i}} q_{\lambda_i} \mathbf{d}_{\lambda_i}^{\mathcal{S}} \\
&\text{with } q_{\lambda_i} \geq 0, \\
&\text{and } \sum_{i=1,2,3} \sum_{\lambda_i} q_{\lambda_i} = 1.
\end{aligned} \tag{4.28}$$

For no-signaling bilocal set  $\mathcal{NS}_2$  we have,

$$\begin{aligned}
v_{\text{crit}} &= \max v \\
\text{s. t. } \mathbf{p}_v &= \sum_{i=1,2,3} \sum_{q_{\lambda_i}} q_{\lambda_i} \mathbf{d}_{\lambda_i}^{\mathcal{NS}} \\
&\text{with } q_{\lambda_i} \geq 0, \\
&\text{and } \sum_{i=1,2,3} \sum_{\lambda_i} q_{\lambda_i} = 1.
\end{aligned} \tag{4.29}$$

The feasible region of the above LP tasks, i.e., the sets  $\mathcal{L}$ ,  $\mathcal{S}_2$  and  $\mathcal{NS}_2$  are the convex hull of a finite number of points, therefore each defining a polytope. The local deterministic points  $\mathbf{d}_\lambda$  correspond to the vertices, or extreme points, of the polytope. We can also transform these problems (4.27) and (4.28) into their dual formulation to get a hyperplane (defined by the normal plane  $\mathbf{S}$  and a constant  $S$ ), which separates the point  $\mathbf{p}$  from the respective polytope. This way by solving the dual LP we obtain a linear inequality  $\mathbf{S} \cdot \mathbf{d}_\lambda \leq S$  satisfied by all the vertices  $\mathbf{d}_\lambda$ , but violated by the correlation point  $\mathbf{p}(v)$  such that

$$\mathbf{S} \cdot \mathbf{p}(v) \geq S \quad \text{for } v > v_{\text{crit}}. \tag{4.30}$$

In order to determine the probability of violation, we repeat the LP procedure for randomly sampled set of settings (according to the Haare measure) and count how many times we observe violation of the models,  $\mathcal{L}$ ,  $\mathcal{S}_2$  and  $\mathcal{NS}_2$ , for  $v_{crit} < 1.0$ . For sufficiently high statistics, the frequency approaches the probability.

## 4.2 Results

### 4.2.1 Qubits

Now we apply the optimization method to investigate different tripartite states. For this we consider the following three states which are well known and often considered as very crucial resource in quantum information processing protocols:

- (i) Greenberger-Horne-Zeilinger state [197]:

$$|\text{GHZ}\rangle = \frac{1}{\sqrt{2}}(|000\rangle + |111\rangle) \quad (4.31)$$

- (ii) W state [239]:

$$|\text{W}\rangle = \frac{1}{\sqrt{3}}(|001\rangle + |010\rangle + |100\rangle), \quad (4.32)$$

- (iii) A state in  $(3, 2, 2)$  scenario given [240] showing significant  $\mathcal{L}$  violation:

$$|\psi_s\rangle = \frac{1}{\sqrt{6}}(|001\rangle + |010\rangle - |100\rangle) + \frac{1}{\sqrt{2}}|111\rangle. \quad (4.33)$$

In Tab. (4.2) we present numerical results containing probabilities of violation  $\mathcal{P}_V$  and the maximal nonlocality strengths  $\mathcal{S}_{max}$  for an increasing number of measurement settings per site and different nonlocality scenarios:  $\mathcal{L}$ ,  $\mathcal{S}_2$ ,  $\mathcal{NS}_2$ . From the numerical evidences we make the following observations.

(1) It is evident that the probability of violation  $\mathcal{P}_V$  steadily increases with  $m$ . In case of L scenario, we observe almost certain violations once the number of settings  $m > 2$  for each state has been considered. For  $m > 3$  the probability of violation is also very high, greater than 99.99%. However, the trait seems to be slightly weaker in the  $\mathcal{NS}_2$  scenario. For  $m = 2$ ,  $\mathcal{P}_v$  values are significantly smaller for  $\mathcal{NS}_2$  than for L. Although, starting from  $m = 4$  they start to become closer together for the GHZ state and the same is noticed at  $m = 5$  for the W and  $\psi_2$  states. However, in the case of  $\mathcal{S}_2$ , the percentage remains considerably small, especially for the W state, even for  $m = 6$ . In other words, according to numerical evidences, increasing number of settings does not increase the probability of violation for with respect

to Svetlichny-local constraint.

(2) It also appears that  $v_{crit}$  practically depends on the number of settings only for the W state and L problem. For other cases, either we do not observe any dependence up to 6 decimal places (GHZ:  $\mathcal{S}_2, \mathcal{NS}_2$ ;) or we see slight improvement on the 4th of 5th decimal place (GHZ:  $\mathcal{L}$ ; W:  $\mathcal{S}_2, \mathcal{NS}_2$ ;  $\psi_2$ :  $\mathcal{L}$ ) which is not conclusive. One should note that the above improvements are a real effect and not the result of numerical inaccuracy.

### Asymmetric GHZ state

For the tripartite qubit systems, we also investigate nonlocal feature of the asymmetric GHZ state which has the form,

$$|\psi_{\text{GHZ}}(\alpha)\rangle = \cos \alpha |000\rangle + \sin \alpha |111\rangle \quad (4.34)$$

We calculate probability of violation  $\mathcal{P}_V$  for no-signaling bilocal scenario ( $\mathcal{NS}_2$ ). The numerical results are presented in Tab. 4.1. Interestingly, dependency can be observed concerning changes in the probability of violation with increasing  $\alpha$ . For  $m = 2, 3, 4$  we observe expected monotonic increase of with  $\alpha$ . However, this monotonicity is disrupted for  $m = 4, 5$  where there is a local decrease of (minimum) around  $\alpha = 40^\circ$ . Although the effect manifests itself at the 4th decimal place, it is not due to numerical inaccuracies. It is worth noting that a similar effect is not observed for the standard nonlocality problem ( $\mathcal{NL}$ ).

$m$	$\psi_{\text{GHZ}}(10^\circ)$	$\psi_{\text{GHZ}}(20^\circ)$	$\psi_{\text{GHZ}}(30^\circ)$	$\psi_{\text{GHZ}}(40^\circ)$	$\psi_{\text{GHZ}}(45^\circ)$
2	0.0097	0.0413	0.0852	0.1127	0.1157
3	0.1364	0.4162	0.6361	0.7052	0.7081
4	0.4383	0.8473	0.9581	0.9684	0.9672
5	0.7249	0.9807	0.9979	0.9980	0.9977
6	0.8829	0.9985	0.99993	0.99990	0.99987

Table 4.1: Probability of violation for asymmetric GHZ state ( $\psi_{\text{GHZ}}(\alpha)$ ) determined from  $10^7$  ( $m = 2$ ) and  $10^6$  ( $m > 2$ ) random samples for  $\mathcal{NS}_2$  model.

### 4.2.2 Qutrits

In this section, we investigate nonlocal properties of qutrit systems. However, we limit our research to the violation of  $\mathcal{L}$  and  $\mathcal{NS}_2$  constraint.

We investigate probabilities of violation and maximal nonlocality strengths for  $m = 2$  and  $m = 3$  measurement settings and for the following three qutrit states:

N	State	m	Standard nonlocality		Genuine multipartite nonlocality			
			L		S <sub>2</sub>		NS <sub>2</sub>	
			$\mathcal{P}_V$	$\mathcal{S}_{max}$	$\mathcal{P}_V$	$\mathcal{S}_{max}$	$\mathcal{P}_V$	$\mathcal{S}_{max}$
3	GHZ	2	74.69	0.5	0.5413	0.2929	11.57	0.2929
		3	99.54	0.5	6.6282	0.2929	70.81	0.2929
		4	> 99.99	0.50301	23.255	0.2929	96.73	0.2929
		5	> 99.99	-	46.01	-	99.77	-
		6	> 99.99	-	66.67	-	99.99	-
		3	W	2	54.89	0.3558	0.0085	0.082107
3	97.80	0.395		0.01951	0.082107	41.29	0.1992	
4	> 99.99	0.3985		1.3797	0.082107	86.69	0.80014	
5	> 99.99	-		5.49	-	98.71	-	
6	> 99.99	-		14.33	-	99.93	-	
3	$\psi_s$	2		64.38	0.46445	0.2019	-	6.8637
3		99.03	0.46455	2.9871	-	58.9212	-	
4		> 99.99	0.4669	12.3838	-	94.55	-	
5		> 99.99	0.46699	28.91	-	99.6594	-	
6		> 99.99	0.46747	48.32	-	-	-	

Table 4.2: Probabilities of violation  $\mathcal{P}_V$  and the maximal nonlocality strengths  $\mathcal{S}_{max}$  for an increasing  $m$  per site and different nonlocality scenarios:  $\mathcal{L}$ ,  $\mathcal{S}_2$ ,  $\mathcal{NS}_2$ .

(i) 3-qutrit GHZ-type state

$$|\text{GHZ}\rangle = \frac{1}{\sqrt{3}}(|000\rangle + |111\rangle + |222\rangle). \quad (4.35)$$

(ii) 3-qutrit GHZ-type state reduced to qubit subspace, i.e., rank-2 state

$$|\text{rank} - 2\rangle = \frac{1}{\sqrt{2}}(|000\rangle + |111\rangle). \quad (4.36)$$

(iii) 3-qutrit Dicke states [241]

$$|D_3^1\rangle = \frac{1}{\sqrt{3}}(|001\rangle + |010\rangle + |100\rangle), \quad (4.37)$$

$$|D_3^2\rangle = \frac{1}{\sqrt{15}}(|002\rangle + |020\rangle + |200\rangle + 2(|011\rangle + |101\rangle + |110\rangle)), \quad (4.38)$$

$$|D_3^3\rangle = \frac{1}{\sqrt{10}}(|012\rangle + |021\rangle + |102\rangle + |120\rangle + |201\rangle + |210\rangle + 2|111\rangle). \quad (4.39)$$

(iv) 3-singlet state [242, 243]

$$|\text{Aharonov}\rangle = \frac{1}{\sqrt{6}}(|012\rangle - |021\rangle - |102\rangle + |120\rangle + |201\rangle - |210\rangle). \quad (4.40)$$

State	$m$	$\mathcal{L}$	$\mathcal{NS}_2$
GHZ	2	81.1435	0.5516
	3		16.5618
rank-2	2	33.1366	0.1854
	3		3.2805
$D_3^1$	2	17.2009	0.0190
	3		0.3483
$D_3^2$	2	39.3363	0.0506
	3		1.2658
$D_3^3$	2	42.5216	0.0807
	3		2.0036
Aharonov	2	68.7038	0.0056
	3		0.1643

Table 4.3: Probabilities of violation (in %) obtained for qutrit states from  $10^6$  random samples for  $\mathcal{L}$  and  $\mathcal{NS}_2$  models.

The results are presented Tab. 4.3. It is interesting to observe that the probability of revealing genuine multipartite nonlocality ( $\mathcal{NS}_2$ ) is negligible. The only case for which a considerable value can be observed is the GHZ state with three measurement settings ( $m = 3$ ), i.e., 16.56%. For three measurement settings if we compare these probabilities of violation with the values for the case of standard nonlocality ( $\mathcal{L}$ ), it turns out that they are smaller by two (GHZ, rank-2), three ( $D_3^1, D_3^2, D_3^3$ ) and even five (Aharonov) orders of magnitude.

The probability of violation for the  $\mathcal{NS}_2$  problem increases from 17-30 times depending on the state when the number of settings is increased to  $m = 3$ . We recall that, for qubits, the increment was smaller and varies in the range 6-11 times. These two cases, however, are not necessarily comparable due to the fact that different states were considered to investigate both the cases. But, if we limit ourselves to comparing only the family of the GHZ states then in the case of qubits the increment was 6.12 times, while for qutrits it is 30.02 times. This implies that the probability of violation tend to increase with increasing dimension of the subsystems.

### 4.3 Conclusion

In this chapter we have proposed linear programming scheme to investigate different kind of genuinely multipartite nonlocal correlations. For this task, we have considered three families of correlations, namely, Standard nonlocal  $\mathcal{L}$  correlations, Svetlichny-nonlocal correlations and no-signaling non-bilocal correlations. To witness GMNL, we have used two

quantifiers, namely, the strength of nonlocality and probability of violation and ran extensive optimization code to generate statistics for several states that are often considered as crucial resource in several quantum information processing tasks. Due to the increasing complexity of the task, we limited our numerical search for tripartite qubit and qutrit systems. From the numerical evidences we tried to judge the dependencies that genuinely multipartite nonlocal correlations may have on different key parameters of the construction of the experiment such as number of settings of the measurements and dimension of the subsystems. We also compared how the states behave for different kind of genuinely multipartite nonlocal correlations.

# Bibliography

- [1] E. Schrödinger. Discussion of probability relations between separated systems. *Mathematical Proceedings of the Cambridge Philosophical Society*, 31(4):555–563, 1935.
- [2] L Henderson and V Vedral. Classical, quantum and total correlations. *Journal of Physics A: Mathematical and General*, 34(35):6899–6905, aug 2001.
- [3] Patrick Hayden, Debbie W. Leung, and Andreas Winter. Aspects of generic entanglement. *Communications in Mathematical Physics*, 265(1):95–117, Mar 2006.
- [4] Borivoje Dakić, Vlatko Vedral, and Časlav Brukner. Necessary and sufficient condition for nonzero quantum discord. *Phys. Rev. Lett.*, 105:190502, Nov 2010.
- [5] Shunlong Luo. Quantum discord for two-qubit systems. *Phys. Rev. A*, 77:042303, Apr 2008.
- [6] Shunlong Luo and Shuangshuang Fu. Geometric measure of quantum discord. *Phys. Rev. A*, 82:034302, Sep 2010.
- [7] Eric Chitambar. Quantum correlations in high-dimensional states of high symmetry. *Phys. Rev. A*, 86:032110, Sep 2012.
- [8] Sai Vinjanampathy and A R P Rau. Quantum discord for qubit–qudit systems. *Journal of Physics A: Mathematical and Theoretical*, 45(9):095303, Feb 2012.
- [9] Kavan Modi, Tomasz Paterek, Wonmin Son, Vlatko Vedral, and Mark Williamson. Unified view of quantum and classical correlations. *Phys. Rev. Lett.*, 104:080501, Feb 2010.
- [10] Mazhar Ali, A. R. P. Rau, and G. Alber. Quantum discord for two-qubit  $x$  states. *Phys. Rev. A*, 81:042105, Apr 2010.
- [11] Chang-shui Yu and Haiqing Zhao. Direct measure of quantum correlation. *Phys. Rev. A*, 84:062123, Dec 2011.

- [12] Karol Bartkiewicz, Karel Lemr, Antonín Černoch, and Jan Soubusta. Measuring nonclassical correlations of two-photon states. *Phys. Rev. A*, 87:062102, Jun 2013.
- [13] Davide Girolami, Tommaso Tufarelli, and Gerardo Adesso. Characterizing nonclassical correlations via local quantum uncertainty. *Phys. Rev. Lett.*, 110:240402, Jun 2013.
- [14] Chang shui Yu, Shao xiong Wu, Xiaoguang Wang, X. X. Yi, and He shan Song. Quantum correlation measure in arbitrary bipartite systems. *EPL (Europhysics Letters)*, 107(1):10007, jul 2014.
- [15] Charles H. Bennett, Andrzej Grudka, Michał Horodecki, Paweł Horodecki, and Ryszard Horodecki. Postulates for measures of genuine multipartite correlations. *Phys. Rev. A*, 83:012312, Jan 2011.
- [16] A. J. Scott. Multipartite entanglement, quantum-error-correcting codes, and entangling power of quantum evolutions. *Phys. Rev. A*, 69:052330, May 2004.
- [17] Dardo Goyeneche, Daniel Alsina, José I. Latorre, Arnau Riera, and Karol Życzkowski. Absolutely maximally entangled states, combinatorial designs, and multiunitary matrices. *Phys. Rev. A*, 92:032316, Sep 2015.
- [18] Michael A. Nielsen and Isaac L. Chuang. *Quantum Computation and Quantum Information: 10th Anniversary Edition*. Cambridge University Press, 2010.
- [19] Fernando Pastawski, Beni Yoshida, Daniel Harlow, and John Preskill. Holographic quantum error-correcting codes: toy models for the bulk/boundary correspondence. *Journal of High Energy Physics*, 2015(6), Jun 2015.
- [20] Wolfram Helwig, Wei Cui, José Ignacio Latorre, Arnau Riera, and Hoi-Kwong Lo. Absolute maximal entanglement and quantum secret sharing. *Phys. Rev. A*, 86:052335, Nov 2012.
- [21] Wolfram Helwig and Wei Cui. Absolutely maximally entangled states: Existence and applications, 2013.
- [22] C. Radhakrishna Rao. Factorial experiments derivable from combinatorial arrangements of arrays. *Supplement to the Journal of the Royal Statistical Society*, 9(1):128–139, 1947.
- [23] A. S. Hedayat, N. J. A. Sloane, and J. Stufken. Orthogonal arrays. *Springer Series in Statistics*, (1):XXIII, 417, 1999.
- [24] Davide Girolami, Tommaso Tufarelli, and Cristian E. Susa. Quantifying genuine multipartite correlations and their pattern complexity. *Phys. Rev. Lett.*, 119:140505, Oct 2017.

- [25] Adi Shamir. How to share a secret. *Commun. ACM*, 22(11):612–613, November 1979.
- [26] G. R. Blakley. Safeguarding cryptographic keys. In *Managing Requirements Knowledge, International Workshop on*, page 313, Los Alamitos, CA, USA, jun 1979. IEEE Computer Society.
- [27] Mark Hillery, Vladimír Bužek, and André Berthiaume. Quantum secret sharing. *Phys. Rev. A*, 59:1829–1834, Mar 1999.
- [28] H. Imai, J. Mueller-Quade, A.c.a. Nascimento, P. Tuijls, and A. Winter. An information theoretical model for quantum secret sharing schemes. *Quantum Information and Computation*, 5(1):68–79, 2005.
- [29] Otfried Gühne and Géza Tóth. Entanglement detection. *Physics Reports*, 474(1):1–75, 2009.
- [30] Ryszard Horodecki, Paweł Horodecki, Michał Horodecki, and Karol Horodecki. Quantum entanglement. *Rev. Mod. Phys.*, 81:865–942, Jun 2009.
- [31] Dariusz Chruściński and Gniewomir Sarbicki. Entanglement witnesses: construction, analysis and classification. 47(48):483001, nov 2014.
- [32] Charles H. Bennett, Gilles Brassard, Claude Crépeau, Richard Jozsa, Asher Peres, and William K. Wootters. Teleporting an unknown quantum state via dual classical and einstein-podolsky-rosen channels. *Phys. Rev. Lett.*, 70:1895–1899, Mar 1993.
- [33] Dik Bouwmeester, Jian-Wei Pan, Klaus Mattle, Manfred Eibl, Harald Weinfurter, and Anton Zeilinger. Experimental quantum teleportation. *Nature*, 390(6660):575–579, Dec 1997.
- [34] Charles H. Bennett and Stephen J. Wiesner. Communication via one- and two-particle operators on einstein-podolsky-rosen states. *Phys. Rev. Lett.*, 69:2881–2884, Nov 1992.
- [35] Artur K. Ekert. Quantum cryptography based on bell’s theorem. *Phys. Rev. Lett.*, 67:661–663, Aug 1991.
- [36] Nicolas Gisin, Grégoire Ribordy, Wolfgang Tittel, and Hugo Zbinden. Quantum cryptography. *Rev. Mod. Phys.*, 74:145–195, Mar 2002.
- [37] Charles H. Bennett. Quantum cryptography using any two nonorthogonal states. *Phys. Rev. Lett.*, 68:3121–3124, May 1992.
- [38] A. J. Scott. Multipartite entanglement, quantum-error-correcting codes, and entangling power of quantum evolutions. *Phys. Rev. A*, 69:052330, May 2004.

- [39] Dardo Goyeneche and Karol Życzkowski. Genuinely multipartite entangled states and orthogonal arrays. *Phys. Rev. A*, 90:022316, Aug 2014.
- [40] Dardo Goyeneche, Daniel Alsina, José I. Latorre, Arnau Riera, and Karol Życzkowski. Absolutely maximally entangled states, combinatorial designs, and multiunitary matrices. *Phys. Rev. A*, 92:032316, Sep 2015.
- [41] Dardo Goyeneche, Zahra Raissi, Sara Di Martino, and Karol Życzkowski. Entanglement and quantum combinatorial designs. *Phys. Rev. A*, 97:062326, Jun 2018.
- [42] K. Feng, L. Jin, C. Xing, and C. Yuan. Multipartite entangled states, symmetric matrices, and error-correcting codes. *IEEE Transactions on Information Theory*, 63(9):5618–5627, 2017.
- [43] Wolfram Helwig. Absolutely maximally entangled qudit graph states, 2013.
- [44] Fei Shi, Mao-Sheng Li, Lin Chen, and Xiande Zhang.  $k$ -uniform states and quantum information masking, 2020.
- [45] Zahra Raissi, Christian Gogolin, Arnau Riera, and Antonio Acín. Optimal quantum error correcting codes from absolutely maximally entangled states. *Journal of Physics A: Mathematical and Theoretical*, 51(7):075301, Jan 2018.
- [46] P Facchi, G Florio, U Marzolino, G Parisi, and S Pascazio. Classical statistical mechanics approach to multipartite entanglement. *Journal of Physics A: Mathematical and Theoretical*, 43(22):225303, May 2010.
- [47] A Borrás, A R Plastino, J Batle, C Zander, M Casas, and A Plastino. Multiqubit systems: highly entangled states and entanglement distribution. *Journal of Physics A: Mathematical and Theoretical*, 40(44):13407–13421, Oct 2007.
- [48] A. Higuchi and A. Sudbery. How entangled can two couples get? *Physics Letters A*, 273(4):213–217, Aug 2000.
- [49] Felix Huber, Otfried Gühne, and Jens Siewert. Absolutely maximally entangled states of seven qubits do not exist. *Phys. Rev. Lett.*, 118:200502, May 2017.
- [50] E. M. Rains. Quantum weight enumerators. *IEEE Transactions on Information Theory*, 44(4):1388–1394, 1998.
- [51] E. M. Rains. Quantum shadow enumerators. *IEEE Transactions on Information Theory*, 45(7):2361–2366, 1999.
- [52] Wolfram Helwig and Wei Cui. Absolutely maximally entangled states: Existence and applications, 2013.

- [53] M. Hein, J. Eisert, and H. J. Briegel. Multiparty entanglement in graph states. *Phys. Rev. A*, 69:062311, Jun 2004.
- [54] Steven G. Johnson. The nlopt nonlinear-optimization package. <http://github.com/stevengj/nlopt>.
- [55] Karl R. Gegenfurtner. Praxis: Brent’s algorithm for function minimization. *Behavior Research Methods, Instruments, & Computers*, 24:560–564, 1992.
- [56] M. J. D. Powell. An efficient method for finding the minimum of a function of several variables without calculating derivatives. *The Computer Journal*, 7(2):155–162, 01 1964.
- [57] Stephen Boyd and Lieven Vandenbergh.
- [58] Daniel Gottesman. Class of quantum error-correcting codes saturating the quantum hamming bound. *Phys. Rev. A*, 54:1862–1868, Sep 1996.
- [59] Géza Tóth and Otfried Gühne. Entanglement detection in the stabilizer formalism. *Phys. Rev. A*, 72:022340, Aug 2005.
- [60] Christian Schwemmer, Lukas Knips, Minh Cong Tran, Anna de Rosier, Wiesław Laskowski, Tomasz Paterek, and Harald Weinfurter. Genuine multipartite entanglement without multipartite correlations. *Phys. Rev. Lett.*, 114:180501, May 2015.
- [61] Waldemar Kłobus, Wiesław Laskowski, Tomasz Paterek, Marcin Wieśniak, and Harald Weinfurter. Higher dimensional entanglement without correlations. *The European Physical Journal D*, 73(2), Feb 2019.
- [62] E.M. Rains. Nonbinary quantum codes. *IEEE Transactions on Information Theory*, 45(6):1827–1832, 1999.
- [63] H. J. Briegel, D. E. Browne, W. Dür, R. Raussendorf, and M. Van den Nest. Measurement-based quantum computation. *Nature Physics*, 5:19–26, Jan 2009.
- [64] Vittorio Giovannetti, Seth Lloyd, and Lorenzo Maccone. Quantum-enhanced measurements: Beating the standard quantum limit. *Science*, 306(5700):1330–1336, 2004.
- [65] Bastian Jungnitsch, Tobias Moroder, and Otfried Gühne. Taming multiparticle entanglement. *Phys. Rev. Lett.*, 106:190502, May 2011.
- [66] Samuel L. Braunstein and Carlton M. Caves. Statistical distance and the geometry of quantum states. *Phys. Rev. Lett.*, 72:3439–3443, May 1994.
- [67] Marcin Markiewicz, Zbigniew Puchała, Anna de Rosier, Wiesław Laskowski, and Karol Życzkowski. Quantum noise generated by local random hamiltonians. *Phys. Rev. A*, 95:032333, Mar 2017.

- [68] Philipp Hyllus, Wiesław Laskowski, Roland Krischek, Christian Schwemmer, Witlef Wieczorek, Harald Weinfurter, Luca Pezzé, and Augusto Smerzi. Fisher information and multiparticle entanglement. *Phys. Rev. A*, 85:022321, Feb 2012.
- [69] Géza Tóth. Multipartite entanglement and high-precision metrology. *Phys. Rev. A*, 85:022322, Feb 2012.
- [70] Jacek Gruca, Wiesław Laskowski, Marek Żukowski, Nikolai Kiesel, Witlef Wieczorek, Christian Schmid, and Harald Weinfurter. Nonclassicality thresholds for multiqubit states: Numerical analysis. *Phys. Rev. A*, 82:012118, Jul 2010.
- [71] Anna de Rosier, Jacek Gruca, Fernando Parisio, Tamás Vértesi, and Wiesław Laskowski. Multipartite nonlocality and random measurements. *Phys. Rev. A*, 96:012101, Jul 2017.
- [72] Alba Cervera-Lierta, José Ignacio Latorre, and Dardo Goyeneche. Quantum circuits for maximally entangled states. *Phys. Rev. A*, 100:022342, Aug 2019.
- [73] Weidong Tang, Sixia Yu, and C. H. Oh. Greenberger-horne-zeilinger paradoxes from qudit graph states. *Phys. Rev. Lett.*, 110:100403, Mar 2013.
- [74] TJ Gawne and BJ Richmond. How independent are the messages carried by adjacent inferior temporal cortical neurons? *Journal of Neuroscience*, 13(7):2758–2771, 1993.
- [75] Itay Gat and Naftali Tishby. Synergy and redundancy among brain cells of behaving monkeys. In *Proceedings of the 1998 Conference on Advances in Neural Information Processing Systems II*, page 111–117, Cambridge, MA, USA, 1999. MIT Press.
- [76] Elad Schneidman, William Bialek, and Michael J. Berry. Synergy, redundancy, and independence in population codes. *Journal of Neuroscience*, 23(37):11539–11553, 2003.
- [77] Elad Schneidman, Susanne Still, Michael J. Berry, and William Bialek. Network information and connected correlations. *Phys. Rev. Lett.*, 91:238701, Dec 2003.
- [78] Vinay Varadan, III Miller, David M., and Dimitris Anastassiou. Computational inference of the molecular logic for synaptic connectivity in *C. elegans*. *Bioinformatics*, 22(14):e497–e506, 07 2006.
- [79] Dimitris Anastassiou. Computational analysis of the synergy among multiple interacting genes. *Molecular Systems Biology*, 3(1):83, 2007.
- [80] Dari Trendafilov, Daniel Polani, and Roderick Murray-Smith. Model of coordination flow in remote collaborative interaction, 2015.
- [81] Paul L. Williams and Randall D. Beer. Nonnegative decomposition of multivariate information. *CoRR*, abs/1004.2515, 2010.

- [82] D. L. Zhou, B. Zeng, Z. Xu, and L. You. Multiparty correlation measure based on the cumulant. *Phys. Rev. A*, 74:052110, Nov 2006.
- [83] D. L. Zhou. Irreducible multiparty correlations in quantum states without maximal rank. *Phys. Rev. Lett.*, 101:180505, Oct 2008.
- [84] Dagomir Kaszlikowski, Aditi Sen(De), Ujjwal Sen, Vlatko Vedral, and Andreas Winter. Quantum correlation without classical correlations. *Phys. Rev. Lett.*, 101:070502, Aug 2008.
- [85] Gian Luca Giorgi, Bruno Bellomo, Fernando Galve, and Roberta Zambrini. Genuine quantum and classical correlations in multipartite systems. *Phys. Rev. Lett.*, 107:190501, Nov 2011.
- [86] L Henderson and V Vedral. Classical, quantum and total correlations. *Journal of Physics A: Mathematical and General*, 34(35):6899–6905, aug 2001.
- [87] I. Devetak. The private classical capacity and quantum capacity of a quantum channel. *IEEE Transactions on Information Theory*, 51(1):44–55, 2005.
- [88] Igor Devetak and Jon Yard. Exact cost of redistributing multipartite quantum states. *Phys. Rev. Lett.*, 100:230501, Jun 2008.
- [89] Jon T. Yard and Igor Devetak. Optimal quantum source coding with quantum side information at the encoder and decoder. *IEEE Transactions on Information Theory*, 55(11):5339–5351, 2009.
- [90] Fernando G. S. L. Brandão, Aram W. Harrow, Jonathan Oppenheim, and Sergii Strelchuk. Quantum conditional mutual information, reconstructed states, and state redistribution. *Phys. Rev. Lett.*, 115:050501, Jul 2015.
- [91] Isaac H. Kim. Perturbative analysis of topological entanglement entropy from conditional independence. *Phys. Rev. B*, 86:245116, Dec 2012.
- [92] Alexei Kitaev and John Preskill. Topological entanglement entropy. *Phys. Rev. Lett.*, 96:110404, Mar 2006.
- [93] Michael Levin and Xiao-Gang Wen. Detecting topological order in a ground state wave function. *Phys. Rev. Lett.*, 96:110405, Mar 2006.
- [94] Bei Zeng, Xie Chen, Duan-Lu Zhou, and Xiao-Gang Wen. Quantum information meets quantum matter – from quantum entanglement to topological phase in many-body systems, 2018.
- [95] Matthias Christandl and Andreas Winter. “squashed entanglement”: An additive entanglement measure. *Journal of Mathematical Physics*, 45(3):829–840, 2004.

- [96] Kunal Sharma, Eyuri Wakakuwa, and Mark M. Wilde. Conditional quantum one-time pad. *Phys. Rev. Lett.*, 124:050503, Feb 2020.
- [97] M. Piani. Problem with geometric discord. *Phys. Rev. A*, 86:034101, Sep 2012.
- [98] Chandrashekar Radhakrishnan, Mathieu Laurière, and Tim Byrnes. Multipartite generalization of quantum discord. *Phys. Rev. Lett.*, 124:110401, Mar 2020.
- [99] Eneet Kaur, Xiaoting Wang, and Mark M. Wilde. Conditional mutual information and quantum steering. *Phys. Rev. A*, 96:022332, Aug 2017.
- [100] Mario Berta, Fernando G. S. L. Brandão, Christian Majenz, and Mark M. Wilde. Conditional decoupling of quantum information. *Phys. Rev. Lett.*, 121:040504, Jul 2018.
- [101] Mario Berta, Fernando G. S. L. Brandão, Christian Majenz, and Mark M. Wilde. Deconstruction and conditional erasure of quantum correlations. *Phys. Rev. A*, 98:042320, Oct 2018.
- [102] Thomas M. Cover and Joy A. Thomas. *Elements of Information Theory (Wiley Series in Telecommunications and Signal Processing)*. Wiley-Interscience, USA, 2006.
- [103] Kavan Modi, Tomasz Paterek, Wonmin Son, Vlatko Vedral, and Mark Williamson. Unified view of quantum and classical correlations. *Phys. Rev. Lett.*, 104:080501, Feb 2010.
- [104] N. J. Cerf, C. Adami, and R. M. Gingrich. Reduction criterion for separability. *Phys. Rev. A*, 60:898–909, Aug 1999.
- [105] R. H. Dicke. Coherence in spontaneous radiation processes. *Phys. Rev.*, 93:99–110, Jan 1954.
- [106] R. Prevedel, G. Cronenberg, M. S. Tame, M. Paternostro, P. Walther, M. S. Kim, and A. Zeilinger. Experimental realization of dicke states of up to six qubits for multiparty quantum networking. *Phys. Rev. Lett.*, 103:020503, Jul 2009.
- [107] S K Özdemir, J Shimamura, and N Imoto. A necessary and sufficient condition to play games in quantum mechanical settings. *New Journal of Physics*, 9(2):43–43, feb 2007.
- [108] Mohamed Bourennane, Manfred Eibl, Sascha Gaertner, Nikolai Kiesel, Christian Kurtsiefer, and Harald Weinfurter. Entanglement persistency of multiphoton entangled states. *Phys. Rev. Lett.*, 96:100502, Mar 2006.
- [109] N. Kiesel, C. Schmid, G. Tóth, E. Solano, and H. Weinfurter. Experimental observation of four-photon entangled dicke state with high fidelity. *Phys. Rev. Lett.*, 98:063604, Feb 2007.

- [110] M. Muraio, D. Jonathan, M. B. Plenio, and V. Vedral. Quantum telecloning and multiparticle entanglement. *Phys. Rev. A*, 59:156–161, Jan 1999.
- [111] Géza Tóth. Multipartite entanglement and high-precision metrology. *Phys. Rev. A*, 85:022322, Feb 2012.
- [112] Witlef Wieczorek, Roland Krischek, Nikolai Kiesel, Patrick Michelberger, Géza Tóth, and Harald Weinfurter. Experimental entanglement of a six-photon symmetric dicke state. *Phys. Rev. Lett.*, 103:020504, Jul 2009.
- [113] Luca Pezzè, Augusto Smerzi, Markus K. Oberthaler, Roman Schmied, and Philipp Treutlein. Quantum metrology with nonclassical states of atomic ensembles. *Rev. Mod. Phys.*, 90:035005, Sep 2018.
- [114] Wolfram Helwig, Wei Cui, José Ignacio Latorre, Arnau Riera, and Hoi-Kwong Lo. Absolute maximal entanglement and quantum secret sharing. *Phys. Rev. A*, 86:052335, Nov 2012.
- [115] Philipp Hyllus, Otfried Gühne, and Augusto Smerzi. Not all pure entangled states are useful for sub-shot-noise interferometry. *Phys. Rev. A*, 82:012337, Jul 2010.
- [116] John A. Smolin. Four-party unlockable bound entangled state. *Phys. Rev. A*, 63:032306, Feb 2001.
- [117] Remigiusz Augusiak and Paweł Horodecki. Generalized smolin states and their properties. *Phys. Rev. A*, 73:012318, Jan 2006.
- [118] Remigiusz Augusiak and Paweł Horodecki. Bound entanglement maximally violating bell inequalities: Quantum entanglement is not fully equivalent to cryptographic security. *Phys. Rev. A*, 74:010305, Jul 2006.
- [119] Elias Amsellem and Mohamed Bourennane. Experimental four-qubit bound entanglement. *Nature Physics*, 5(10):748–752, 2009.
- [120] J. Lavoie, R. Kaltenbaek, M. Piani, and K. J. Resch. Experimental bound entanglement? *Nature Physics*, 6(11):827–827, 2010.
- [121] Elias Amsellem and Mohamed Bourennane. Reply to experimental bound entanglement? *Nature Physics*, 6(11):827–827, 2010.
- [122] Jonathan Lavoie, Rainer Kaltenbaek, Marco Piani, and Kevin J. Resch. Experimental bound entanglement in a four-photon state. *Phys. Rev. Lett.*, 105:130501, Sep 2010.
- [123] Julio T. Barreiro, Philipp Schindler, Otfried Gühne, Thomas Monz, Michael Chwalla, Christian F. Roos, Markus Hennrich, and Rainer Blatt. Experimental multiparticle entanglement dynamics induced by decoherence. *Nature Physics*, 6(12):943–946, 2010.

- [124] Elias Amselem, Muhammad Sadiq, and Mohamed Bourennane. Experimental bound entanglement through a pauli channel. *Scientific Reports*, 3(1), 2013.
- [125] Mark M Wilde. Optimized quantumf-divergences and data processing. *Journal of Physics A: Mathematical and Theoretical*, 51(37):374002, 2018.
- [126] Harold Ollivier and Wojciech H. Zurek. Quantum discord: A measure of the quantumness of correlations. *Phys. Rev. Lett.*, 88:017901, Dec 2001.
- [127] Lucas C. Céleri, Jonas Maziero, and Roberto M. Serra. Theoretical and experimental aspects of quantum discord and related measures. *International Journal of Quantum Information*, 09(07n08):1837–1873, 2011.
- [128] D. L. Zhou. Irreducible multiparty correlations can be created by local operations. *Phys. Rev. A*, 80:022113, Aug 2009.
- [129] T. Kahle, E. Olbrich, J. Jost, and N. Ay. Complexity measures from interaction structures. *Phys. Rev. E*, 79:026201, Feb 2009.
- [130] Tobias Galla and Otfried Gühne. Complexity measures, emergence, and multiparticle correlations. *Phys. Rev. E*, 85:046209, Apr 2012.
- [131]
- [132] Christian Schwemmer, Lukas Knips, Minh Cong Tran, Anna de Rosier, Wiesław Laskowski, Tomasz Paterek, and Harald Weinfurter. Genuine multipartite entanglement without multipartite correlations. *Phys. Rev. Lett.*, 114:180501, May 2015.
- [133] S. Designolle, O. Giraud, and J. Martin. Genuinely entangled symmetric states with no  $n$ -partite correlations. *Phys. Rev. A*, 96:032322, Sep 2017.
- [134] Minh Cong Tran, Margherita Zuppardo, Anna de Rosier, Lukas Knips, Wiesław Laskowski, Tomasz Paterek, and Harald Weinfurter. Genuine  $n$ -partite entanglement without  $n$ -partite correlation functions. *Phys. Rev. A*, 95:062331, Jun 2017.
- [135] Waldemar Kłobus, Wiesław Laskowski, Tomasz Paterek, Marcin Wieśniak, and Harald Weinfurter. Higher dimensional entanglement without correlations. *The European Physical Journal D*, 73(2), 2019.
- [136] Damian Markham and Barry C. Sanders. Graph states for quantum secret sharing. *Phys. Rev. A*, 78:042309, Oct 2008.
- [137] Adrian Keet, Ben Fortescue, Damian Markham, and Barry C. Sanders. Quantum secret sharing with qudit graph states. *Phys. Rev. A*, 82:062315, Dec 2010.

- [138] Damian Markham and Barry C. Sanders. Erratum: Graph states for quantum secret sharing [phys. rev. a 78, 042309 (2008)]. *Phys. Rev. A*, 83:019901, Jan 2011.
- [139] Michał Horodecki, Jonathan Oppenheim, and Andreas Winter. Partial quantum information. *Nature*, 436(7051):673–676, 2005.
- [140] Omar Fawzi and Renato Renner. Quantum conditional mutual information and approximate markov chains. *Communications in Mathematical Physics*, 340(2):575–611, 2015.
- [141] Man-Duen Choi. Completely positive linear maps on complex matrices. *Linear Algebra and its Applications*, 10(3):285–290, 1975.
- [142] Benjamin Schumacher. Sending entanglement through noisy quantum channels. *Phys. Rev. A*, 54:2614–2628, Oct 1996.
- [143] Benjamin Schumacher and M. A. Nielsen. Quantum data processing and error correction. *Phys. Rev. A*, 54:2629–2635, Oct 1996.
- [144] Howard Barnum, M. A. Nielsen, and Benjamin Schumacher. Information transmission through a noisy quantum channel. *Phys. Rev. A*, 57:4153–4175, Jun 1998.
- [145] H. Barnum, E. Knill, and M.A. Nielsen. On quantum fidelities and channel capacities. *IEEE Transactions on Information Theory*, 46(4):1317–1329, 2000.
- [146] Seth Lloyd. Capacity of the noisy quantum channel. *Phys. Rev. A*, 55:1613–1622, Mar 1997.
- [147] Howard Hua Yang and John Moody. Data visualization and feature selection: New algorithms for nongaussian data. In *Proceedings of the 12th International Conference on Neural Information Processing Systems, NIPS'99*, page 687–693, Cambridge, MA, USA, 1999. MIT Press.
- [148] Gavin Brown, Adam Pocock, Ming-Jie Zhao, and Mikel Luján. Conditional likelihood maximisation: A unifying framework for information theoretic feature selection. *Journal of Machine Learning Research*, 13(2):27–66, 2012.
- [149] Jie-Dong Yue, Yu-Ran Zhang, and Heng Fan. Quantum-enhanced metrology for multiple phase estimation with noise. *Scientific Reports*, 4(1):5933, Aug 2014.
- [150] Magdalena Szczykulska, Tillmann Baumgratz, and Animesh Datta. Multi-parameter quantum metrology. *Advances in Physics: X*, 1(4):621–639, 2016.
- [151] Sammy Ragy, Marcin Jarzyna, and Rafał Demkowicz-Dobrzański. Compatibility in multiparameter quantum metrology. *Phys. Rev. A*, 94:052108, Nov 2016.

- [152] Manuel Gessner, Luca Pezzè, and Augusto Smerzi. Sensitivity bounds for multiparameter quantum metrology. *Phys. Rev. Lett.*, 121:130503, Sep 2018.
- [153] Jing Liu, Haidong Yuan, Xiao-Ming Lu, and Xiaoguang Wang. Quantum fisher information matrix and multiparameter estimation. *Journal of Physics A: Mathematical and Theoretical*, 53(2):023001, dec 2019.
- [154] Wojciech Górecki, Sisi Zhou, Liang Jiang, and Rafał Demkowicz-Dobrzański. Optimal probes and error-correction schemes in multi-parameter quantum metrology. *Quantum*, 4:288, July 2020.
- [155] Jasminder S. Sidhu and Pieter Kok. Geometric perspective on quantum parameter estimation. *AVS Quantum Science*, 2(1):014701, 2020.
- [156] Emanuele Polino, Mauro Valeri, Nicolò Spagnolo, and Fabio Sciarrino. Photonic quantum metrology. *AVS Quantum Science*, 2(2):024703, 2020.
- [157] Roman Schnabel, Nergis Mavalvala, David E. McClelland, and Ping K. Lam. Quantum metrology for gravitational wave astronomy. *Nature Communications*, 1(1):121, 2010.
- [158] Mikhail I. Kolobov. The spatial behavior of nonclassical light. *Rev. Mod. Phys.*, 71:1539–1589, Oct 1999.
- [159] Catxere A. Casacio, Lars S. Madsen, Alex Terrasson, Muhammad Waleed, Kai Barnscheidt, Boris Hage, Michael A. Taylor, and Warwick P. Bowen. Quantum-enhanced nonlinear microscopy. *Nature*, 594(7862):201–206, 2021.
- [160] Yoad Michael, Leon Bello, Michael Rosenbluh, and Avi Pe’er. Squeezing-enhanced raman spectroscopy. *npj Quantum Information*, 5(1):81, 2019.
- [161] Masahito Hayashi. Parallel treatment of estimation of  $su(2)$  and phase estimation. *Physics Letters A*, 354(3):183–189, 2006.
- [162] Hiroshi Imai and Masahito Hayashi. Fourier analytic approach to phase estimation in quantum systems. *New Journal of Physics*, 11(4):043034, apr 2009.
- [163] Masahito Hayashi. Comparison between the cramer-rao and the mini-max approaches in quantum channel estimation. *Communications in Mathematical Physics*, 304(3):689–709, 2011.
- [164] Jing Liu, Mao Zhang, Hongzhen Chen, Lingna Wang, and Haidong Yuan. Optimal scheme for quantum metrology. *Advanced Quantum Technologies*, 5(1):2100080, Nov 2021.

- [165] Carl W. Helstrom. Quantum detection and estimation theory. *Journal of Statistical Physics*, 1(2):231–252, Jun 1969.
- [166] Alexander S Holevo. *Probabilistic and Statistical Aspects of Quantum Theory; 2nd ed.* Publications of the Scuola Normale Superiore. Monographs. Springer, Dordrecht, 2011.
- [167] Aaron Z. Goldberg, Ilaria Gianani, Marco Barbieri, Fabio Sciarrino, Aephraim M. Steinberg, and Nicolò Spagnolo. Multiphase estimation without a reference mode. *Phys. Rev. A*, 102:022230, Aug 2020.
- [168] C. Helstrom. *Quantum Detection and Estimation Theory*. New York: Academic Press, 1976.
- [169] T. Brougham, V. Košťák, I. Jex, E. Andersson, and T. Kiss. Entanglement preparation using symmetric multiports. *The European Physical Journal D*, 61(1):231–236, Jan 2011.
- [170] Nicolò Spagnolo, Lorenzo Aparo, Chiara Vitelli, Andrea Crespi, Roberta Ramponi, Roberto Osellame, Paolo Mataloni, and Fabio Sciarrino. Quantum interferometry with three-dimensional geometry. *Scientific Reports*, 2(1):862, Nov 2012.
- [171] Mario A. Ciampini, Nicolò Spagnolo, Chiara Vitelli, Luca Pezzè, Augusto Smerzi, and Fabio Sciarrino. Quantum-enhanced multiparameter estimation in multiarm interferometers. *Scientific Reports*, 6(1):28881, Jul 2016.
- [172] Chenglong You, Sushovit Adhikari, Yuxi Chi, Margarite L LaBorde, Corey T Matyas, Chenyu Zhang, Zuen Su, Tim Byrnes, Chaoyang Lu, Jonathan P Dowling, and Jonathan P Olson. Multiparameter estimation with single photons—linearly-optically generated quantum entanglement beats the shotnoise limit. *Journal of Optics*, 19(12):124002, oct 2017.
- [173] Emanuele Polino, Martina Riva, Mauro Valeri, Raffaele Silvestri, Giacomo Corrielli, Andrea Crespi, Nicolò Spagnolo, Roberto Osellame, and Fabio Sciarrino. Experimental multiphase estimation on a chip. *Optica*, 6(3):288–295, Mar 2019.
- [174] Xinwei Li, Jia-Hao Cao, Qi Liu, Meng Khoon Tey, and Li You. Multi-parameter estimation with multi-mode ramsey interferometry. *New Journal of Physics*, 22(4):043005, apr 2020.
- [175] Marcin Zwierz, Carlos A. Pérez-Delgado, and Pieter Kok. General optimality of the heisenberg limit for quantum metrology. *Phys. Rev. Lett.*, 105:180402, Oct 2010.
- [176] Michael J. W. Hall, Dominic W. Berry, Marcin Zwierz, and Howard M. Wiseman. Universality of the heisenberg limit for estimates of random phase shifts. *Phys. Rev. A*, 85:041802, Apr 2012.

- [177] Roy S. Bondurant and Jeffrey H. Shapiro. Squeezed states in phase-sensing interferometers. *Phys. Rev. D*, 30:2548–2556, Dec 1984.
- [178] D. J. Wineland, J. J. Bollinger, W. M. Itano, F. L. Moore, and D. J. Heinzen. Spin squeezing and reduced quantum noise in spectroscopy. *Phys. Rev. A*, 46:R6797–R6800, Dec 1992.
- [179] Vittorio Giovannetti, Seth Lloyd, and Lorenzo Maccone. Quantum-enhanced measurements: Beating the standard quantum limit. *Science*, 306(5700):1330–1336, 2004.
- [180] Vittorio Giovannetti, Seth Lloyd, and Lorenzo Maccone. Quantum metrology. *Phys. Rev. Lett.*, 96:010401, Jan 2006.
- [181] Jonathan P. Dowling. Quantum optical metrology – the lowdown on high-n00n states. *Contemporary Physics*, 49(2):125–143, 2008.
- [182] Vittorio Giovannetti, Seth Lloyd, and Lorenzo Maccone. Advances in quantum metrology. *Nature Photonics*, 5(4):222–229, Apr 2011.
- [183] Matthias D. Lang and Carlton M. Caves. Optimal quantum-enhanced interferometry using a laser power source. *Phys. Rev. Lett.*, 111:173601, Oct 2013.
- [184] Lorenzo Maccone and Alberto Riccardi. Squeezing metrology: a unified framework. *Quantum*, 4:292, July 2020.
- [185] Igor Jex, Stig Stenholm, and Anton Zeilinger. Hamiltonian theory of a symmetric multiport. *Optics Communications*, 117(1):95 – 101, 1995.
- [186] Sailes K. Sengupta and Steven M. Kay. Fundamentals of statistical signal processing: Estimation theory. *Technometrics*, 37(4):465, 1995.
- [187] Y.C. Eldar. Minimum variance in biased estimation: bounds and asymptotically optimal estimators. *IEEE Transactions on Signal Processing*, 52(7):1915–1930, 2004.
- [188] Zvika Ben-Haim and Yonina C. Eldar. On the constrained cramÉr–rao bound with a singular fisher information matrix. *IEEE Signal Processing Letters*, 16(6):453–456, 2009.
- [189] Peter C. Humphreys, Marco Barbieri, Animesh Datta, and Ian A. Walmsley. Quantum enhanced multiple phase estimation. *Phys. Rev. Lett.*, 111:070403, Aug 2013.
- [190] P. A. Knott, T. J. Proctor, A. J. Hayes, J. F. Ralph, P. Kok, and J. A. Dunningham. Local versus global strategies in multiparameter estimation. *Phys. Rev. A*, 94:062312, Dec 2016.
- [191] Jing Liu, Xiao-Ming Lu, Zhe Sun, and Xiaoguang Wang. Quantum multiparameter metrology with generalized entangled coherent state. *Journal of Physics A: Mathematical and Theoretical*, 49(11):115302, feb 2016.

- [192] Lu Zhang and Kam Wai Clifford Chan. Quantum multiparameter estimation with generalized balanced multimode noon-like states. *Phys. Rev. A*, 95:032321, Mar 2017.
- [193] A. S. Holevo. *Probabilistic and statistical aspects of quantum theory*. North-Holland, 1982.
- [194] Mankei Tsang, Francesco Albarelli, and Animesh Datta. Quantum semiparametric estimation. *Phys. Rev. X*, 10:031023, Jul 2020.
- [195] Jonathan Arthur Gross and Carlton M Caves. One from many: Estimating a function of many parameters. *Journal of Physics A: Mathematical and Theoretical*, sep 2020.
- [196] Jun Suzuki, Yuxiang Yang, and Masahito Hayashi. Quantum state estimation with nuisance parameters. *Journal of Physics A: Mathematical and Theoretical*, 53(45):453001, oct 2020.
- [197] D. M. Greenberger, M. A. Horne, and A. Zeilinger. Going beyond bell’s theorem. *arXiv:0712.0921 [quant-ph]*, 2007.
- [198] Lu Zhang and Kam Wai Clifford Chan. Scalable generation of multi-mode noon states for quantum multiple-phase estimation. *Scientific Reports*, 8(1):11440, Jul 2018.
- [199] A. Einstein, B. Podolsky, and N. Rosen. Can quantum-mechanical description of physical reality be considered complete? *Phys. Rev.*, 47:777–780, May 1935.
- [200] J. S. Bell. On the Einstein Podolsky Rosen paradox. *Physica Physique Fizika*, 1:195–200, Nov 1964.
- [201] John F. Clauser, Michael A. Horne, Abner Shimony, and Richard A. Holt. Proposed experiment to test local hidden-variable theories. *Phys. Rev. Lett.*, 23:880–884, Oct 1969.
- [202] Nicolas Brunner, Daniel Cavalcanti, Stefano Pironio, Valerio Scarani, and Stephanie Wehner. Bell nonlocality. *Rev. Mod. Phys.*, 86:419–478, Apr 2014.
- [203] Rodrigo Gallego, Lars Erik Würflinger, Antonio Acín, and Miguel Navascués. Operational framework for nonlocality. *Phys. Rev. Lett.*, 109:070401, Aug 2012.
- [204] R. Augusiak, M. Demianowicz, J. Tura, and A. Acín. Entanglement and nonlocality are inequivalent for any number of parties. *Phys. Rev. Lett.*, 115:030404, Jul 2015.
- [205] Reinhard F. Werner. Quantum states with Einstein-Podolsky-Rosen correlations admitting a hidden-variable model. *Phys. Rev. A*, 40:4277–4281, Oct 1989.
- [206] R. Horodecki, P. Horodecki, and M. Horodecki. Violating Bell inequality by mixed spin-12 states: necessary and sufficient condition. *Physics Letters A*, 200(5):340–344, 1995.

- [207] Jonathan Barrett. Nonsequential positive-operator-valued measurements on entangled mixed states do not always violate a Bell inequality. *Phys. Rev. A*, 65:042302, Mar 2002.
- [208] A. A. Methot and V. Scarani. An anomaly of non-locality, 2006.
- [209] Wojciech Hubert Zurek. Decoherence, einselection, and the quantum origins of the classical. *Rev. Mod. Phys.*, 75:715–775, May 2003.
- [210] H. M. Wiseman, S. J. Jones, and A. C. Doherty. Steering, entanglement, nonlocality, and the einstein-podolsky-rosen paradox. *Phys. Rev. Lett.*, 98:140402, Apr 2007.
- [211] Joseph Bowles, Tamás Vértesi, Marco Túlio Quintino, and Nicolas Brunner. One-way einstein-podolsky-rosen steering. *Phys. Rev. Lett.*, 112:200402, May 2014.
- [212] Marco Túlio Quintino, Tamás Vértesi, Daniel Cavalcanti, Remigiusz Augusiak, Maciej Demianowicz, Antonio Acín, and Nicolas Brunner. Inequivalence of entanglement, steering, and bell nonlocality for general measurements. *Phys. Rev. A*, 92:032107, Sep 2015.
- [213] Zhih-Ahn Jia, Rui Zhai, Shang Yu, Yu-Chun Wu, and Guang-Can Guo. Hierarchy of genuine multipartite quantum correlations. *Quantum Information Processing*, 19:419, 2020.
- [214] George Svetlichny. Distinguishing three-body from two-body nonseparability by a bell-type inequality. *Phys. Rev. D*, 35:3066–3069, May 1987.
- [215] Michael Seevinck and George Svetlichny. Bell-type inequalities for partial separability in  $n$ -particle systems and quantum mechanical violations. *Phys. Rev. Lett.*, 89:060401, Jul 2002.
- [216] Daniel Collins, Nicolas Gisin, Sandu Popescu, David Roberts, and Valerio Scarani. Bell-type inequalities to detect true  $n$ -body nonseparability. *Phys. Rev. Lett.*, 88:170405, Apr 2002.
- [217] Peter Mitchell, Sandu Popescu, and David Roberts. Conditions for the confirmation of three-particle nonlocality. *Phys. Rev. A*, 70:060101, Dec 2004.
- [218] Nick S. Jones, Noah Linden, and Serge Massar. Extent of multiparticle quantum nonlocality. *Phys. Rev. A*, 71:042329, Apr 2005.
- [219] Jean-Daniel Bancal, Nicolas Brunner, Nicolas Gisin, and Yeong-Cherng Liang. Detecting genuine multipartite quantum nonlocality: A simple approach and generalization to arbitrary dimensions. *Phys. Rev. Lett.*, 106:020405, Jan 2011.

- [220] Igor Devetak and Andreas Winter. Distillation of secret key and entanglement from quantum states. *Proceedings of the Royal Society A: Mathematical, Physical and Engineering Sciences*, 461(2053):207–235, 2005.
- [221] Daniel Cavalcanti, Mafalda L. Almeida, Valerio Scarani, and Antonio Acín. Quantum networks reveal quantum nonlocality. *Nature Communications*, 2:184, 2011.
- [222] Sandu Popescu and Daniel Rohrlich. Generic quantum nonlocality. *Physics Letters A*, 166(5):293–297, 1992.
- [223] Mariami Gachechiladze and Otfried GÃEhne. Completing the proof of generic quantum nonlocality. *Physics Letters A*, 381(15):1281–1285, 2017.
- [224] Patricia Contreras-Tejada, Carlos Palazuelos, and Julio I. de Vicente. Genuine multipartite nonlocality is intrinsic to quantum networks. *Phys. Rev. Lett.*, 126:040501, Jan 2021.
- [225] R. Augusiak, M. Demianowicz, and J. Tura. Constructing genuinely entangled multipartite states with applications to local hidden variables and local hidden states models. *Phys. Rev. A*, 98:012321, Jul 2018.
- [226] Jean-Daniel Bancal, Jonathan Barrett, Nicolas Gisin, and Stefano Pironio. Definitions of multipartite nonlocality. *Phys. Rev. A*, 88:014102, Jul 2013.
- [227] Joseph Bowles, JÃ©rÃ©mie Francfort, Mathieu Fillettaz, Flavien Hirsch, and Nicolas Brunner. Genuinely multipartite entangled quantum states with fully local hidden variable models and hidden multipartite nonlocality. *Phys. Rev. Lett.*, 116:130401, Mar 2016.
- [228] N. Gisin. Hidden quantum nonlocality revealed by local filters. *Physics Letters A*, 210(3):151–156, 1996.
- [229] Lluís Masanes. Asymptotic violation of bell inequalities and distillability. *Phys. Rev. Lett.*, 97:050503, Aug 2006.
- [230] Lluís Masanes, Yeong-Cherng Liang, and Andrew C. Doherty. All bipartite entangled states display some hidden nonlocality. *Phys. Rev. Lett.*, 100:090403, Mar 2008.
- [231] Flavien Hirsch, Marco TÃºlio Quintino, Joseph Bowles, and Nicolas Brunner. Genuine hidden quantum nonlocality. *Physical Review Letters*, 111(16), Oct 2013.
- [232] Flavien Hirsch, Marco TÃºlio Quintino, Joseph Bowles, Tamás VÃ©rtesi, and Nicolas Brunner. Entanglement without hidden nonlocality. *New Journal of Physics*, 18(11):113019, Nov 2016.

- [233] Sixia Yu and C. H. Oh. Tripartite entangled pure states are tripartite nonlocal, 2013.
- [234] Anna de Rosier, Jacek Gruca, Fernando Parisio, Tamás Vértesi, and Wiesław Laskowski. Multipartite nonlocality and random measurements. *Phys. Rev. A*, 96:012101, Jul 2017.
- [235] Yeong-Cherng Liang, Nicholas Harrigan, Stephen D. Bartlett, and Terry Rudolph. Nonclassical correlations from randomly chosen local measurements. *Phys. Rev. Lett.*, 104:050401, Feb 2010.
- [236] Nicolas Brunner, Daniel Cavalcanti, Stefano Pironio, Valerio Scarani, and Stephanie Wehner. Bell nonlocality. *Rev. Mod. Phys.*, 86:419–478, Apr 2014.
- [237] I. Pitowsky. *Quantum Probability — Quantum Logic*. Lecture Notes in Physics. Springer Berlin Heidelberg, 1989.
- [238] Stephen Boyd and Lieven Vandenberghe. *Convex Optimization*. Cambridge University Press, 2004.
- [239] W. Dür, G. Vidal, and J. I. Cirac. Three qubits can be entangled in two inequivalent ways. *Phys. Rev. A*, 62:062314, Nov 2000.
- [240] Sheila López-Rosa, Zhen-Peng Xu, and Adán Cabello. Maximum nonlocality in the (3,2,2) scenario. *Phys. Rev. A*, 94:062121, Dec 2016.
- [241] Wiesław Laskowski, Junghee Ryu, and Marek Żukowski. Noise resistance of the violation of local causality for pure three-qutrit entangled states. *Journal of Physics A: Mathematical and Theoretical*, 47(42):424019, oct 2014.
- [242] Matthias Fitzi, Nicolas Gisin, and Ueli Maurer. Quantum solution to the byzantine agreement problem. *Phys. Rev. Lett.*, 87:217901, Nov 2001.
- [243] Adán Cabello.  $n$ -particle  $n$ -level singlet states: Some properties and applications. *Phys. Rev. Lett.*, 89:100402, Aug 2002.

